The Institute of Paper Science and Technology

Atlanta, Georgia

Doctor's Dissertation

The Effect of Pulping, Bleaching, and Refining Operations on the Electrokinetic Properties of Wood Fiber Fines

Mike T. Goulet

June, 1989

THE EFFECT OF PULPING, BLEACHING, AND REFINING OPERATIONS ON THE ELECTROKINETIC PROPERTIES OF WOOD FIBER FINES

A thesis submitted by

Mike T. Goulet

B.S. 1983, Western Michigan University
Kalamazoo, Michigan

M.S. 1986, Lawrence University - The Institute of Paper Chemistry
Appleton, Wisconsin

in partial fulfillment of the requirements
of The Institute of Paper Chemistry
for the degree of Doctor of Philosophy
from Lawrence University
Appleton, Wisconsin

June, 1989

TABLE OF CONTENTS

ABSTRACT

The average electrophoretic mobility (E.M.) of wood fiber fines has been shown to play a role in many of the colloidal interactions involved in papermaking. Limited literature data suggest the E.M. distribution in a papermaking furnish is also very important and that attempts to correlate observed phenomena with a single (average) value may not be adequate. Wood pulp processing operations, such as pulping, bleaching, and refining, are known to modify the chemical nature of wood fibers and fiber fines. These chemical changes would be expected to affect the electrokinetic properties of the pulp. An understanding of how electrokinetic properties are influenced by fiber processing operations would be useful for predicting and controlling wet-end chemistry on the papermachine.

The objective of this work was to determine the effect of various processing operations on the E.M. distribution of fiber fines. The variables studied included pulping method, pulp yield, chemical bleaching, and degree of refining. The chemical changes occurring in the long fibers and fiber fines during these operations were measured independently and correlated with electrokinetic properties. The results indicate that a relationship exists between the weak acid content of the fines and their average E.M. Fiber modification processes that increase the weak acid content of the pulp (i.e., bleaching with hydrogen peroxide) produce fines with a more negative E.M. Processes that reduce the weak acid content (i.e., decreasing kraft pulp yield and bleaching of kraft pulp using a CEDED bleaching sequence) produce fines with a less negative E.M. Increasing the level of refining did not appreciably affect the weak acid content, and also had little effect on the average E.M. The width of the E.M. distribution was not significantly affected by pulp yield, bleaching, or refining.

INTRODUCTION

Wood fibers and fiber fragments (fines) acquire a negative surface charge when suspended in water. The origin of the surface charge in wood fibers is believed to be dependent upon the chemical nature of the surface. Many wood fiber processing operations change the overall chemical composition of wood fibers and also would be expected to alter their surface chemical nature. Although it is difficult to measure the actual surface charge of wood fibers and fiber fines, the electrokinetic (or zeta) potential that results from the charged surface can be determined. The zeta potential has been shown by many researchers to play a significant role in colloidal interactions that take place during paper formation. An increased understanding of how fiber processing operations affect the electrokinetic potential of wood fibers and fiber fines would be beneficial.

Electrokinetics involves the study of charged surfaces and their influence on the distribution of neighboring ions in solution. Many of the current theories used to explain electrokinetic phenomena are derived from the Gouy-Chapman theory of the diffuse double layer. An important modification of the Gouy-Chapman theory was later made by Stern to include an adsorbed layer of counterions adjacent to the solid surface. Many researchers have since modified these basic theories to explain various observed phenomena, and the historical development of the electric double layer has been reviewed several times.[1-4] Because of these available reviews, the following discussion will focus on general electrokinetic theories and their application to wood fibers and fiber fines.

ELECTROKINETIC PHENOMENA

The Electric Double Layer

Most substances acquire a surface electric charge when suspended in a polar medium, such as water. In general, there are three ways in which this surface charge may originate:

1. The charge can originate from chemical reaction of surface functional groups. For example, a negative surface charge will result from the ionization of surface acid groups, while protonation of surface amino groups results in a positive surface charge.

2. Surface charges can originate from lattice imperfections at the surface of crystalline solids, or by the unequal dissolution of oppositely charged ions.

3. Surface charges can be established by the adsorption of ions via London-van der Waals forces or hydrogen bonding.

A charged surface in an aqueous suspension will influence the distribution of nearby ions. Ions of opposite charge (counterions) will migrate toward this surface, while ions of like charge (co-ions) will be repelled This separation of charges in solution leads to the formation of an electric double layer. The double layer is comprised of the charged surface and a neutralizing excess of counterions, over co-ions, distributed in a diffuse manner in the surrounding liquid.

The diffuse double layer model was developed independently by Gouy (1910) and Chapman (1913) from purely theoretical considerations.[5] The ions in the diffuse part of the double layer were assumed to be point charges distributed according to the Boltzmann distribution above a flat, uniformly charged surface. An

important formula resulting from the work of Gouy and Chapman (Equation 1) correlates surface charge density (σ_o) and surface potential (φ_o). Although derived for a charged plane, Equation 1 may be used to describe the double-layer structure of colloidal particles if the minimum value for the radius of curvature of its surface is greater than the thickness of the double layer.[3]

$$\sigma_o = (2\varepsilon\varepsilon_o kN_A Tc/\pi)^{0.5} \sinh(ze\varphi_o/2kT) \qquad [1]$$

where:
- ε = dielectric constant of the medium
- ε_o = permittivity of free space
- k = Boltzmann's constant
- N_A = Avagadro constant
- T = absolute temperature
- c = ion concentration in the bulk of the electrolyte
- z = electrovalence of ion
- e = electron charge

The double layer thickness is generally expressed as the reciprocal of the Debye-Huckel parameter (i.e., $1/\kappa$). The Debye-Huckel parameter (κ) is defined by Equation 2.[4] The units of κ are $(\text{length})^{-1}$.

$$\kappa = [e^2 N_A \Sigma(c_i z_i^2)/\varepsilon\varepsilon_o kT]^{0.5} \qquad [2]$$

where:
- c_i = concentration of ion "i"
- z_i = electrovalence of ion "i"

The general expression for the thickness of the electric double layer for aqueous 1:1 electrolytes at 25°C is given in Equation 3.[3] Values of $1/\kappa$ for the solution conditions to be used in this thesis range from 21.6nm (c = 0.0002M) to 6.84nm (c = 0.002M) to 3.06nm (c = 0.01M).

$$\kappa^{-1} \text{ (nm)} = 0.306(c)^{-0.5} \qquad [3]$$

Hunter,[4] however, shows that the double layer extends appreciably beyond $1/\kappa$, and reaches a distance of about $3/\kappa$ before the potential has decayed to approximately 2% of its value at the surface.

Smoluchowski (1921) and Freundlich (1922) recognized that counterions adjacent to the charged surface were restricted in their movement due to the presence of the strong electric field, and that only part of the diffuse layer ions were involved in electrokinetic phenomena.[3] They proposed that a distinction should therefore be made between the surface potential (φ_o) and the electrokinetic potential (ζ). The term electrokinetic (or zeta) potential was used to describe the potential (measured with respect to the bulk of the solution) at the plane of shear between restricted ions and ions free to move independently of the particle. By differentiating between the surface and zeta potentials many experimentally observed phenomena could now be explained, including the effect of indifferent (i.e., non-potential-determining) electrolytes. The surface potential is essentially unaltered when an indifferent electrolyte is introduced, while the magnitude of the electrokinetic potential is decreased considerably due to a decrease in the double-layer thickness.

While the double-layer theory developed by Gouy and Chapman can be used to explain the difference between surface and zeta potentials, it failed to take into account the volume associated with hydrated ions in solution by regarding them as point charges. At high electrolyte concentrations the theory predicts excessively high counterion concentrations at the solid-liquid interface. Stern (1924) modified the theory of Gouy and Chapman by accounting for the dimensions of ions and the role of specific ion adsorption. The major result of Stern's work was the subdivision of the double layer into an inner and outer region. The inner

region was defined as an adsorbed layer of counterions. A Langmuir-type adsorption isotherm was used to describe the equilibrium between adsorbed ions and those in the diffuse part of the double layer. In the outer region, ionic dimensions and adsorption forces are neglected and the Gouy-Chapman theory can therefore be applied. The plane separating the inner and outer regions of the double layer is called the Stern plane, and is located approximately one hydrated ionic radius from the surface.

A schematic representation of the electric double layer is shown in Fig. 1. The potential changes from φ_o (the surface potential) to φ_d (the Stern potential) within the Stern layer, and decays from φ_d to zero in the diffuse layer.

The position of the shear plane is still somewhat obscure.[3] Some authors have assumed that it coincides with the boundary between the Stern layer and the diffuse layer, and that $\varphi_d \equiv \zeta$. In general, the shear plane is regarded as being located within the diffuse layer and therefore, $\zeta < \varphi_d$ (absolute magnitude). The net charge per unit area at the shear plane is called the electrokinetic charge density (σ_e).[4] The electrokinetic charge density can be calculated using Eq. 1 by substituting σ_e for σ_o and ζ for φ_o.

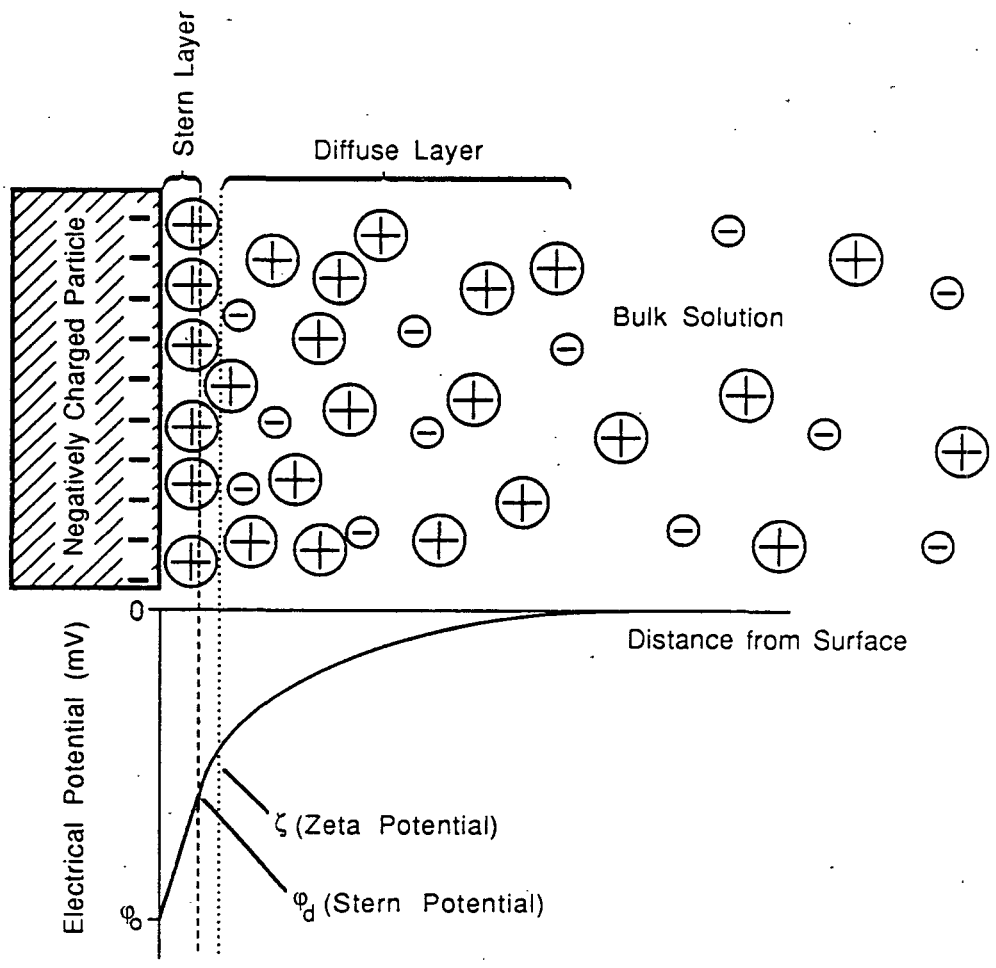

Figure. 1. Schematic representation of electric double layer and electrical potential as a function of distance from surface.

According to the Gouy-Chapman theory, the variation in potential with distance from the surface is given by Equation 4.[3] The potential φ_x equals ζ when x equals "δ", the distance from the particle surface to the shear plane.

$$e^{-\kappa x} = \tanh(ze\varphi_x/4kT)/\tanh(ze\varphi_o/4kT) \qquad [4]$$

where: x = distance from surface
φ_x = potential of the double layer at distance x from surface

It is important to keep in mind that many assumptions have been made regarding the nature of the charged surface and the distribution of the surrounding ions during the development of the Gouy-Chapman theory.[1-5] Because of these assumptions, and the uncertainty in the position of the shear plane, it has often been difficult to interpret electrokinetic measurements on the basis of this theory.[6] Herrington and Midmore[7] used the Gouy-Chapman theory (Eq. 1) to calculate the surface potential (φ_o) for cotton linters and bleached kraft fibers. The authors assumed that $\varphi_o \equiv \varphi_d$ and compared φ_d to measured values of ζ for the samples. They found that the calculated values of φ_d were much larger than the measured zeta potentials. Herrington and Midmore concluded that zeta potential, therefore, is not a good measure of the surface charge. The present author believes that limitations in the Gouy-Chapman theory are probably responsible for the observed difference between φ_d and ζ. Several other researchers have reported similar problems when attempting to evaluate experimental measurements of zeta potential in terms of the Gouy-Chapman theory.[4] Some authors have made modified the values used for the shear plane distance (δ)[8,9] and the dielectric constant of the medium[10] to account for observed differences between experimental data and the values predicted from theory.

To summarize, although it is recognized that the Gouy-Chapman theory of the electric double layer contains many inherent assumptions and may not be sophisticated enough to accurately predict experimentally obtained results, it is nevertheless a useful framework through which to interpret electrokinetic phenomena.

Techniques for Measuring Electrokinetic Potential

Four types of electrokinetic phenomena can be measured for the purpose of calculating the zeta potential. The four phenomena are defined as follows:[5]

1) Electrophoresis -- the movement of a charged surface relative to stationary liquid by an applied field.

2) Electroosmosis -- the movement of liquid relative to a stationary charged surface by an applied electric field.

3) Streaming potential -- the electric field created when liquid is made to flow along a stationary charged surface.

4) Sedimentation potential -- the electric field created when charged particles move relative to stationary liquid.

The most commonly used measurement technique, and the method used in this study, is particle electrophoresis (or microelectrophoresis). Microelectrophoresis involves the measurement of individual particle velocities under a known external electric field. The velocity per unit field strength is called the electrophoretic mobility. The velocity is usually expressed in "μm/second", and the field strength in "volts/centimeter".

An advantage of the microelectrophoresis technique is that it is possible to measure many individual particles and obtain a distribution of electrophoretic mobilities within a colloidal system. All other techniques yield an average value for the system under study.

One disadvantage of microelectrophoresis is that both the particles and the liquid are affected by the imposed electric field. If the wall of the electrophoresis cell is negatively charged and an external electric field is applied, electroosmosis will

cause the fluid near the cell wall to flow toward the cathode. Because the system is closed, there will be a return flow through the center of the cell. An accurate estimate of particle velocity can only be obtained by making measurements at the so-called "stationary level" within the electrophoresis cell where the liquid velocity is zero. Microelectrophoresis is therefore restricted to small diameter particles. In the case of wood pulp, only the fines fraction below approximately 50 μm in size may be measured.[11] Larger particles will extend beyond the stationary level and be subjected to the flow of the surrounding fluid. Measurement of such particles will result in erroneous velocities.

The Smoluchowski equation (Eq. 5) can be used to calculate the zeta potential from the electrophoretic mobility (E.M.) when the $|\zeta|$ is less than approximately 25mV.[4] The theory for larger values has been given by Wiersema, Loeb, and Overbeek[12] and tabulated correction factors to the Smoluchowski equation are available.[13] The Smoluchowski equation is valid for nonspherical particles only when the value of $(\kappa \cdot r)$ is greater than 100 (where: κ = the reciprocal of the thickness of the Debye-Huckel ionic atmosphere; and r = the local radius of curvature). For papermaking fibers (and fines) in systems of moderate ionic strength, the electric double layer will be suppressed and the quantity $(\kappa \cdot r)$ can be assumed to be greater than 100.[11] Other assumptions involved in applying the Smoluchowski equation are that the dielectric constant and viscosity measured in the bulk solution are valid for the region surrounding the particle. To avoid any uncertain assumptions, the data obtained from microelectrophoresis measurements in this work are expressed in terms of electrophoretic mobility.

$$\text{E.M.} = \frac{\varepsilon\varepsilon_0\zeta}{4\pi\eta} \qquad [5]$$

where: η = viscosity of medium surrounding particle

SURFACE CHARGE OF CELLULOSE FIBERS

Cellulose (wood) fibers develop a negative surface charge when suspended in an aqueous medium. The origin of this surface charge has been the subject of continued research. Several theories have been proposed suggesting that either surface group ionization, adsorption of suitable ions, or the structure of water at the solid-liquid interface is responsible for surface charge development.

Neale and Peters[14] used streaming current to measure the zeta potential of cotton fibers, derivatized cotton fibers, and vinyon (copolymer of vinyl chloride and vinyl acetate) fibers. The authors ruled out dissociation of surface acidic groups as the origin of surface charge based on two observations: (1) the chemically neutral vinyon fibers possessed the largest negative potential; and (2) the introduction of excess carboxylic acid groups into cotton by oxidation was found to decrease, not increase, its negative potential. The authors claimed the negative potential may arise from orientation of water molecules at the surface, although no direct experimental evidence was given. The theory of oriented water molecules has also been cited by Aksel'rod[15] as the source of negative surface charge on wood fibers.

Clapp[16] studied the role of carboxyl groups on zeta potential development of synthetic fibers. Polyacrylic acid (PAA) was adsorbed onto dacron fibers to provide fibers of varying surface carboxyl content. The zeta potential of the treated fibers was measured using a streaming current technique. Clapp found that fibers with low amounts of adsorbed PAA had a more negative zeta potential than either the untreated dacron or the dacron with the high amount of adsorbed PAA. Solvent orientation effects were again used to explain these results. Clapp concluded that the orientation of water molecules into high density layers at the

surface increased the thickness of the immobilized solvent, forcing the shear plane to move further into the medium and thus lowering the zeta potential.

Stamm[17] attributes the negative electrokinetic potential of cellulose to the ionization of surface hydroxyl groups. Balodis[18] uses the same reasoning to explain his results with esterified bleached kraft pulp fibers. Hydroxyl groups in both the lignin and cellulose fractions of wood have been cited by Ingruber[19] as a potential reserve of ionizable hydrogen in addition to conventional carboxylic acid groups. Reported pK_a values for cellulosic hydroxyl groups range from 13.4 to 13.7.[20,21] The pK_a calculations were made assuming only one acidic hydroxyl group per glucose unit. A recalculated pK_a for individual hydroxyl groups would be approximately 14,[22] with the 2-hydroxyl probably a slightly stronger acid than the 3- and 6- hydroxyl groups. The measured pK_a of phenolic hydroxyl (in lignin) ranges from 10.5-11.0.[23] Therefore, the ionization of a significant number of hydroxyl groups on wood fibers would not be expected below pH 10.5, thus limiting the role of hydroxyl ionization as a source of surface charge under conventional papermaking conditions.

The acidity of cellulose has generally been attributed to occasional carboxyl groups within the cellulose structure, probably at the C6 position.[24] The pK_a of carboxymethylcellulose is approximately 4.[25] The pK_a of carboxyl groups on the surface of latex particles was calculated to be 4.64 from zeta potential measurements and 4.6 by titration.[3] Pulp demineralization with EDTA was found to increase the magnitude of the zeta potential of kraft pulp in a study conducted by Jacquelin and Bourlas.[26] This result is consistent with the hypothesis that carboxyl groups are responsible for the negative charge of pulp fibers. Several other researchers have concluded that the negative surface charge of cellulose arises from the ionization of weak acid (i.e., carboxyl) groups.[11,27,28]

Rozalinov[29] measured the zeta potential of various oxidized bleached kraft pulp fractions using streaming potential. Carboxyl content (via a calcium ion exchange technique) and hydrodynamic specific surface area were also measured. These values were used to calculate a surface charge density. Rozalinov found that the zeta potential became more negative with increasing surface charge density. However, a change of only 3mV (from -32mV to -35mV) was observed over the calculated surface charge density range of 20 to 120 (x 10^{-9}) equivalents/cm^2.

Neale and Standring[30] studied the Donnan potential of cellulose and oxidized cellulose membranes in aqueous electrolyte solutions. They observed that the Donnan potential vanished when the dissociation of carboxylic acid groups had been repressed by lowering the pH. A plot of Donnan potential versus carboxylic acid content for various oxycellulose samples is shown in Fig. 2. Lines drawn through the data points passed through the origin, indicating that the intrinsic negative charge of cellulose was due solely to the presence of carboxyl groups.

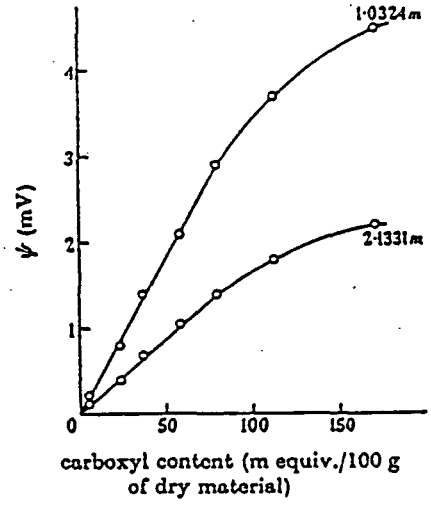

Figure 2.[30] Donnan potentials of oxycelluloses in solutions of 1.0324 and 2.1331 molal KCl.

Electrokinetics of Wood Fibers and Fiber Fines

Because only the fines fraction of a pulp is measured using micro-electrophoresis, it is unclear whether the long fibers possess similar electrokinetic properties. Unfortunately, none of the methods available for measuring the electrokinetic potential can be used to accurately measure both the fines and long fiber fractions independent of one another. Differences among sample preparation methods and the techniques used to measure the electrokinetic potential can make direct comparison between published results difficult.

Strazdins[31] presents the following points to argue that wood fibers and fiber fines have the same electrokinetic properties:

1) In most pulps, the fines represent a variety of debris that has originated from the cell wall. Therefore, it is reasonable to expect that the potential-determining surfaces of the fines should be very similar to the surfaces of the long fibers (for chemical pulps).

2) The surfaces of cellulose fibers (and fines) are always contaminated since a variety of polyelectrolytes and partially solubilized hemicelluloses can adsorb onto them.

3) The electrokinetic potential is strictly a surface property and as such depends upon the composition of the surface and has little to do with the average composition of the fiber as a whole. (Therefore, fines derived from long fibers should have electrokinetic potentials similar to the fiber surface from which they were obtained.)

Experimentally, Strazdins[32] has shown that sheet density reaches a minimum, while pulp freeness reaches a maximum, when the electrophoretic mobility of the fines is zero. These conditions would be expected when flocculation has been maximized (i.e., at the isoelectric point). Thus, by correlating whole pulp properties with the electrophoretic mobility of the fines fraction, Strazdins has

provided indirect evidence to substantiate the claim that long fibers and fiber fines are electrokinetically similar.

Jaycock and Pearson[33] measured the zeta potential of a bleached kraft pulp using both streaming potential and microelectrophoresis techniques. The streaming potential measurements were conducted using a fibrous pad containing both long fibers and fiber fines. The microelectrophoresis measurements were conducted on the nonsettling fines material. The zeta potential of both fractions was very similar over the pH range of 3 to 9, leading the authors to conclude that the assumption of electrokinetic similarity between long fibers and fiber fines had been verified. Stratton and Swanson[11] point out, however, that there is no rigorous method available to calculate the zeta potential from streaming potential measurements on pads of compressible fibers, and that such values "must be regarded as only assumptions of undetermined validity."

The technique of electroosmosis was used by Hinton and Quinn[34] to measure the zeta potential of bleached sulphite long fibers (>60-mesh) and fiber fines (<60-mesh). The pulp had been sized with 2% rosin and 4% alum prior to measuring the electrokinetic properties. Zeta potentials ranged from -7.8mV to -2.8mV for the long fibers and from -28mV to -10mV for the fines, depending on the sample packing density. The authors use the observed difference in zeta potential between fibers and fines, along with surface area differences, to explain the increased affinity of dyestuffs for the fines fraction. The dependence of zeta potential on the packing density leaves their results open to question, especially when comparisons are made between two dissimilarly shaped particles (i.e., fibers and fiber fines).

Branion and Arcelus[35] argue that fiber fines are not representative of long fibers in terms of their electrokinetic properties. The authors used micro-electrophoresis to measure the zeta potential of fines (<200-mesh) from both a bleached kraft and newsprint furnish. As they were making the measurements, the authors classified the fines as "small" (approximately 10μm), "medium" (approx. 30μm), and "large" (approx. 65μm). The average zeta potentials calculated for the small, medium, and large bleached kraft fines were -16, -20, and -27mV, respectively. For the newsprint furnish fines, the authors obtained average zeta potentials of -17, -19, and -26mV corresponding to the small, medium, and large fines. Their results indicate that a distribution of zeta potentials, possibly based on particle size, exists for fines less than 200-mesh (75μm). If this is the case, the average zeta potential may not be the most appropriate way to characterize the electrokinetic properties of the furnish. In theory, the electrophoretic mobility of a colloidal particle is independent of particle size or shape, provided the surface conductivity is negligible and the local particle radius is much greater than $1/\kappa$.[36]

The distribution of zeta potentials in a newsprint furnish was studied by Smith.[37] The mobilities of one-hundred individual particles (<100-mesh) from each sample were measured to produce zeta potential histograms, as shown in Fig. 3. Smith found that kraft pulps generally exhibited a unimodal, Gaussian distribution, while all of the groundwood and TMP pulps examined had bimodal distributions. The author suggests that the lower and higher (magnitude) zeta potential peaks observed in the mechanical pulp samples correspond to particles with predominantly cellulose and lignin surfaces, respectively.

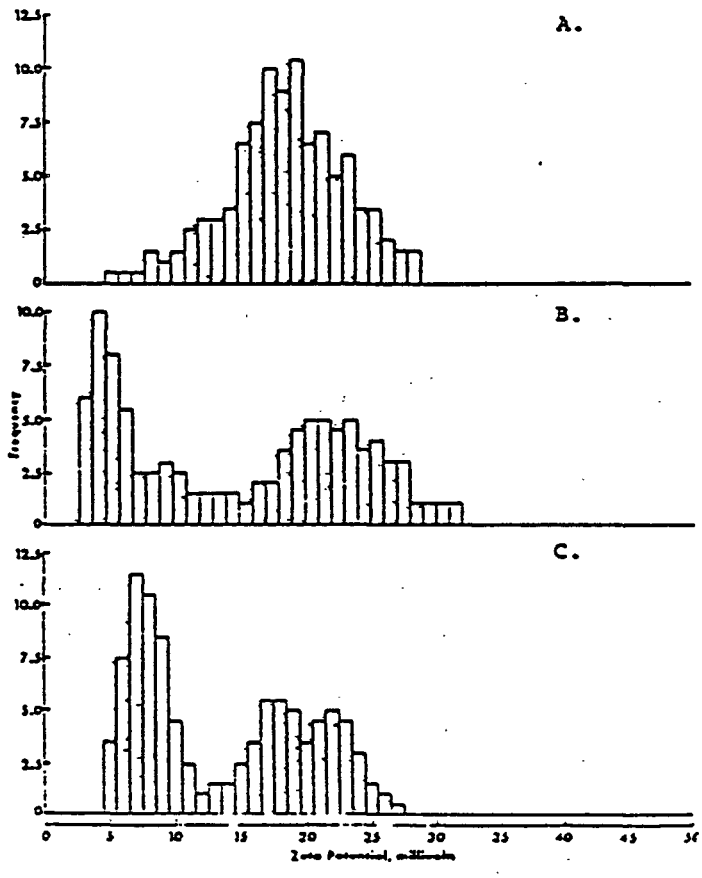

Figure 3.[37] Zeta potential histograms of various pulp sample fines.
(A = semi-bleached kraft; B = groundwood; C = thermomechanical pulp)

Smith also found that zeta potential distributions were better than calculated average values for interpreting the electrokinetic effects of fines in a newsprint furnish. While the average zeta potential of two different samples can be very similar, the underlying distribution can be quite different. Pulps with different zeta potential distributions were found to act independently with respect to their electrokinetic contributions when mixed together in a furnish. These results suggest that measurement of only a few particles, a common practice in microelectrophoresis, may not be sufficient to accurately characterize a pulp.

Although much has been published regarding the electrokinetic properties of wood fibers and fiber fines, in many instances the authors do not adequately describe the system under study. In particular, information concerning the wood species, pulping method, pulp yield, chemical analysis of the pulp, concentration of the suspending electrolyte, pH of the electrolyte, and the degree of uncertainty associated with average electrophoretic mobility values is often lacking. The present author would like to emphasize that it is very difficult to interpret the electrokinetic properties of wood fiber fines without also knowing a history of the pulp sample and the experimental conditions under which the measurements were performed.

Effect of Fiber Modification Processes

A limited amount of research has been published concerning the effects of pulping and bleaching on wood fiber electrokinetic properties. McKenzie[38] measured the electrophoretic mobility of fines from a number of different papermaking pulps. Considerable variations in zeta potential were found among different wood species pulped using the same method, as shown in Table 1.

Table 1. Zeta potential of fines from unbleached chemical pulps.[38]

Sample	Zeta Potential (mV)
Araucaria hunsteinii sulfate	-23.5
Pinus radiata sulfate A	-24.5
Pinus radiata sulfate B	-28.1
Populus angulata sulfate	-31.4
Eucalyptus regnans sulfate	-30.1
Eucalyptus regnans sulfite	-24.9
Picea spp. sulfite	-33.7

Within the same wood species, different pulping methods produced fibers with considerably different zeta potentials. Chemical bleaching also changed the zeta potential of sulfate pulp. Table 2 shows the effect of pulping method and bleaching on the zeta potential of Pinus radiata fines. Differences in zeta potential were attributed to chemical changes which had occurred during the pulping and bleaching processes, although no chemical analysis results were reported.

Table 2. Zeta potential of Pinus radiata pulp fines.[38]

Sample	Zeta Potential (mV)
Unbleached sulfate A	-24.5
Unbleached sulfate B	-28.1
Bleached sulfate (hypochlorite)	-21.1
Unbleached groundwood	-17.2
Unbleached cold soda	-34.4
Unbleached neutral sulfite semi-chemical	-46.1

Conflicting results appear in the literature regarding the effect of refining on the electrokinetic potential. Jaycock and Pearson[33] have reported that increased refining produces a more negative zeta potential for bleached sulfate pulps. The authors attribute this decrease in zeta potential to either the adsorption of negative species during refining or to an increase in the number of negative sites on the fibers. No experimental evidence was given to support either hypothesis. Their results are summarized in Fig. 4.[33] The authors used streaming potential to measure the zeta potential of the refined pulps, but do not indicate how the differences in fiber pad density that would be expected over this freeness range were accounted for in their calculations. Strazdins[31] has also reported a more negative zeta potential with increased refining of bleached sulfite pulp. Anderson and Penniman,[39] however, report no change in the electrophoretic mobility of spruce sulfite fines with increased refining over the freeness range of 800mL CSF to 200mL CSF. Davison and Cates[40] report similar results with bleached kraft fines.

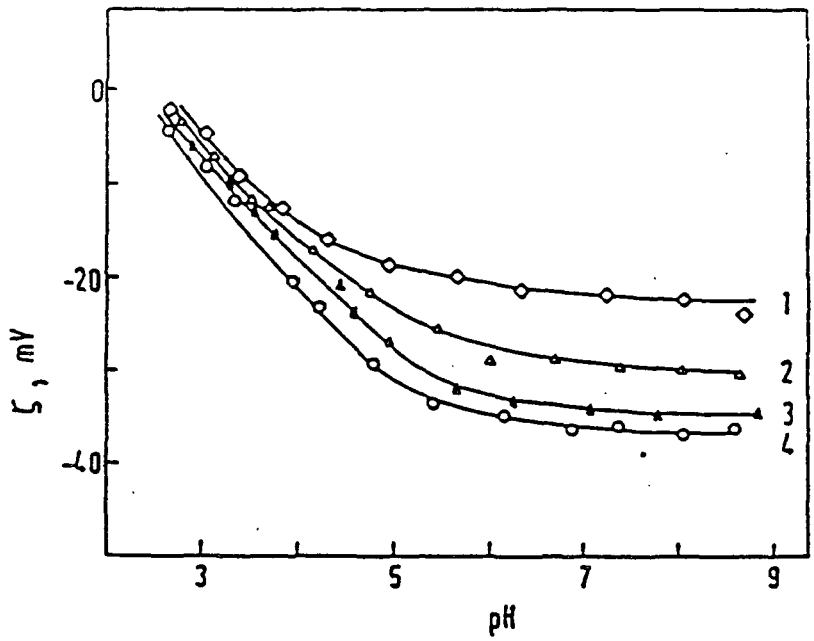

Figure 4.[33] The effect of beating on the zeta potential of cellulose fibers. (1) 550 mL, (2) 236 mL, (3) 179 mL, (4) 110 mL CSF.

In support of the hypothesis offered by Jaycock and Pearson, Lindström and coworkers[41] found that hemicellulosic material and lignin were released from Scotch pine kraft pulp during refining in a PFI mill. Increasing the pH increased the amount of dissolved substance, while increasing the electrolyte concentration decreased dissolution. The authors suggest that soluble polymers, prior to dissolution, are trapped in the microcavities of the cell wall during pulping. The polymers are released to the surrounding liquid during refining as the pores in the cell wall open and close due to mechanical action. The liberated polymers would be free to re-adsorb onto the surface of pulp, possibly creating a more negative surface.

Bryson[42] reported a change in average zeta potential from -20mV to -17mV with increased refining over a freeness range of 14°SR to 48°SR. Adsorption of metal ions from the refiner casing was offered as a possible explanation of these

results. Jacquelin and Bourlas[26] studied the effect of refining on a beech kraft pulp. These authors found that the zeta potential changed from -19.8mV at 17°SR freeness (i.e., no refining) to -9.8mV at 30°SR. Adsorption of metallic cations from the refining apparatus was suspected to be the cause of the change in zeta potential. After demineralization of the refined pulp with EDTA the zeta potential was -15.9mV. Therefore, they concluded that only a slight reduction in the magnitude of the zeta potential had occurred during refining. The above authors provide no indication of the experimental uncertainty associated with their calculated zeta potential values. Therefore it is difficult to determine if the observed changes are statistically significant. Nevertheless, their results demonstrate the importance of removing adsorbed metal ions from a pulp prior to making electrokinetic measurements.

PRESENTATION OF THE PROBLEM AND THESIS OBJECTIVES

The electrokinetic properties of wood fibers and fiber fines have been reported to be important in papermachine wet-end chemistry. The electrokinetic potential, or zeta potential, has been cited as a controlling factor in pigment retention,[43-46] chemical additives retention,[34,46-48] polymer adsorption,[32,46,49-51] fiber bonding,[18,52] flocculation,[28,53-55] wastewater treatment,[49,56] and other colloidal interactions. Claims that the entire paper forming process can be optimized by adjusting the electrokinetic potential of the system to zero, or some other predetermined value, appear in the literature.[39,40,57-59] These generalizations are often based on observed effects in the laboratory and have not always been observed in paper mill environments.[11,37,42,60]

The inability to utilize electrokinetic properties in the mill environment may be due to a lack of knowledge concerning the origin of wood fiber surface charge and the factors affecting it. The effects of common fiber processing operations such as pulping, bleaching, and refining on the electrokinetic properties of the pulp are not well understood. McKenzie[38] studied the effect of various pulping methods on the average zeta potential of wood fiber fines and found that different pulping methods produced fines with considerably different zeta potentials. He also found that bleaching with hypochlorite decreased the magnitude of the zeta potential. McKenzie attributed the zeta potential differences to chemical changes occurring during pulping and bleaching, however, no chemical analysis results were presented to substantiate this conclusion. Several researchers have studied the effect of refining on the average zeta potential of wood fibers and fiber fines. Their conclusions range from increased refining resulting in a more negative zeta potential,[31,33] to increased refining having no effect on the average zeta

potential,[39,40] to increased refining resulting in a less negative zeta potential.[26,42] Limited literature data indicates that the distribution of electrokinetic potentials in a papermaking furnish is very important and attempts to correlate observed phenomena with a single (average) value may not be adequate.[37,61,62] The factors influencing the zeta potential distribution and its role in papermaking operations have not been studied.

The purpose of this work was to investigate the effect of pulping, bleaching, and refining operations on the average electrophoretic mobility and electrophoretic mobility distribution of wood fiber fines. Chemical changes occurring in the fibers and fiber fines during these operations were also measured. Changes in chemical composition were correlated with changes in the electrokinetic properties. The specific objectives of the work were:

(1) To measure the average electrophoretic mobility and electrophoretic mobility distribution of wood fiber fines and to document the changes resulting from pulping, bleaching, and refining operations.

(2) To identify the physical and chemical changes occurring in the fibers and fiber fines during pulping, bleaching, and refining operations.

(3) To provide a better understanding of the effects of pulping, bleaching, and refining on the electrokinetic properties of fiber fines, and to identify the chemical changes responsible for these effects.

SCOPE OF THESIS OBJECTIVES

The thesis was limited in scope to the study of a single wood source, consisting of a mixture of white and black spruce. On the basis of McKenzie's results,[38] other wood species would probably behave differently with respect to electrokinetic property development. Two pulping methods common to the papermaking industry were used in this study, thermomechanical pulping (TMP) and kraft pulping. The effect of bleaching on the electrokinetic properties of the fiber fines was the only variable studied with the TMP pulp. With the kraft pulps, the effects of pulp yield, bleaching, and level of refining on the electrokinetic properties of the fines fraction were studied. Electrophoretic mobility measurements were conducted at one pH in three background electrolyte concentrations. The electrokinetic properties studied in this thesis were the average electrophoretic mobility and the standard deviation of the electrophoretic mobility distribution. A more detailed description of the materials and the experimental procedures used in this work is presented in the EXPERIMENTAL section.

EXPERIMENTAL

DESIGN

A schematic of the overall experimental design developed for accomplishing the objectives of this thesis is shown in Fig. 5. The experimental design can be divided into two parts: (1) a mechanical pulping (thermomechanical) phase, and (2) a chemical pulping (kraft) phase.

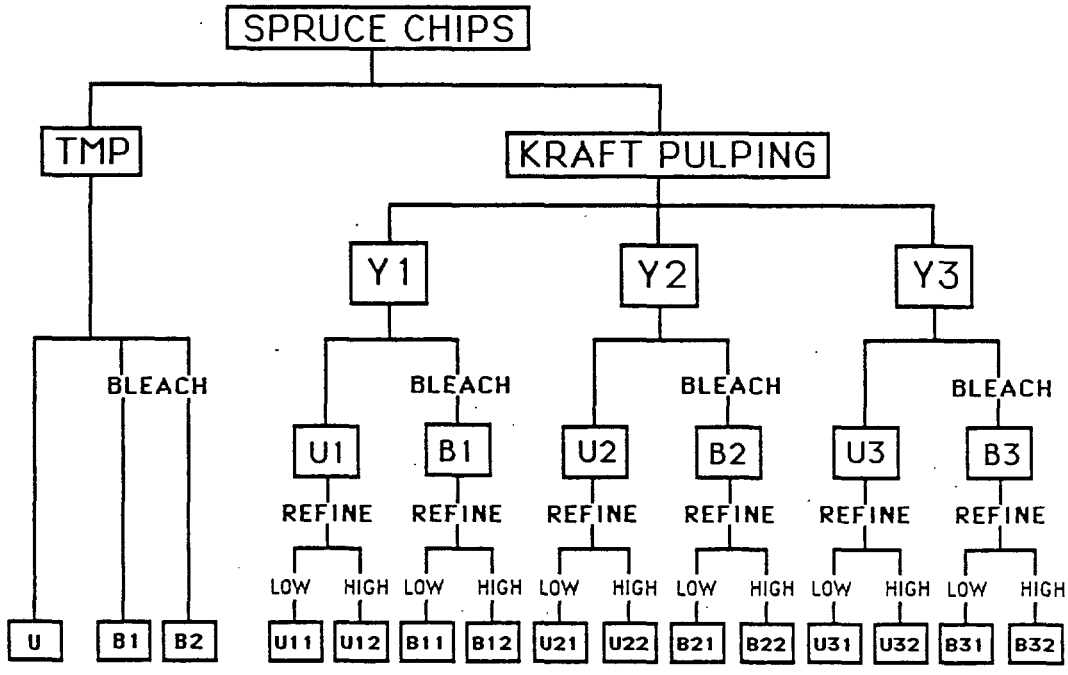

Figure 5. Schematic of experimental design.

Mechanical Pulping Phase

Only one variable was studied in the mechanical pulping phase: the effect of bleaching on the electrokinetic properties of thermomechanical pulp (TMP) fines. Referring to Fig. 5, B1 and B2 designate duplicate bleaching trials. Replicate

bleaching treatments were performed to determine the reproducibility of the operation. The effect of bleaching can be determined by comparing the electrokinetic properties of unbleached and bleached TMP fines.

Chemical Pulping Phase

The kraft pulping process was used in the chemical pulping phase of the work. The variables of interest included: pulp yield (Y); bleaching (B); and degree of refining. Three pulp yields were studied at two levels of bleaching (unbleached and bleached) and two degrees of refining (arbitrarily, "low" and "high"), as shown in Fig. 5. By making the proper comparisons, the effect of pulp yield, bleaching, and degree of refining on the electrokinetic properties of kraft pulp fines can be determined.

Parameters of Study

Two parameters were studied to evaluate the electrokinetic properties of a sample of fiber fines. These were: (1) the average electrophoretic mobility; and (2) the standard deviation of the electrophoretic mobility distribution. The use of the standard deviation to characterize the shape of distribution was justified on the basis of preliminary experiments where both kraft and TMP fines exhibited unimodal distributions that resembled a Gaussian distribution. Electrophoretic mobility distributions for all kraft and TMP fines measured in this study were also unimodal, and resembled a Gaussian distribution. Other properties relating to the chemical composition of pulp fibers and fiber fines were also measured. The specific properties and the procedures used are described in the "Analysis of Pulps" section.

MATERIALS

Thermomechanical Pulp and Wood Chips

The goal in selecting the wood supply for study was to obtain both a thermomechanical pulp sample and a sample of the chips used to produce the TMP for use in subsequent kraft pulping experiments. This would provide a homogeneous fiber supply and allow comparisons to be made between pulping methods. The wood chips and TMP used in this work were donated by Consolidated Papers, Inc. (Biron Division). Both the wood chips and TMP were reported to be a mixture of black spruce (Picea mariana) and white spruce (Picea glauca).[63] The exact mixture is unknown, however, the two species are essentially identical with respect to microscopic structure and chemical properties[64] and thus provide a homogeneous wood supply for study.

Approximately 65 pounds of spruce chips (air dry) were obtained from the hopper immediately preceding the TMP steaming vessels. The chips were stored in polyethylene bags at -4°C. No preservative was added. Microscopic analysis of a kraft pulp produced from the wood chips revealed no evidence of hardwood contamination.

Approximately 40 pounds of a 7.24% consistency slurry of spruce TMP were obtained. The pulp was stored a -4°C in polyethylene containers with no preservative added to the pulp. Fines fractionation of a sample of TMP was performed using a Dynamic Drainage Jar. The fines fraction, defined as the quantity of pulp passing through a 200-mesh screen with 76μm diameter circular openings,[65] was 33.0% by weight

EQUIPMENT

Electrokinetic Measurements

All electrophoretic mobility measurements were performed using the Zetasizer IIc Particle Electrophoresis and Submicron Particle Size Analyzer (Malvern Instruments). The Zetasizer IIc uses the technique of differential laser Doppler anemometry to measure the velocity of suspended particles moving under the influence of an applied electric field. For an excellent review of laser Doppler theory, refer to Drain.[66]

During a measurement, light from a 5mW helium-neon laser (633nm wavelength) is split into two beams which are focused to cross within a 4mm diameter quartz capillary containing the sample. A pattern of constructive and destructive interference fringes is formed (perpendicular to the direction of the applied electric field) in this crossover region, as shown in Fig. 6. The vertical arrow represents the direction of the applied electric field. The spacing between the fringes is determined by the angle of intersection and the wavelength of the light. The beam crossing region is referred to as the 'probe volume', and is approximately 50μm in extent. As particles pass through the probe volume, they experience a modulation of light intensity. The frequency of the scattered light signal from a particle moving perpendicular to the fringes is proportional to the particle velocity.

To measure the direction of a moving particle, the frequency of one of the split beams is modulated by the application of a ramp wave function to a stack of piezoelectric cells which are mounted behind one of the mirrors used to direct the path of the beam. Modulating the frequency of one beam causes the optical fringe pattern to move with velocity V_f in a direction parallel to the applied electric field (see arrow in Fig. 6). A stationary particle within the probe volume produces a

signal with a frequency equal to the modulation frequency. A particle moving in the same direction as the fringes produces a signal with a lower frequency, while particles moving in the opposite direction give higher frequency signals.

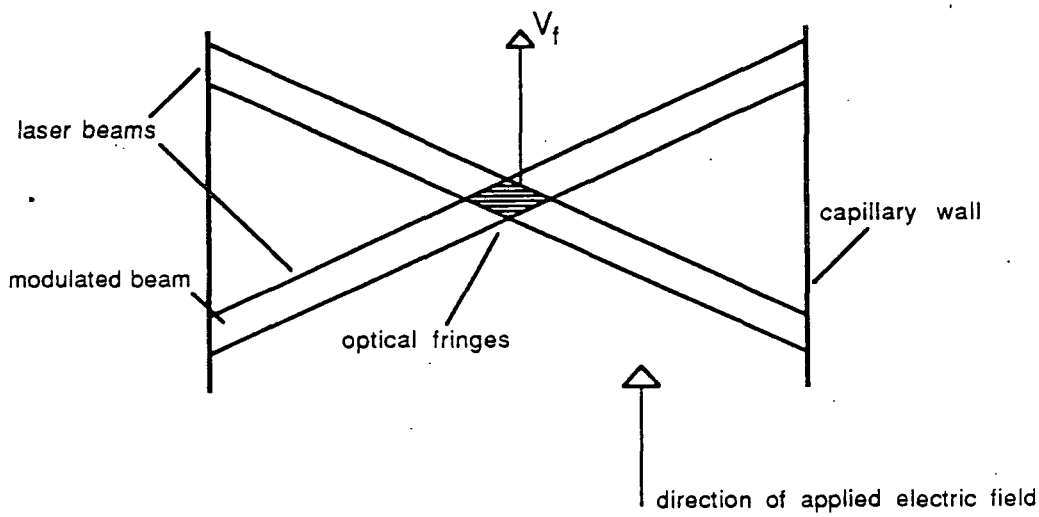

Figure 6. The moving fringe pattern produced by crossing two beams of different frequency (V_f = velocity vector of optical fringe pattern).

Scattered light from the moving particles is imaged by the receiving optics onto the cathode of the photomultiplier. The detected light is converted into an electrical signal and sent to the digital correlator. A correlation function is then calculated and mathematically analyzed to compute a velocity histogram. By simultaneously measuring the electric field strength, electrophoretic mobility distributions can be determined.

PROCEDURES

Hydrogen Peroxide Bleaching of Thermomechanical Pulp

The procedure outlined in IPC Pulping Group Procedure 73[67] was used, with some modifications, to bleach the TMP. Refer to Appendix I for a detailed

description of the procedures used for liquor preparation and bleaching. Duplicate bleaching treatments using 2.0% hydrogen peroxide on 30g (oven dry) pulp samples were performed.

Prior to bleaching, the pulp was washed extensively over a fritted glass funnel to replace mill process water with deionized water. The washed pulp was soaked in 0.2% DTPA (diethylenetriaminepentaacetic acid) for 30 minutes. The DTPA acts as a chelating agent to remove metal ions from the system. The pulp was then filtered using a fritted glass funnel and washed thoroughly with deionized water.

During bleaching, the initial pH of the liquor was adjusted to 11.5 with a solution of 50 g/L NaOH. The pH was checked periodically over the 4-hour bleaching period and adjusted to 11.0 with NaOH as required. Upon completion, the residual bleach liquor was filtered from the pulp and analyzed for pH and residual hydrogen peroxide concentration. The bleach liquor analysis results are summarized in Table 3.

Table 3. Analysis of hydrogen peroxide bleach liquor before and after bleaching.

Sample	% Peroxide on Pulp	Initial Peroxide (g/L)	Residual Peroxide (g/L)	Final pH	% Peroxide Consumed
1	2.0	1.051	0.476	11.16	54.7
2	2.0	1.046	0.468	10.92	55.3

The pulp was washed with deionized water and stored in a refrigerator under a nitrogen atmosphere at approximately 16% solids. An unbleached "control" was treated with DTPA, washed, and stored under identical conditions.

Kraft Pulping

Prior to pulping, the spruce chips were screened using a Sweco vibratory screen. Chips smaller than one inch square and larger than 0.25 inch square were selected for pulping and dried overnight in an ambient temperature forced air oven. The dried chips had a moisture content of 5.16% (o.d.).

White liquor was prepared from stock solutions of sodium hydroxide (100 g/L) and sodium sulfide (162.5 g/L) and analyzed using the ABC liquor titration technique.[68]

Pulping was conducted using the M&K laboratory batch digester in the IPC pulping laboratory. The digester has a total volume of 6 liters and is equipped with a liquor circulation pulp, electrical heater, thermocouple for temperature monitoring, and a temperature controller. The digester temperature is controlled by heating the circulating liquor. An additional heat exchanger on the liquor recirculation line provides rapid cooling at the end of a cook.

All cooks were conducted on an 800g (o.d.) charge of screened chips. A liquor-to-wood ratio of 3.5:1 was used for all three cooks. The effective alkali concentration was 19% with a sulfidity of 28%. Target unscreened pulp yields for the cooks were 55%, 50%, and 45%. Pulp yield was varied by cooking to three different H-Factors under identical conditions. (The H-Factor value represents the area under the curve of relative delignification reaction rate plotted against time and is useful for expressing cooking time and temperature as a single variable.) The approximate H-Factors necessary to achieve the target yields were selected on the basis of a preliminary kraft pulping study. The target H-Factors were 580, 933, and 4200 for the 55%, 50% and 45% pulp yields, respectively.

After loading the digester with chips and pulping chemicals, a warm-up time of 90 minutes was used to bring the temperature from 25°C to the final cooking temperature of 173°C. An Apple II+ personal computer was used to monitor and control the digester temperature (± 0.2°C). H-Factor calculations were also performed by the computer. Because of a digester control malfunction, cook number 2 cooled to 165°C toward the end of the cooking period. The final H-Factor for cook 2 was calculated from the time/temperature data collected during the cook using the procedure described in Ref. 68.

At the end of a cook, the black liquor was drained and discarded. The chips were removed from the digester, dispersed in tap water, and defibered using a Williams stirrer. The pulp was then washed thoroughly with deionized water. After dewatering the pulp to approximately 30% solids using an industrial centrifuge, the pulps were weighed for unscreened yield determinations.

The pulps were redispersed using a Williams stirrer prior to screening. Screening was conducted using a slotted flat vibratory screen with 0.008 inch openings. Rejects remaining on the screen were collected and weighed to determine the screened yield. Table 4 summarizes the unscreened and screened yield results.

Table 4. Unscreened and screened yield results for spruce kraft pulps.

Cook no.	H-Factor	Unscreened yield (%)	Rejects (%)	Screened yield (%)
3	576	54.35	5.61	48.74
1	927	49.92	1.61	48.31
2	3300	44.71	0.41	44.30

Primary fines were removed by passing a dilute slurry of screened pulp over a Sweco vibratory screen equipped with a 200-mesh screen. The long fibers were collected, dewatered in an industrial centrifuge, and stored under nitrogen in a

refrigerator for approximately two months. After some initial testing, the fibers were placed in a freezer until needed for further testing.

Bleaching of Kraft Pulps

A 50g (o.d.) sample of each of the three kraft pulps was bleached using the sequence shown below:

Stage 1. Chlorination
Stage 2. Caustic extraction
Stage 3. Chlorine dioxide
Stage 4. Caustic extraction
Stage 5. Chlorine dioxide

The CEDED sequence is common in industrial kraft pulp bleaching.[69] The goal was to obtain a high brightness pulp in each sample. Because of the wide range of lignin contents, the amount of chlorine added in the first stage was adjusted for each sample to obtain a similar final brightness. The specific conditions for each of the five stages were recommended by Tom Paulson of the Institute of Paper Chemistry,[70] and are shown in Table 5.

Table 5. Experimental conditions for CEDED bleaching of kraft pulps.

Stage	% Solids	Temp. (C)	Time (hr)	Addition Level (on o.d. pulp)
Chlorination	3	25	1	% Cl_2 = Kappa x 0.23
Extraction 1	10	70	1	%NaOH = %Cl_2 x 0.55
Chlorine dioxide 1	10	70	4	%ClO_2 = 1.0; %NaOH = 0.50
Extraction 2	10	70	1	% NaOH = 0.50
Chlorine dioxide 2	10	70	4	%ClO_2 = 0.60; %NaOH = 0.10

The following procedure was used for each bleaching stage. The pulp was broken-up into approximately 0.5 inch square pieces and placed in a heat-

sealable bag. The bleaching chemicals and water were then added and the bag was sealed. The pulp and chemicals were mixed by kneading until uniform in appearance. Bleaching was performed in a temperature controlled bath. During the reaction period, the bag was removed from the bath and kneaded frequently to assure uniform mixing. At the end of the period, the bag was opened and the pulp washed thoroughly with deionized water using a fritted glass funnel. The resulting pad was then broken up in preparation for the next stage.

Refining of Kraft Pulps

Prior to refining, the kraft pulps were fractionated through a 200-mesh screen using a Dynamic Drainage Jar to remove all primary fines. Bleached and unbleached kraft pulps were then refined using a PFI Mill.[71] The pulp was refined at 10% consistency using a gap clearance of 0.20mm between beating elements. The two levels of refining used in this work were 7,500 revolutions and 15,000 revolutions. Table 6 summarizes the refining results for both bleached and unbleached kraft pulps. In general, the 7,500 revolution refining level resulted in pulps with a Canadian Standard Freeness around 500mL. The 15,000 revolution level produced pulps in the 200mL - 250mL CSF range. The lower yield pulps refined more quickly than the high yield pulps.

Table 6. Results of refining kraft pulp in PFI Mill.

Pulp Type*	PFI Revolutions	CSF (mL)
54.35% - U	7,500	598
54.35% - U	15,000	271
49.92% - U	7,500	513
49.92% - U	15,000	217
44.71% - U	7,500	437
44.71% - U	15,000	152
54.35% - B	7,500	498
54.35% - B	15,000	247
49.92% - B	7,500	511
49.92% - B	15,000	262
44.71% - B	7,500	460
44.71% - B	15,000	196

(* % unscreened yield - Unbleached or - Bleached)

Analysis of Pulps

Lignin Analysis

Various pulp properties were used as a measure of the lignin content of the pulp. These included hypochlorite number,[72] kappa number,[73] pulp brightness,[74] and Klason lignin analysis.[75]

Selected pulp samples were also analyzed using diffuse reflectance Fourier-transform infrared (FTIR) spectrometry according to the method described in Ref. 76. Pulp samples were prepared for measurement by critical point drying from liquid carbon dioxide after solvent exchange with absolute ethanol. Diffuse reflectance infrared spectrometry measurements were performed on a Nicolet Instrument Corporation model 7199 FTIR spectrometer. With this method, the diffuse reflectance FTIR spectrum of cotton linters (Fig. 7) is subtracted from the FTIR spectrum of wood pulp (Figs 8, 10) resulting in a "lignin spectrum" of the

sample (Figs. 9, 11). The area under the 1510 cm^{-1} peak of the lignin spectrum is integrated and used as a relative measure of lignin content. An advantage of this method is that sample sizes of a few milligrams are used, allowing fiber fines to be easily analyzed and compared to long fibers from the same sample.

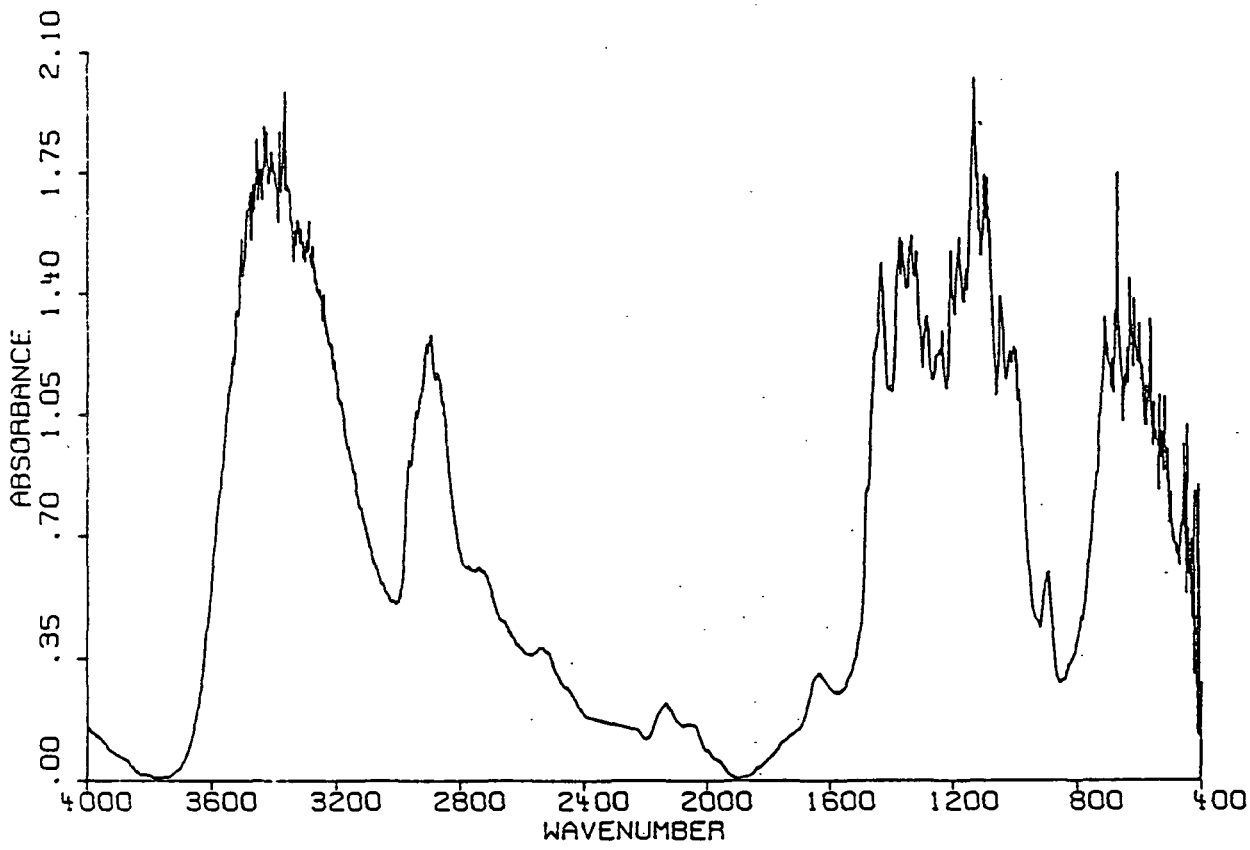

Figure 7. Diffuse reflectance spectrum of cotton linters.

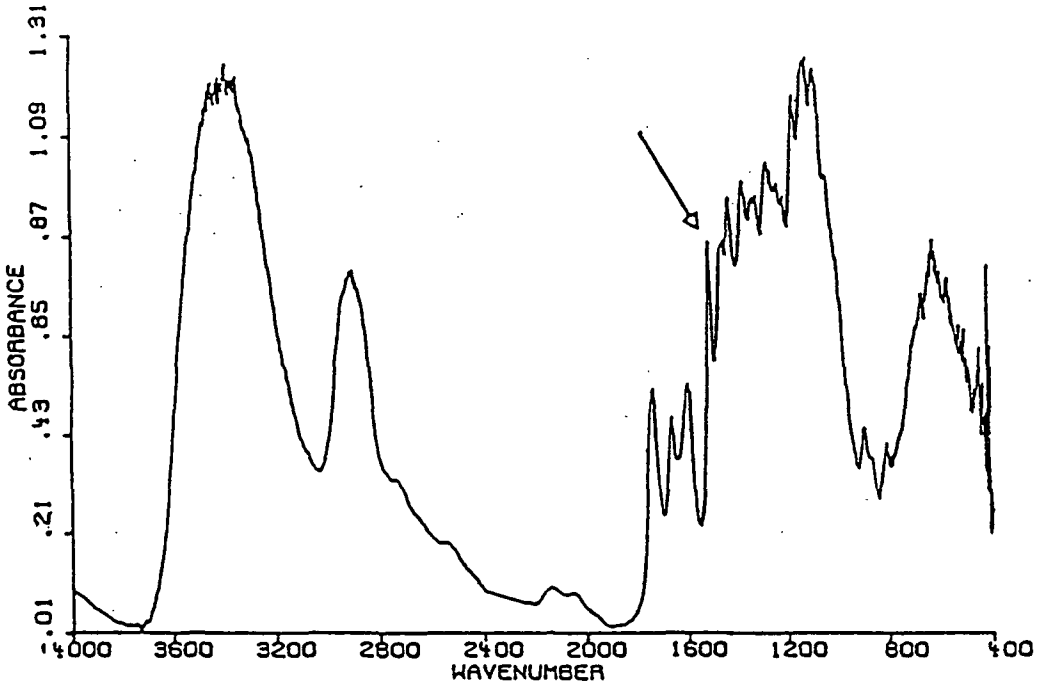

Figure 8. Diffuse reflectance spectrum of unbleached TMP long fibers.

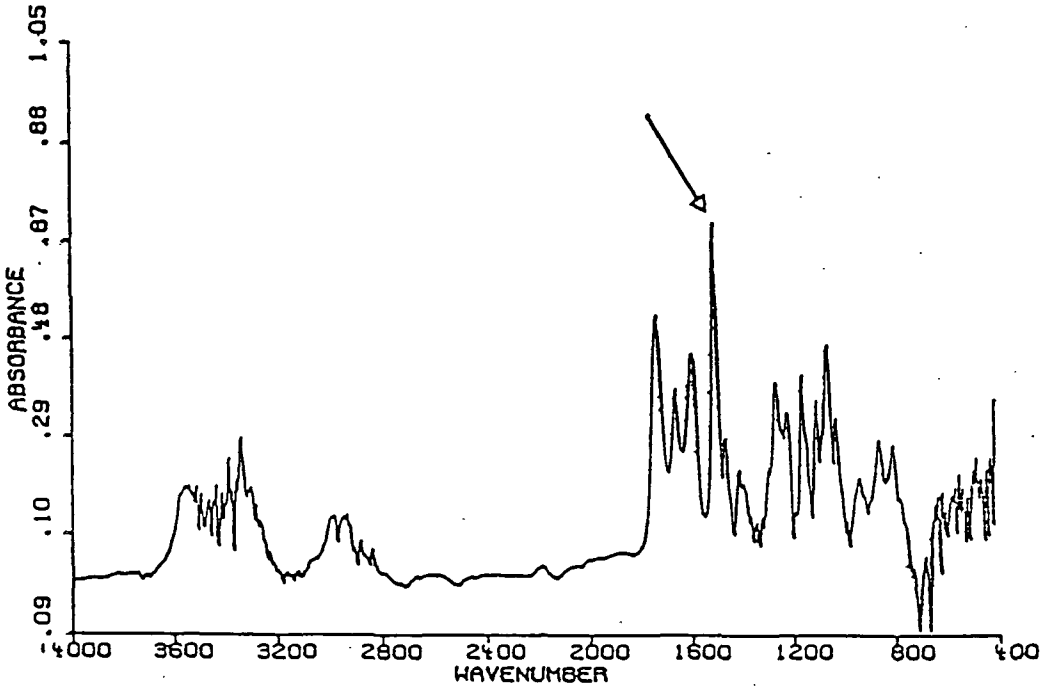

Figure 9. "Lignin spectrum" of unbleached TMP long fibers showing peak at 1510 cm^{-1}.

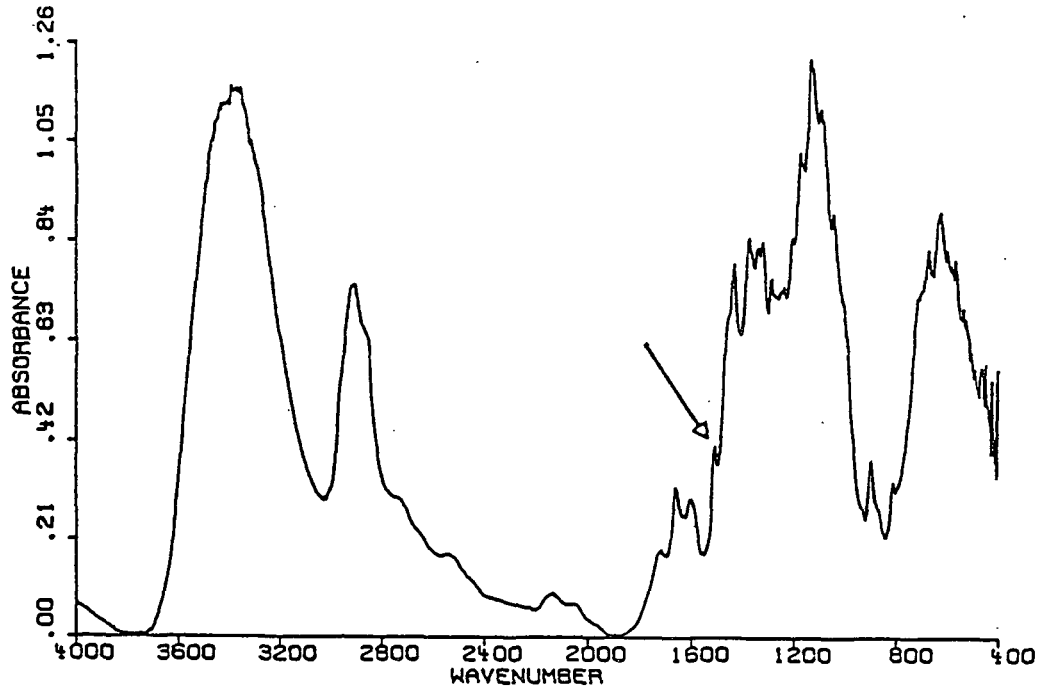

Figure 10. Diffuse reflectance spectrum of unbleached kraft long fibers (54.4% yield).

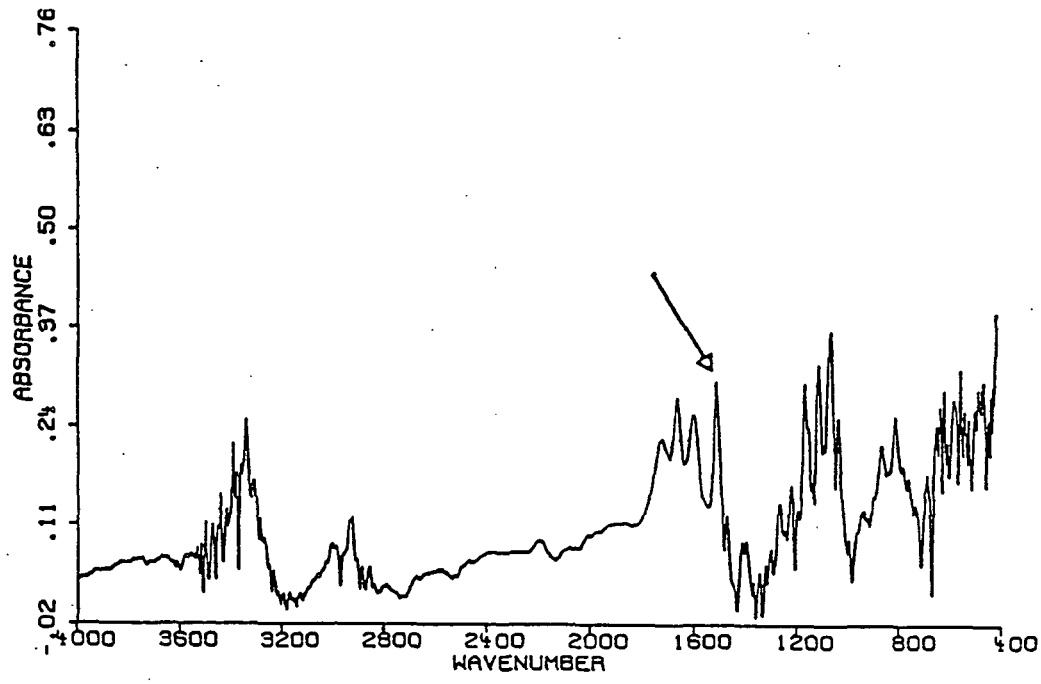

Figure 11. "Lignin spectrum" of unbleached kraft long fibers (54.4% yield) showing peak at 1510 cm^{-1}.

Carbohydrate Analysis

Selected pulp samples were analyzed for carbohydrate composition. The purpose of the analysis was to determine the effect of pulp yield and bleaching on the carbohydrate composition of pulp fibers and fiber fines. Carbohydrate analysis was conducted using a gas chromatographic method.[77] Measurements were performed using a Hewlett Packard model 5890 gas chromatograph, equipped with a flame ionization detector.

Extractives Analysis

The kraft pulping process removes most water-soluble and volatile compounds present in the wood. There remains, however, a fraction of material that can not be classified as either carbohydrate or lignin, the so-called "solvent extractables". This fraction consists primarily of resin and fatty acids and their esters, along with waxes and unsaponifiable substances. After removal of the primary fines fraction of the kraft pulps, this fraction would be expected to be very small. With the TMP pulps the extractives content should be somewhat higher due to the presence of primary fines. Selected pulp samples were analyzed to determine the extractives content.

No single solvent is capable of removing all "extractable" substances, and different solvents remove different combinations of this fraction. For this study, an ethanol-benzene mixture was chosen because it appears to provide the most complete removal of residual solvent-extractable substances in pulp.[78] Extraction was conducted for 6 hours with a 1:2 volume ratio of ethanol:benzene using a Soxhlet extraction flask according to the procedure outlined in Ref. 78. The air-dry samples were held in cellulose extraction thimbles (Whatman) during the extraction. The extracted material was then collected in tared flasks and evaporated

to dryness in an exhaust hood under ambient conditions. The residue was weighed to determine the percent extractives (air dry). The ether soluble fraction was extracted from the air dry residue, derivatized to form the methyl ester, and analyzed using gas chromatography to determine the resin acid and fatty acid content.

Analysis of Weak Acid Content

Several methods were used in this study to measure the carboxyl content, or more accurately the weak acid content, of wood pulps. These included the current TAPPI Standard method,[79] the conductometric titration method described by Katz and coworkers,[80] and a procedure involving the adsorption of methylene blue dye.[81]

The current TAPPI Standard method involves soaking the pulp in acid to protonate acidic groups on the fibers, followed by ion exchange of the acid groups with a base (sodium bicarbonate), and titration of the liberated hydrogen ions with sodium hydroxide to the methyl red endpoint.

The conductometric titration method for determining the weak acid content of pulp fibers involves soaking the pulp in acid to protonate the weak acid groups, dispersing the pulp in a dilute electrolyte solution (0.001M NaCl), and titrating the liberated hydrogen ions with a dilute (0.025 - 0.1M), accurately standardized solution of sodium hydroxide. The titration is monitored by measuring the specific conductance. To determine the weak acid content it is necessary to plot the specific conductance versus the volume of NaOH added as shown in Fig. 12. The equivalence point is located by extrapolating the two linear portions of the curve (see arrow). The weak acid content is then calculated using the following equation:

$$\text{Weak acid content (meq/100g)} = \frac{\text{(M NaOH)x(mL NaOH at eq. pt.)x100}}{\text{(dry fiber weight)}} \qquad [6]$$

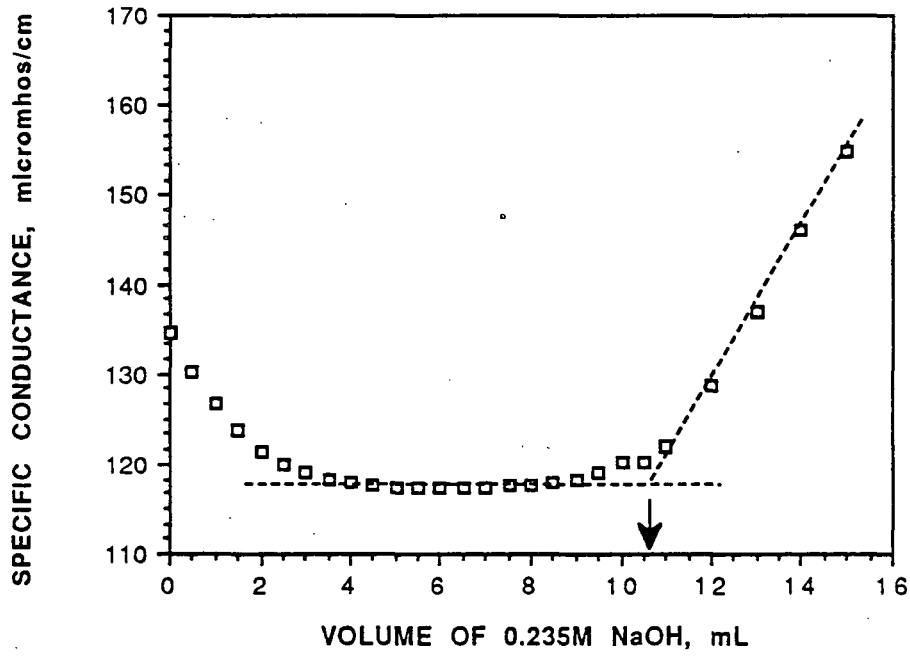

Figure 12. Specific conductance versus volume of NaOH for spruce TMP pulp.

A detailed description of the methylene blue dye adsorption procedure can be found in Appendix II. The procedure was adapted from the method described by Wilson and Mandel.[81] An advantage of the methylene blue dye adsorption technique is that it can be adapted for use on small sample sizes. This allows the weak acid content of long fibers and fiber fines to be measured separately. For this reason, the methylene blue dye adsorption technique was used extensively throughout this work.

A sample of mixed softwood bleached kraft fibers was analyzed for weak acid content using each of the three methods previously described. The results, shown in Table 7, indicate excellent agreement among the three techniques.

Table 7. Weak acid content analysis of bleached softwood kraft fibers.

Method	Fiber Weight (g)	Weak Acid Content (meq/100g)
TAPPI Standard	3.143	3.40
	1.551	3.56
	0.334	3.75
Conductometric Titration	3.172	3.56
	2.733	3.53
	2.756	3.41
Methylene Blue Dye	0.275	3.64
	0.0985	3.05

Scanning Electron Microscopy

Scanning electron photomicrographs were taken of selected long fiber and fiber fines samples to observe the effects of fiber modification processes on the morphology of the fibers and fiber fines. The samples were prepared by solvent exchange of the water with absolute ethanol followed by critical point drying from liquid carbon dioxide.

Electrokinetic Measurements

Prior to measuring the electrophoretic mobility of fines derived from the experimental design pulps, preliminary experiments were performed to determine the concentration and pH of the supporting electrolyte to be used in this work. A background level of ionic strength was provided to eliminate the effect of small variations in ionic strength on the electrophoretic mobility. A simple 1:1 electrolyte (NaCl) was chosen as the background electrolyte.

A study was performed to determine the effect of electrolyte concentration on the electrophoretic mobility of bleached kraft fines. Electrophoretic mobility measurements were made over a wide range of background electrolyte

concentrations ranging from distilled water to 0.01M NaCl. Multiple measurements (three to six) were made on each sample. The average electrophoretic mobility results are summarized in Table 8 and Fig. 13. Increasing the sodium chloride concentration causes the electrical double layer to collapse. The net result is the electrophoretic mobility becomes less negative with increasing electrolyte concentration.

Table 8. Electrophoretic mobility of bleached kraft fines.

Sample	NaCl [M]	Sp. Cond.*	pH	Elec. Mobility (st. dev.)
1.1	none added	2.63	5.31	-2.40 (± 0.18)
2.1	0.0002	26.57	5.24	-1.71 (± 0.02)
3.1	0.001	121.8	5.21	-1.13 (± 0.04)
4.1	0.002	379.4	5.19	-0.74 (± 0.04)
5.1	0.01	1457	5.18	-0.44 (± 0.05)
5.2	0.01	1480	6.16	-0.34 (± 0.03)

*Specific Conductance (μmhos/cm)

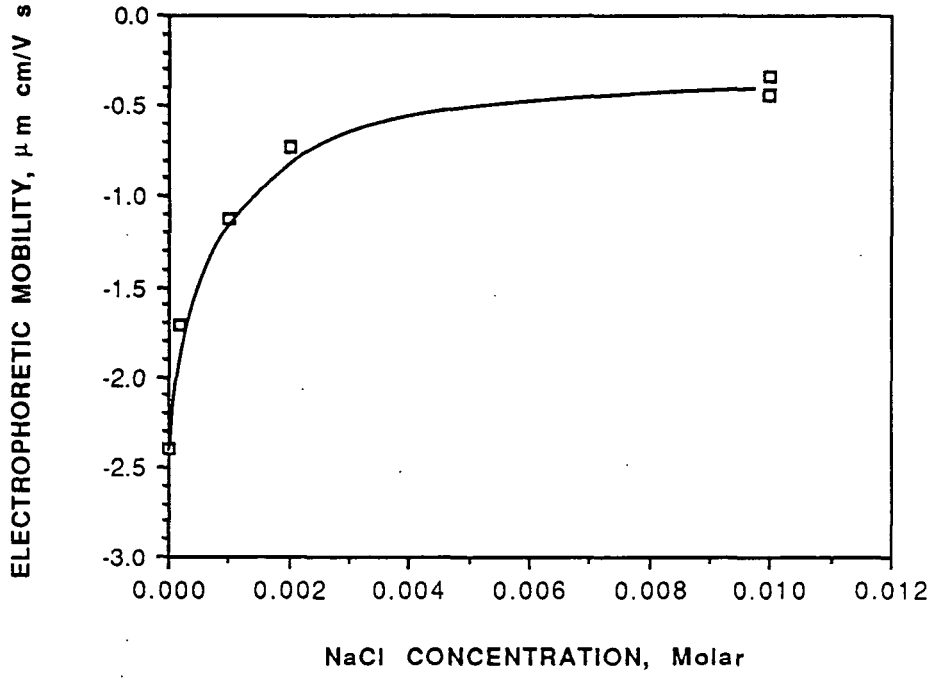

Figure 13. Electrophoretic mobility of bleached kraft fines in sodium chloride solutions.

The plot of electrophoretic mobility versus the logarithm of the sodium chloride concentration is linear, as shown in Fig. 14. Linear relationships between zeta potential and the logarithm of the electrolyte concentration have also been demonstrated for many other systems, including B. coli bacteria (sic) and glass particles in dilute KCl solutions.[82] A theoretical discussion of the linearity of this relationship is presented by Anderson.[83] Three electrolyte concentrations were selected for this work to provide a broad range over which to study the electrokinetic properties. These were 0.0002M, 0.002M, and 0.01M NaCl .

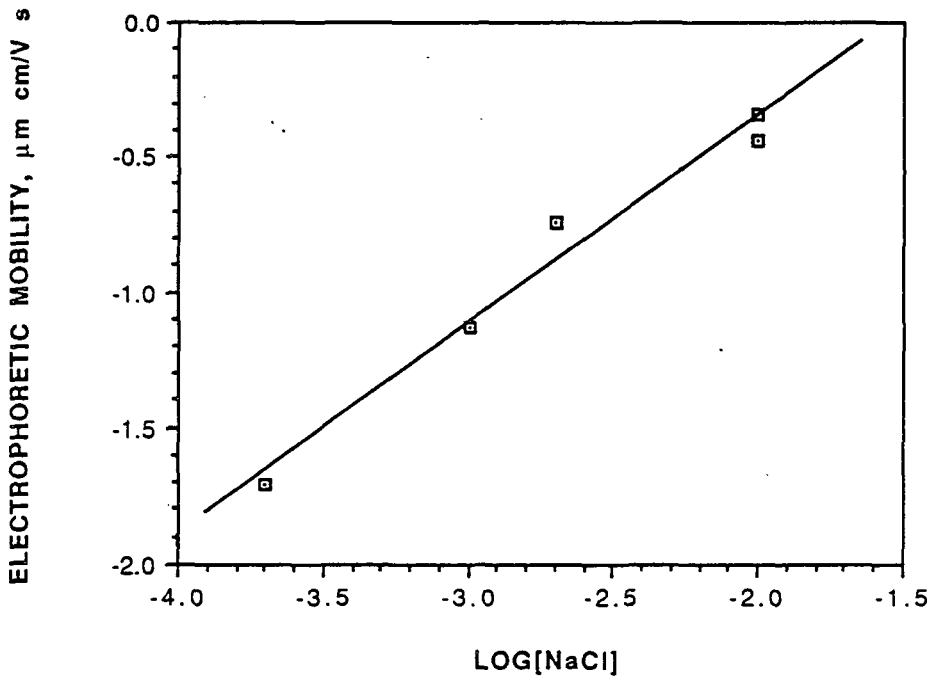

Figure 14. Electrophoretic mobility of bleached kraft fines versus log[NaCl].

A second preliminary study was conducted to determine the effect of the suspending electrolyte's pH on the electrophoretic mobility of unbleached spruce TMP fines. The fines were first dispersed in 0.004M NaCl with an initial pH of 6.66.

The pH was then varied over the range of 2.5 to 9.6 using solutions of 0.10M HCl and 0.07M NaOH. Multiple electrophoretic mobility measurements (three to five) were made at each pH. The average results are presented in Table 9 and Fig. 15.

Table 9. Electrophoretic mobility of unbleached TMP fines in 0.004M NaCl.

Sample	pH	Sp. Cond.	Elec. Mobility (st. dev.)
1	2.53	941.6	-0.32 (± 0.02)
2	3.05	637.8	-0.47 (± 0.01)
3	3.46	522.1	-0.62 (± 0.04)
4	3.72	494.3	-0.66 (± 0.04)
5	4.62	459.5	-0.87 (± 0.04)
6	5.20	450.8	-0.86 (± 0.03)
7	6.43	448.1	-0.91 (± 0.03)
8	6.66	439.2	-0.87 (± 0.05)
9	7.35	458.9	-0.88 (± 0.06)
10	9.62	469.3	-0.91 (± 0.04)

At pH values greater than 4.6 the electrophoretic mobility is essentially independent of solution pH. For pH values smaller than approximately 4.5 (see arrow in Fig. 15), the electrophoretic mobility becomes less negative with decreasing pH. This can be explained in terms of acid group ionization. At high pH values all of the acidic groups would be ionized, thus giving the particle its maximum negative surface charge. Below a certain pH value, however, significant numbers of acidic groups become protonated and the negative charge of the particle is reduced. This results in a less negative electrophoretic mobility. A similar relationship has been reported for polystyrene latex particles with carboxyl functional groups[3].

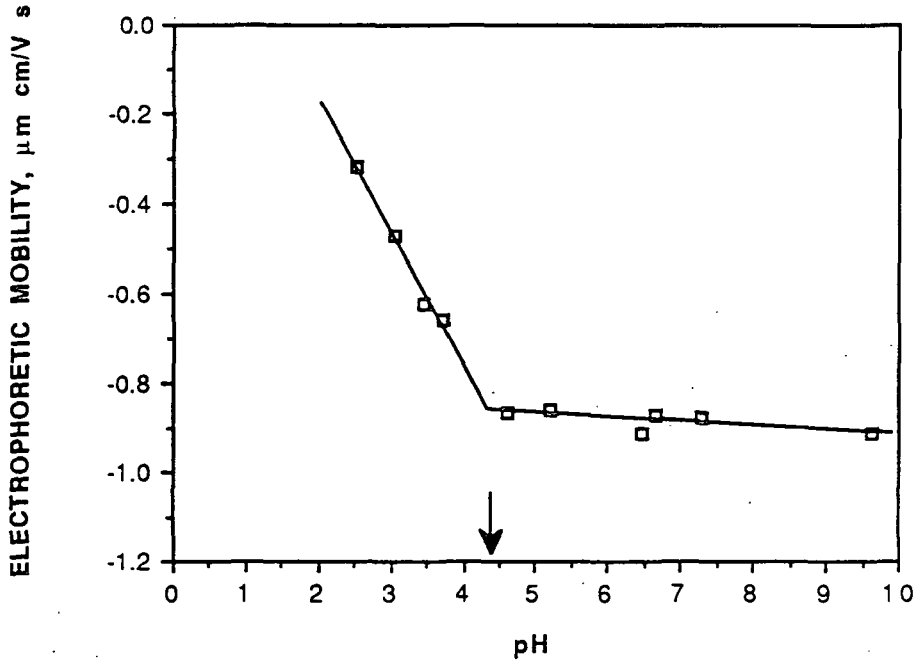

Figure 15. Electrophoretic mobility of TMP fines in 0.004M NaCl versus pH.

For this work a pH of 6.0 was selected because it is relatively easy to control and lies within the region where the electrophoretic mobility is essentially independent of pH.

Prior to measuring the electrophoretic mobility of the fines, the whole pulp (i.e., long fibers and fines) was soaked in 0.10M HCl for 45 minutes (twice) to remove metal ions, and washed thoroughly with distilled water to a constant conductance. Electrophoretic mobility measurements were performed on the fines fraction <400-mesh (38μm diameter circular openings) because preliminary experiments indicated that fines <200-mesh contained particles too large to be accurately measured using the Zetasizer IIc. Fines <400-mesh could be readily measured. Fractionation of fines <400-mesh was facilitated by first dispersing the whole pulp in the appropriate electrolyte and fractionating through a 200-mesh

screen using the Dynamic Drainage Jar (DDJ). The filtrate was then fractionated through a 400-mesh screen using the DDJ to obtain the fines fraction for electrophoretic mobility measurement. The filtrate, containing fines which had passed through a 400-mesh screen, was diluted with the electrolyte solution and the pH adjusted to 6.00 ($\pm$0.05) using dilute HCl or NaOH.

The quartz capillary containing the fines sample during measurement was coated internally with methylcellulose to reduce the electroosmotic velocity profile of the supporting electrolyte. Details of the procedure followed are described in Appendix III.

Ten measurements were performed on every sample, two measurements each on five consecutive loadings of the capillary. The applied voltage was 150V for every measurement. The length of each experiment was 30 seconds, which gave final photon detection counts of between 800,000 and 1,100,000 for the fines concentration used in the study. All of the data were stored to a 5.25 in. flexible disk. The mean electrophoretic mobility and "% width" of the electrophoretic mobility distribution were calculated by the Zetasizer IIc computer program using the following equations.

$$\text{mean E.M.} = \Sigma [(E.M._i)p(E.M._i)]/\Sigma\, p(E.M._i) \qquad [7]$$

$$\%\ \text{width} = (100/\text{mean E.M.})\{\Sigma [(E.M._i)^2\, p(E.M._i) - (\text{mean E.M.})^2]/\Sigma\, p(E.M._i)\}^{0.5} \qquad [8]$$

where: $p(E.M._i)$ = percentage of particles having electrophoretic mobility "i"

The standard deviation of the distribution was calculated by multiplying the "% width" by the mean E.M. and dividing by 100. The standard deviation was used as the measure of the electrophoretic mobility distribution throughout this work.

RESULTS AND DISCUSSION

The RESULTS AND DISCUSSION section will be structured in the following manner. The results of the thermomechanical pulp chemical analyses and electrokinetic measurements will be presented and discussed in the beginning of this section, followed by a presentation and discussion of the results from the kraft pulps. These discussions will be followed by a comparison of the average electrophoretic mobility data and the weak acid content of the fiber fines from both the kraft and TMP pulps. The section will conclude with an analysis of the results in terms of the electrokinetic theory developed by Gouy and Chapman.

THERMOMECHANICAL PULP

Microscopic Analysis

Selected samples of TMP long fibers and fiber fines were examined using a scanning electron microscope. The purpose was to examine the morphology of the fines and to determine where the fines originated (i.e., primary wall/middle lamella or secondary wall). A photomicrograph of the long fiber (>200-mesh) fraction is shown in Fig. 16. An analysis of the long fiber fraction revealed two distinct fiber types: (1) fibers with the primary wall still intact, or beginning to peel away (Fig. 17), and (2) fibers with the primary wall removed and the secondary wall beginning to show severe damage (Fig. 18). The line in Figs. 16 - 18, and in all subsequent photomicrographs, represents the indicated distance in micrometers.

A photomicrograph of the fines (<200-mesh) fraction is shown in Fig. 19. As with the long fiber fraction, two types of fines were observed: (1) flake-like fines originating from middle lamella and primary wall fragments, and (2) ribbon-like

fines derived from the secondary wall. Figure 20 is a more highly magnified photograph showing the flake-like and ribbon-like fines more clearly. Other researchers have reported observing similar types of fines from TMP pulps.[84,85]

The two distinct fractions in both the long fiber and fiber fines would be expected to have very different surface chemistries. The surfaces of fibers with the primary wall still intact, and the flake-like fines originating from the primary wall, would be expected to be lignin-rich. Fibers with secondary wall surfaces and ribbon-like fines would be expected to have relatively carbohydrate-rich surfaces.

Figure 16. Unbleached TMP fibers (>200-mesh): 100x (magnification)

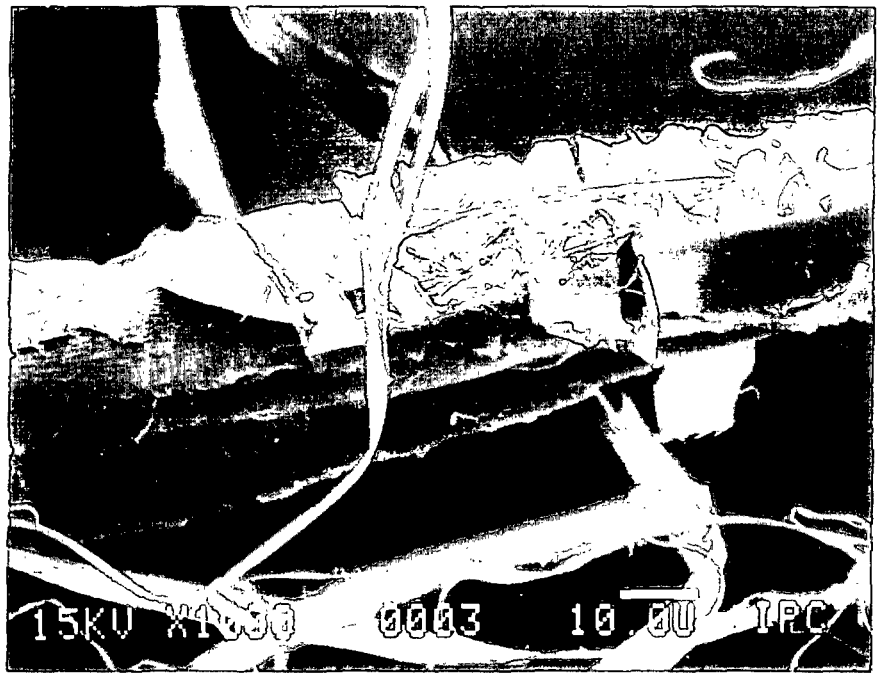

Figure 17. Unbleached TMP fiber showing primary wall removal: 1,000x.

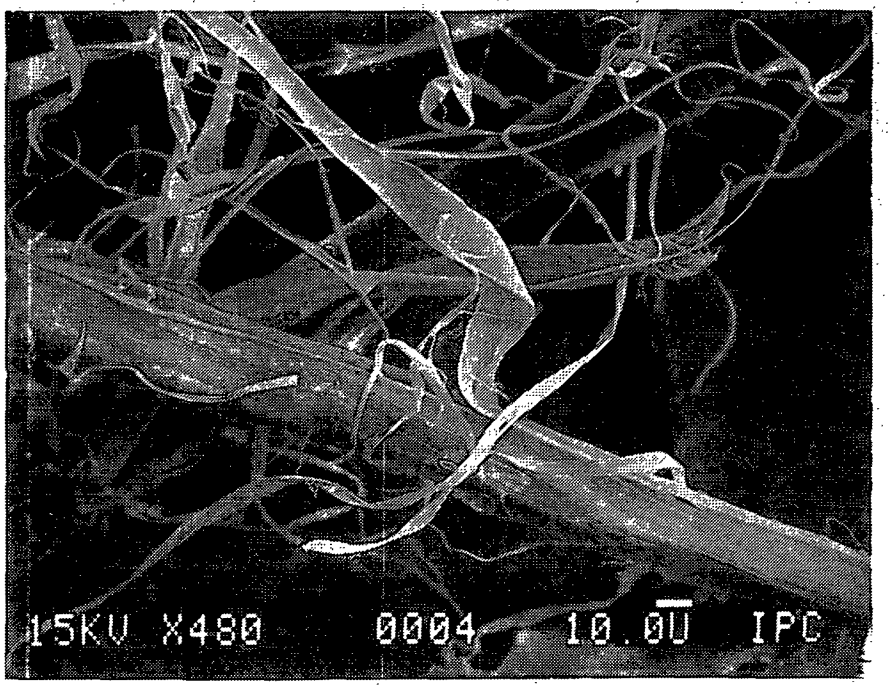

Figure 18. Unbleached TMP fiber showing peeling of the secondary wall: 480x.

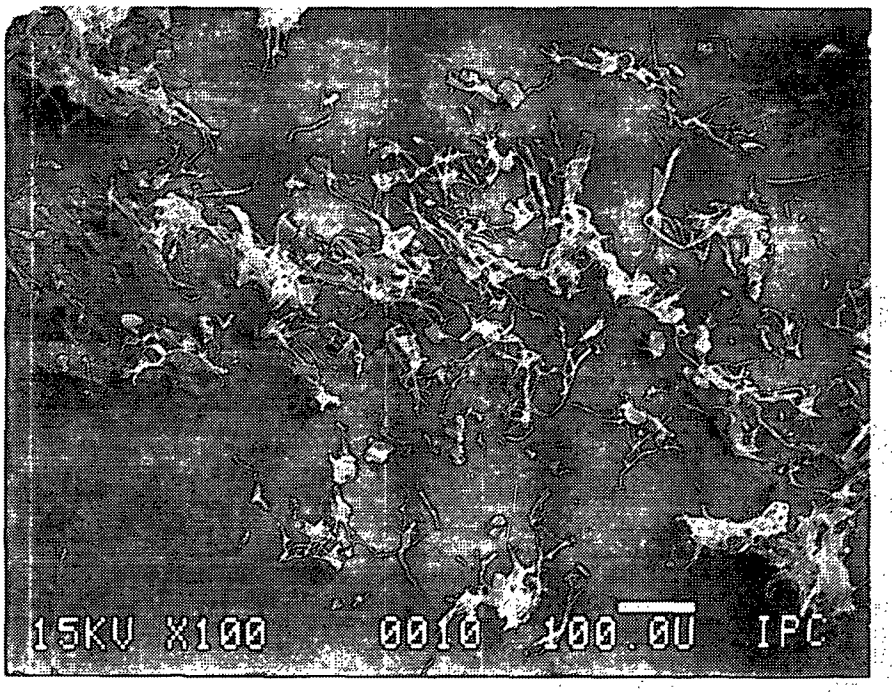

Figure 19. Bleached TMP fines (<200-mesh) showing flake-like and ribbon-like fractions: 100x.

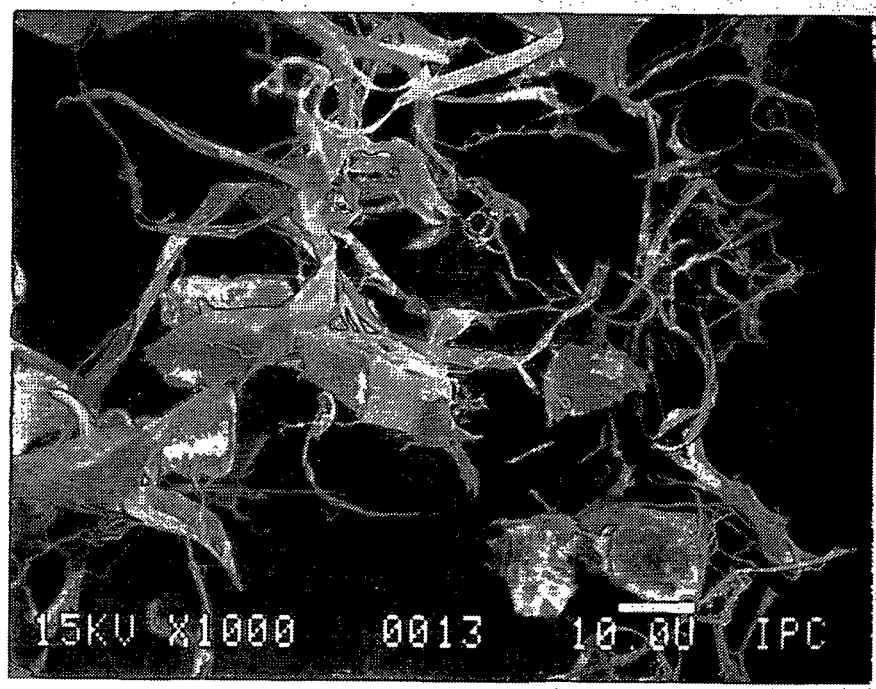

Figure 20. Bleached TMP fines (<400-mesh) showing flake-like and ribbon-like fractions: 1,000x.

Chemical Analysis

Treatment of pulp with alkaline hydrogen peroxide solutions results in the conversion of the conjugated chromophoric groups present in lignin to carboxylic acids and other degradation products.[86,87] The elimination of chromophores produces a whiter (i.e., bleached) pulp with little or no yield loss. Decomposition of hydrogen peroxide to oxygen or hydroxy and hydroperoxy radicals can, however, result in a certain degree of color reversion and lignin degradation.[87] Lignin degradation was prevented by the addition of a stabilizer (magnesium sulfate) in the bleach liquor to minimize hydrogen peroxide decomposition. The pulp

was soaked in 0.2% DTPA (diethylenetriaminepentaacetic acid) prior to bleaching to remove metal ions that can catalyze the decomposition of hydrogen peroxide.

The unbleached and bleached TMP chemical analysis results are presented in Tables 10, 11, and 12. As shown in Table 10, bleaching with 2% hydrogen peroxide resulted in a ten point increase in TAPPI brightness. The hypochlorite numbers indicate that very little delignification occurred during bleaching. The weak acid content of the bleached pulps was more than twice that of the unbleached pulps, indicating the oxidative nature of the treatment. The replicate bleached pulps were very similar with respect to lignin content, brightness, and weak acid content.

Table 10. Results of TMP whole pulp analysis.

Sample	Hypo No.	TAPPI Brightness	Weak Acid Content (meq/100g)
U	28.01	60.40	11.38
B1	26.62	69.86	25.13
B2	27.07	70.35	23.81

An analysis of the carbohydrate composition of spruce TMP is presented in Table 11. Glucose is the predominant sugar found in spruce, since cellulose comprises approximately 40 to 50 percent of the weight of a tree. The other sugars measured in the carbohydrate analysis represent the hemicellulose fraction. With softwoods, hemicelluloses represent 20 to 30 percent by weight of the tree.[88] The two major hemicelluloses present in softwoods are glucomannan, and 4-O-methyl-glucuronoarabinoxylan. Other polysaccharides found in softwoods include arabinogalactan, galactoglucomannan, pectic acid, and starch. It has been shown that

polysaccharides are distributed nonuniformly across the wood fiber wall, and that the distribution varies with wood species.[89,90] Meier[89] studied the distribution of polysaccharides in Norway spruce tracheids and found the middle lamella/primary wall (M+P) fraction had a much higher concentration of galactose and arabinose than the secondary wall. The concentration of glucose and mannose in the M+P fraction was lower than the secondary wall, while the xylose concentrations in the two fractions were approximately equal.

Differences in carbohydrate composition between the spruce TMP long fibers and fiber fines used in this study are shown in Table 11. The results are presented as percentages of oven-dry sample weight. For purposes of comparison, the carbohydrate analysis of white spruce wood (extractive-free basis) is also presented in Table 11.

Table 11. Carbohydrate analysis of TMP long fibers and fines (% o.d. weight).

Sample	Araban (%)	Xylan (%)	Mannan (%)	Galactan (%)	Glucan (%)
U-L. Fiber	1.2	6.2	12.9	2.4	50.8
U-Fines	2.0	6.4	9.2	3.7	34.2
B1-L. Fiber	1.2	6.3	13.2	2.6	56.6
B1-Fines	1.9	6.5	10.2	3.8	37.1
white spruce[68]	1.6	6.8	11.6	1.2	46.5

The results show the fines possess higher araban and galactan contents than the long fibers. The mannan and glucan content of the fines is lower than the fibers. These findings are consistent with those of Meier,[89] and indicate that the fines fraction is enriched with middle lamella (M) and primary wall (P) material. The TMP results compare favorably to the reference wood with respect to carbohydrate content. Differences in galactan content between the TMP samples

used in this work and the white spruce reference may be due to a loss of galactan during extraction of the reference wood.

Bleaching with hydrogen peroxide did not affect the carbohydrate composition of either the fines or the long fiber fractions. These results agree with those published by Willis and Herring[91] for white spruce using solid-state carbon-13 NMR analysis.

Table 12 shows the results of weak acid, Klason lignin content, and ethanol-benzene extractives analyses for TMP long fibers and fiber fines. Published results for white spruce are also presented.

Table 12. Chemical analysis of TMP long fibers and fines.

Sample	W. Acid (meq/100g)	Klason (%)	Extractives* (%)	Fatty and Resin* Acids (%)
U-L. Fiber	8.24	22.8	0.9	0.08
U-Fines	13.88	36.8	3.3	0.17
B1-L. Fiber	17.37	23.1	---	---
B1-Fines	35.88	36.1	---	---
B2-L. Fiber	17.51	---	0.7	0.03
B2-Fines	35.33	---	1.9	0.14
white spruce[92]		27.5	2.1	

* = % of air-dry pulp
"---" = not measured

The TMP fines fraction has a much higher Klason lignin content than the long fibers. As shown in the SEM photomicrographs, the fines fraction is enriched in middle lamella and primary wall fragments. This enrichment is considered to be responsible for the difference in lignin content between fines and long fibers.

The weak acid content of the fines fraction was also found to be considerably higher than that of the long fibers for both the unbleached and bleached samples. The results are summarized in Fig. 21. The difference in weak acid content is believed to result from differences in hemicellulose, lignin, and extractives content between the long fibers and the fines.

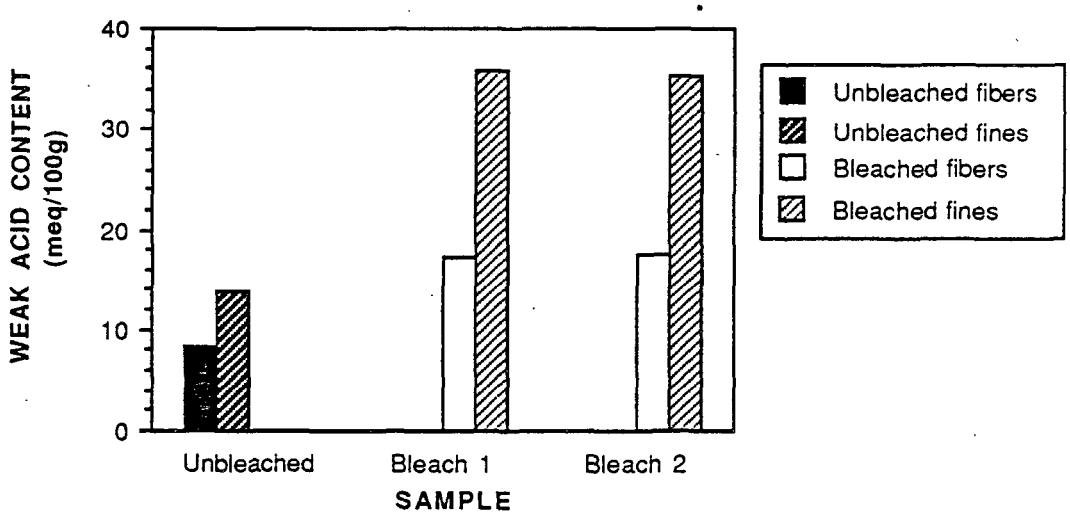

Figure 21. Weak acid content of TMP long fibers (>200-mesh) and fiber fines (<200-mesh).

For the unbleached pulp, it is interesting to note that the ratio of the Klason lignin content between the long fibers and fiber fines (0.620) and the ratio of the weak acid content between the two fractions (0.594) are approximately equal. In a study of black spruce trachieds, Whiting and Goring[93] found both a high lignin and high carboxyl content associated with the middle lamella tissue. The authors also found a linear relationship between percent lignin and carboxyl group content. They speculated that the increased pectic acid content, also associated with the middle lamella fraction,[89,94] is contributing to the high carboxyl content and that the

lignin does not necessarily contain carboxyl groups. Other researchers have reported that kraft lignin does possess base-exchange (i.e., acidic) properties.[95,96] Marton and Adler[97] found evidence of carboxyl groups on pine kraft lignin. On the basis of model studies, they concluded that the carboxyl groups were of an aliphatic rather than an aromatic nature. Values of pK_a between 4 and 5 have been reported for aliphatic carboxyl groups on lignin.[98]

For the bleached pulps, the weak acid content results would be expected to follow the same trend as the lignin since the hydrogen peroxide bleaching treatment selectively oxidizes the conjugated structures present in the lignin molecule. Hemicelluloses, extractives, and acidic groups present on unmodified lignin would also contribute to the overall measured weak acid content of the bleached pulp.

The extractives content of the fines was higher than the long fibers. This is probably due to the presence of ray tracheid and ray parenchyma cells in the fines fraction. These cells are used for conduction and storage of resins and other extractable materials within the tree. Bleaching with hydrogen peroxide reduced the extractives content somewhat. It should be noted that only small samples were available for extractives analysis, particularly in the case of the fines, and therefore the degree of uncertainty associated with the results is assumed to be high.[99]

Electrophoretic Mobility Measurements

A representative electrophoretic mobility distribution of bleached TMP fines is shown in Fig. 22. All of the distributions measured in this study, for both the unbleached and bleached TMP fines, were unimodal. This is in contrast to results of Smith,[37] who observed bimodal zeta potential distributions with TMP fines. One possible explanation for this difference is that Smith obtained his fines

directly from a paper mill furnish, and the samples may have contained non-fibrous particles. Smith found evidence of non-fibrous contamination in some kraft fines samples and attributed these to precipitated pulping liquor not completely removed during washing.[37]

Smith also used the fines fraction passing through a 100-mesh screen (150μm diameter openings) for microelectrophoresis measurement. This is considerably larger than the fines fraction measured in the present study (i.e., fines <400-mesh). As discussed in a previous section, the application of microelectrophoresis to particles greater than approximately 50μm can lead to erroneous results. The experimental error associated with measuring large particle size fines may have contributed to the observed bimodal distributions.

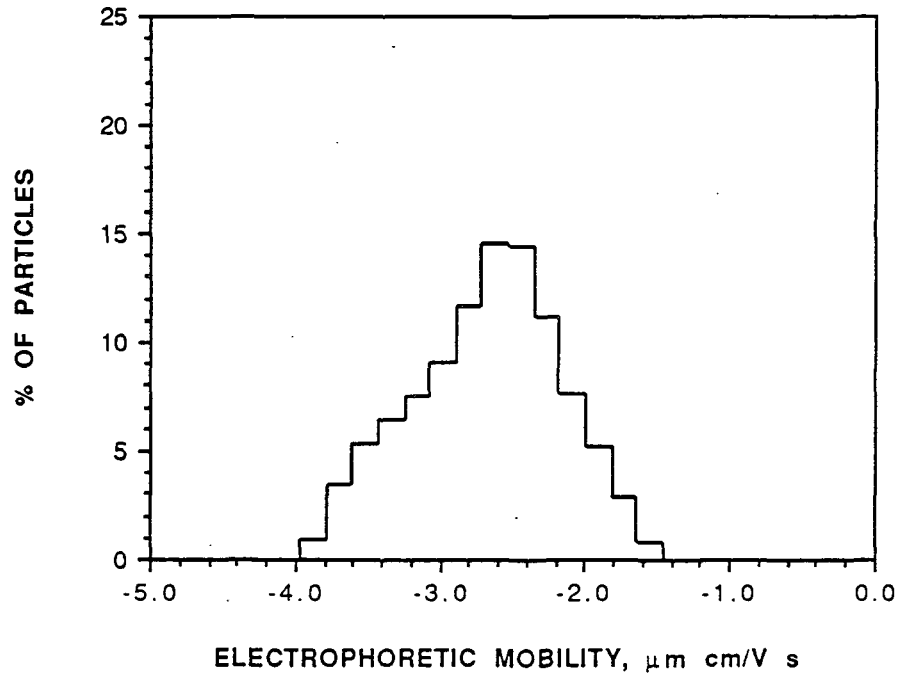

Figure 22. Electrophoretic mobility distribution of bleached TMP fines in 0.0002M NaCl. (average E.M. = -2.67μm cm/V s, distribution st. dev. = 0.507)

The average electrophoretic mobility and distribution standard deviation data for the TMP fines are presented in Table 13. A complete raw data table of electrophoretic mobility results is presented in Appendix IV.

Table 13. Average electrophoretic mobility and distribution results for TMP fines.

	0.0002M NaCl		0.002M NaCl		0.01M NaCl	
Sample	E. Mobility	St. Dev.	E. Mobility	St. Dev.	E. Mobility	St. Dev.
TMP-U	-2.39	0.39	-1.30	0.27	-0.74	0.21
TMP-B1	-2.59	0.43	-1.81	0.27	-1.22	0.22
TMP-B2	-2.52	0.39	-1.84	0.23	-1.18	0.21

The average electrophoretic mobility values for both the unbleached and bleached TMP fines are plotted versus the logarithm of the supporting electrolyte (NaCl) concentration in Fig. 23. The error bars represent one standard deviation on either side of the mean of ten measurements. The lines represent linear regressions of the average electrophoretic mobility data. The results indicate that bleaching with hydrogen peroxide produces fines with a more negative electrophoretic mobility. A statistical analysis of the data is presented in Appendix V.

The average standard deviation of the electrophoretic mobility distribution for each measurement is plotted versus log [NaCl] in Fig. 24. The three data points in each grouping all correspond to the indicated value along the x-axis. The points have been separated for purposes of clarity. With both the unbleached and bleached fines, the distributions becomes narrower with increasing electrolyte concentration, however, there does not appear to be any difference in the distribution standard deviations among the samples. This implies that although the average electrophoretic mobility of TMP fines becomes more negative with bleaching, the shape of the electrophoretic mobility distribution does not change.

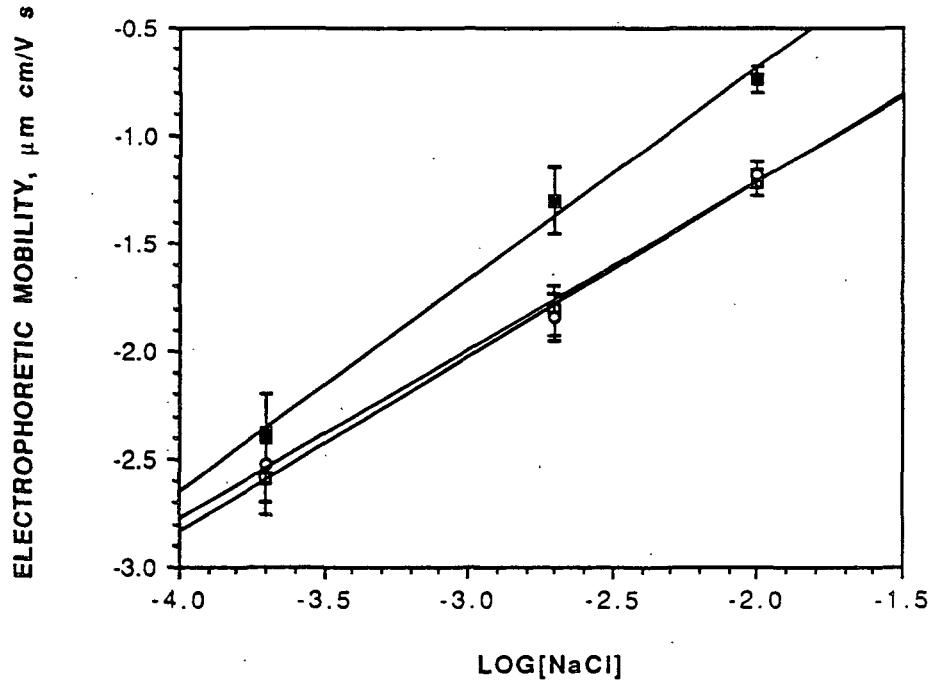

Figure 23. Electrophoretic mobility versus log[NaCl] for TMP fines (■ = unbleached; □ = bleach 1; o= bleach 2).

Linear regression equations for Figure 23:

unbleached:	E.M. = 0.979(log[NaCl]) - 1.265	R^2 = 0.993
bleach 1:	E.M. = 0.805(log[NaCl]) - 0.379	R^2 = 1.000
bleach 2:	E.M. = 0.781(log[NaCl]) - 0.340	R^2 = 0.991

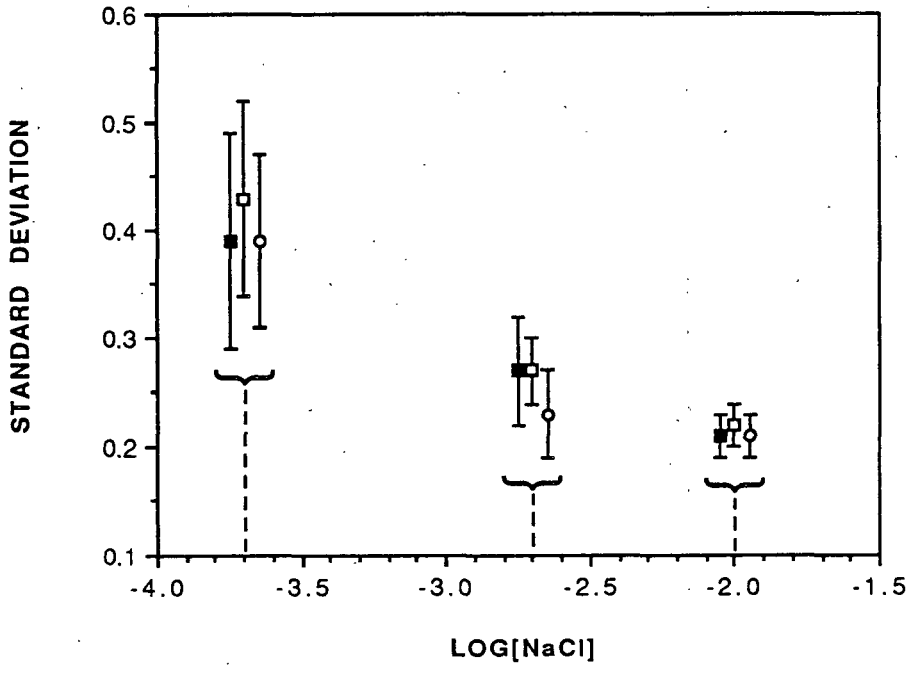

Figure 24. Distribution standard deviation versus log[NaCl] for TMP fines (■ = unbleached; ▫ = bleach 1; o= bleach 2).

KRAFT PULP

Microscopic Analysis

Analysis of the various fractions using the scanning electron microscope revealed that the surface of a substantial percentage of long fibers from the highest yield (Y1) samples had the S1 layer still intact, as evidenced by the high fibril angle with respect to the fiber axis shown in Fig. 25. The fines fraction from the high yield pulp contained many flake-like fines (Fig. 26). Closer examination revealed the flake-like kraft fines to be comprised of a tightly bound network of fibrils.

Figure 25. Bleached kraft fiber (>200-mesh), 54.4% yield, 15,000 revolutions: 1,000x.

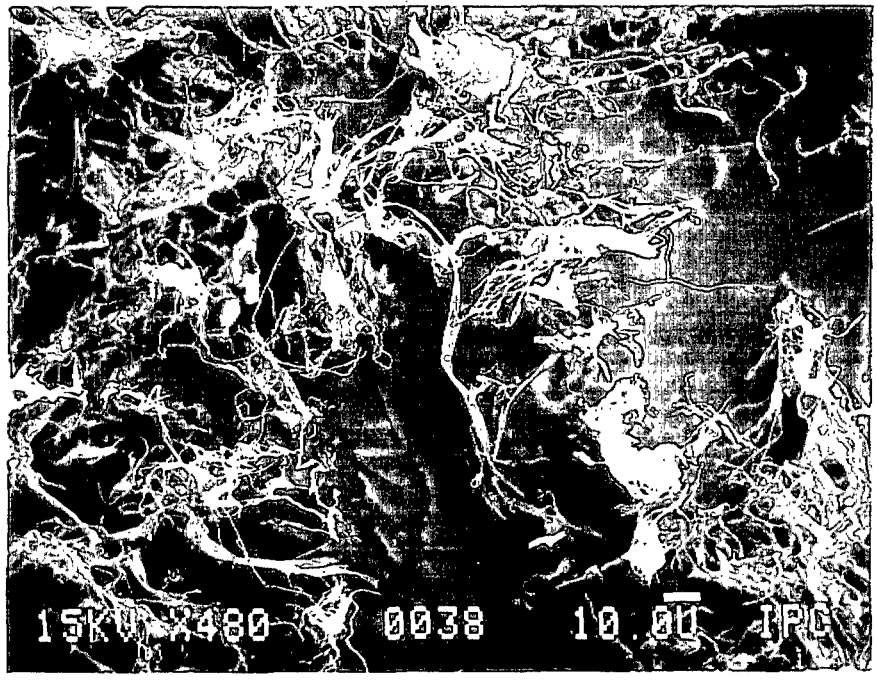

Figure 26. Unbleached kraft fines (<400-mesh), 54.4% yield, 15,000 revolutions: 480x.

The intermediate yield pulp (Y2) also showed evidence of high fibril angle on the surface of some fibers. In contrast, the surfaces of long fibers derived from the lowest yield (Y3) pulp appeared to originate within the S2 layer, based on the angle of the exposed fibrils (Fig. 27). Fines from these pulps were somewhat more fibrillar in nature, as shown in Fig. 28.

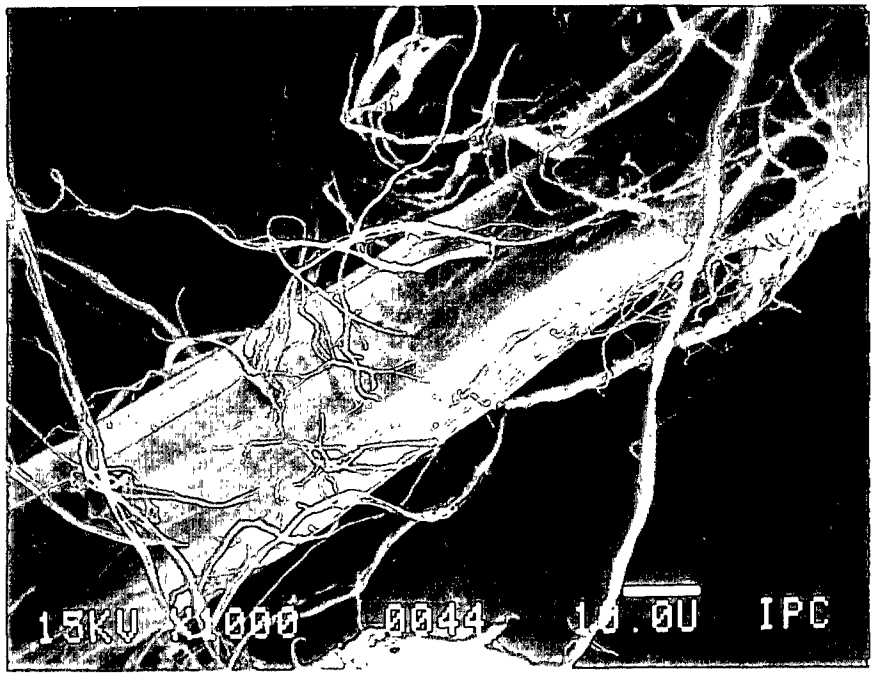

Figure 27. Unbleached kraft fiber (>200-mesh), 44.7% yield, 15,000 revolutions: 1,000x.

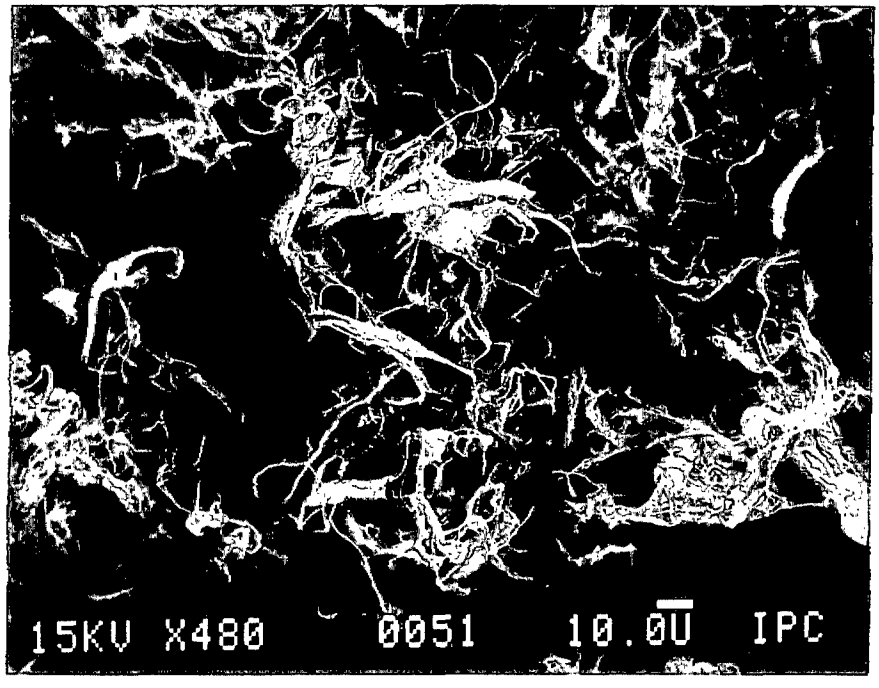

Figure 28. Bleached kraft fines (<200-mesh), 44.7% yield, 15,000 revolutions: 480x.

Chemical Analysis

The unrefined kraft pulp chemical analysis results are presented in Table 14. The results indicate a wide range of lignin contents within the unbleached pulps. Bleaching the pulp using a CEDED sequence resulted in a considerable decrease in the weak acid content. The weak acid content decreased with decreasing yield for both the unbleached (U_i) and bleached (B_i) samples.

Table 14. Unrefined kraft pulp analysis.

Sample	Hypo. No.	Kappa No.	TAPPI Brightness	Weak Acid Content (meq/100g)
U1	10.50	72.58	25.76	13.92
B1	---	---	89.41	4.72
U2	5.41	36.06	30.78	9.13
B2	---	---	86.60	3.95
U3	2.67	17.78	35.20	5.41
B3	---	---	87.35	3.11

Selected kraft pulp samples were analyzed for carbohydrate composition to detect changes resulting from decreasing pulp yield and bleaching. The results are shown in Table 15. Decreasing the pulp yield decreased the araban, mannan, and galactan content of the pulps. The xylan component was more resistant to removal during pulping than the other sugars. The galactan content was reduced by bleaching in the high yield pulp, and was the only carbohydrate significantly affected by this operation.

Table 15. Carbohydrate analysis of kraft long fiber and fiber fines (% o.d. weight).

Sample	Yield* (%)	Araban (%)	Xylan (%)	Mannan (%)	Galactan (%)	Glucan (%)
U12-L. Fiber	54.35	0.7	6.6	7.2	0.8	75.1
U12-Fines	54.35	0.7	5.5	7.2	1.1	67.3
U32-L. Fiber	44.71	0.5	7.8	6.6	0.5	78.6
U32-Fines	44.71	0.4	7.1	6.9	0.4	80.1
B12-L. Fiber	54.35	0.7	7.4	7.3	0.4	81.7
B12-Fines	54.35	0.6	7.4	8.3	0.7	80.8
B32-L. Fiber	44.71	0.6	8.2	7.1	0.5	84.0
B32-Fines	44.71	0.6	7.8	7.5	0.5	87.2

* = unbleached, unscreened yield

The results of kraft pulp lignin content analyses are presented in Table 16. Diffuse reflectance FTIR spectrometry was used to determine the lignin content of long fibers and fiber fines from selected samples. Equations relating the "lignin" spectrum peak area at 1510 cm^{-1} to kappa number and hypo number were obtained from the unrefined kraft pulp data. The equation relating the 1510 cm^{-1} peak area to the Klason lignin content was provided by the analytical department of IPC.[100] These equations are shown below:

kappa number:	kappa = 11.47(area) - 6.93	R^2 = 0.998
hypo. number:	hypo. = 1.63(area) - 0.788	R^2 = 0.997
%Klason lignin:	Klason = 2.16(area) - 2.25	R^2 = 0.943

Table 16. Lignin content analysis of kraft long fibers and fiber fines.

	1510 cm^{-1}	Kappa No.		Hypo. No.		Klason Lignin (%)	
Sample	Peak Area	Meas.	Calc.	Meas.	Calc.	Meas.	Calc.
U1	6.96	72.58	72.90	10.50	10.56	---	12.78
U2	3.64	36.06	34.82	5.41	5.15	---	5.61
U3	2.23	17.78	18.65	2.67	2.85	---	2.57
U12-L. Fiber	5.36	---	54.55	---	7.95	8.7	9.33
U12-Fines	8.23	---	87.47	---	12.63	---	15.53
U22-L. Fiber	4.75	---	47.55	---	6.95	---	8.01
U22-Fines	4.97	---	50.08	---	7.31	---	8.49
U32-L. Fiber	2.66	---	23.58	---	3.55	2.3	3.50
U32-Fines	2.58	---	22.66	---	3.42	---	3.32

The calculated lignin content of the fines was considerably higher than the long fiber for the high yield (U1) kraft pulp. This indicates a possible enrichment of lignin-rich primary wall material in the fines fraction. Long fibers and fiber fines from both the intermediate yield (U2) and low yield (U3) pulps were similar with respect to lignin content.

These results are supported by the findings of Proctor and coworkers.[101] Proctor used an ultraviolet light microscope to study the effect of kraft pulp yield on the distribution of lignin across the double cell wall of adjacent fibers in black spruce chips. In the native wood, the lignin concentration in the middle lamella was much higher than the secondary wall. During kraft pulping, the lignin concentration in the middle lamella and secondary wall decreased at approximately the same rate up to 50% delignification, after which a more rapid removal of lignin occurred in the middle lamella. After approximately 70% lignin removal, the lignin concentration was higher in the secondary wall than in the middle lamella. The

authors found no evidence of a lignin concentration gradient across the secondary wall of individual fibers. In the present work, the Klason lignin content of the unbleached TMP (27.42%) was assumed to equal the lignin content of the original wood. The percentage of lignin removed in the U1, U2, and U3 pulps was calculated to be 53.39%, 79.54%, and 90.63%, respectively. Because the fines originate from the outer surface of fibers, fines from pulps with less than 70% lignin removal (i.e., U1) would be expected to have higher lignin contents than the respective long fibers. Fines from pulps with greater than 70% lignin removal (i.e., U2 and U3) would have similar or lower lignin contents than the long fibers. Therefore, the results of the present study are consistent with those expected on the basis of Proctor's data.

The weak acid content analysis results for the kraft long fibers and fiber fines are summarized in Table 17 and in Figures 29 and 30. For the high yield samples (U11 and U12), the fines fraction had a slightly higher weak acid content than the long fibers. For the intermediate and low yield pulp samples, the weak acid content of the fines was lower than the long fibers. Duplicate measurements were performed on samples U22-fines, U31-fibers, and U31-fines, as shown in Table 17. The results indicate differences of more than approximately 0.5meq/100g are probably significant. The observed differences in weak acid content between the fibers and fines are most likely due to differences in lignin and hemicellulose content In general, pulps refined at the high level (15,000 revolutions) had essentially the same weak acid content as pulps refined at the low level, and any observed differences are probably not significant.

Table 17. Weak acid content analysis of kraft long fiber and fiber fines.

Sample	Weak acid content (meq/100g)	Sample	Weak acid content (meq/100g)
U11-Fiber	13.10	B11-Fiber	4.50
U11-Fines	13.83	B11-Fines	2.78
U12-Fiber	13.60	B12-Fibers	4.46
U12-Fines	13.61	B12-Fines	2.26
U21-Fiber	9.48	B21-Fibers	3.56
U21-Fines	8.95	B21-Fines	2.64
U22-Fiber	9.45	B22-Fibers	3.31
U22-Fines	7.37, 6.97	B22-Fines	2.33
U31-Fiber	5.63, 5.43	B31-Fibers	2.80
U31-Fines	3.47, 3.54	B31-Fines	2.14
U32-Fiber	5.58	B32-Fibers	2.88
U32-Fines	3.17	B32-Fines	2.10

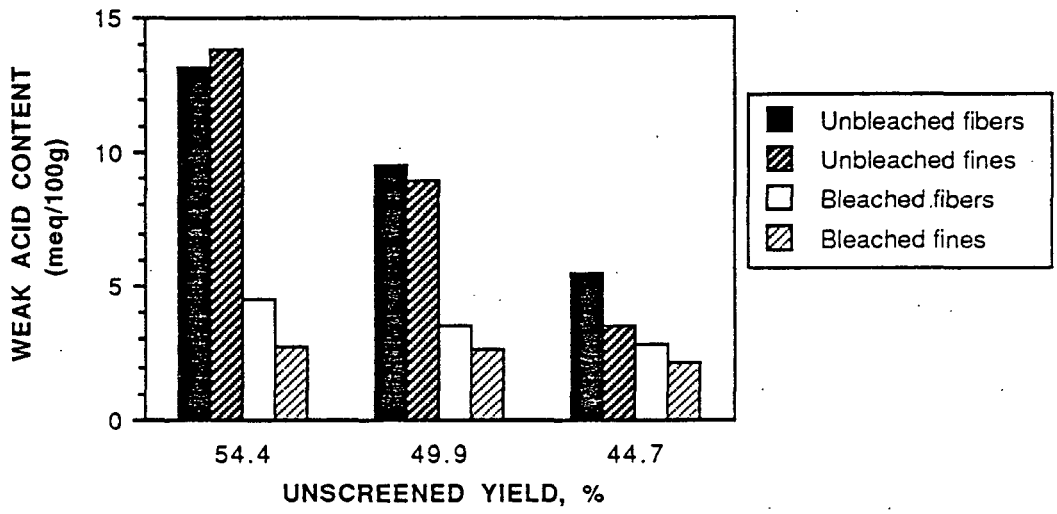

Figure 29. Weak acid content of kraft long fibers (>200-mesh) and fiber fines (<200-mesh): 7,500 revolutions

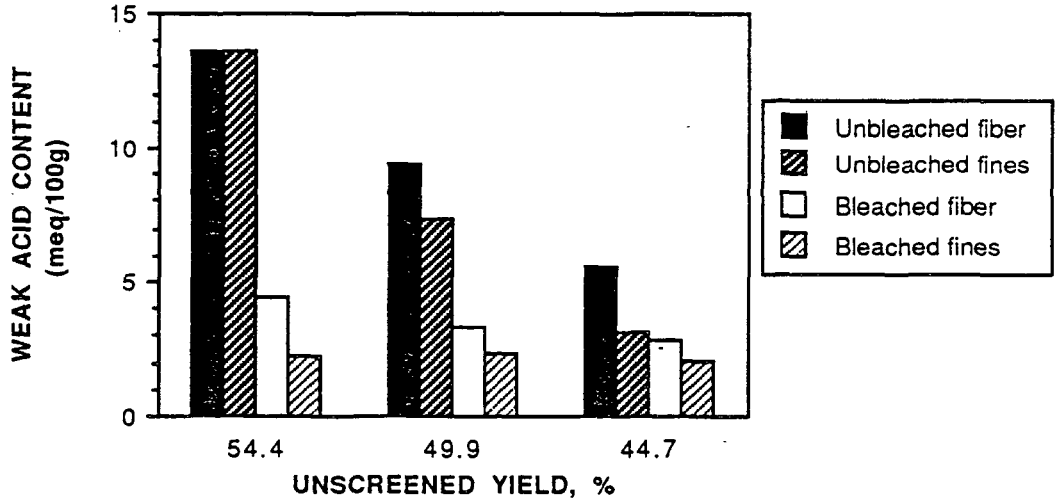

Figure 30. Weak acid content of kraft long fibers (>200-mesh) and fiber fines (<200-mesh): 15,000 revolutions

Electrophoretic Mobility Measurements

A representative electrophoretic mobility distribution of unbleached kraft fines is shown in Fig. 31. All of the distributions measured in this study, for both the unbleached and bleached kraft fines, were unimodal. The electrophoretic mobility distributions of kraft fines were generally narrower than those of TMP fines in the same electrolyte concentration.

The average electrophoretic mobility and distribution standard deviation data for kraft fines are presented in Table 18. These data will be referred to in subsequent discussions of the effect of pulp yield, bleaching, and refining on the electrokinetic properties. A complete raw data table of electrophoretic mobility results appears in Appendix VI. A statistical analysis of the kraft electrophoretic mobility data is presented in Appendix VII.

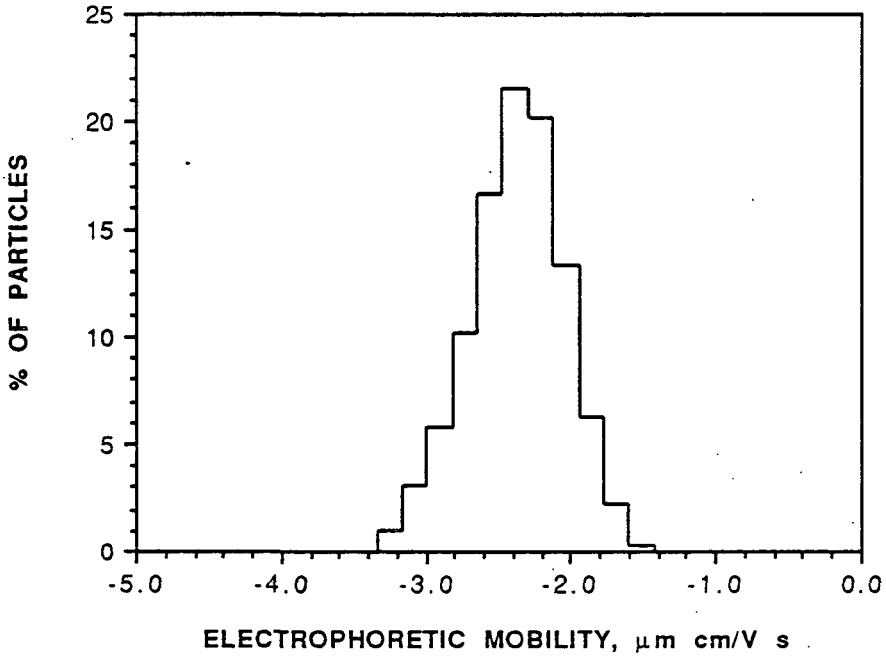

Figure 31. Electrophoretic mobility distribution of unbleached kraft fines in 0.0002M NaCl (average E.M. = -2.36μm cm/V s), distribution st. dev. = 0.314).

Table 18. Average electrophoretic mobility and distribution results for kraft fines.

	0.0002M NaCl		0.002M NaCl		0.01M NaCl	
Sample	E. Mobility	St. Dev.	E. Mobility	St. Dev.	E. Mobility	St. Dev.
U11	-2.40	0.32	-1.68	0.22	-1.12	0.18
U12	-2.38	0.30	-1.68	0.23	-1.13	0.20
U21	-2.29	0.31	-1.54	0.23	-0.99	0.18
U22	-2.39	0.33	-1.59	0.23	-1.05	0.20
U31	-2.16	0.34	-1.34	0.23	-0.80	0.19
U32	-2.14	0.33	-1.45	0.25	-0.79	0.19
B11	-2.19	0.28	-1.39	0.23	-0.82	0.18
B12	-2.19	0.29	-1.41	0.21	-0.84	0.18
B21	-2.10	0.36	-1.31	0.25	-0.64	0.18
B22	-2.11	0.30	-1.35	0.22	-0.73	0.17
B31	-1.95	0.32	-1.19	0.23	-0.64	0.18
B32	-2.01	0.29	-1.23	0.23	-0.71	0.18

The average electrophoretic mobility of unbleached kraft fines from pulps refined at the low level (7,500 revolutions) is plotted in Fig. 32 versus the logarithm of the molar NaCl concentration. The lines represent a linear regression of the data, while the error bars depict one standard deviation on either side of the mean of ten measurements. For the spruce kraft pulps, decreasing pulp yield resulted in fines with a less negative electrophoretic mobility. A similar trend was observed with fines from the pulps refined at the high level (15,000 revolutions), as shown in Fig. 33.

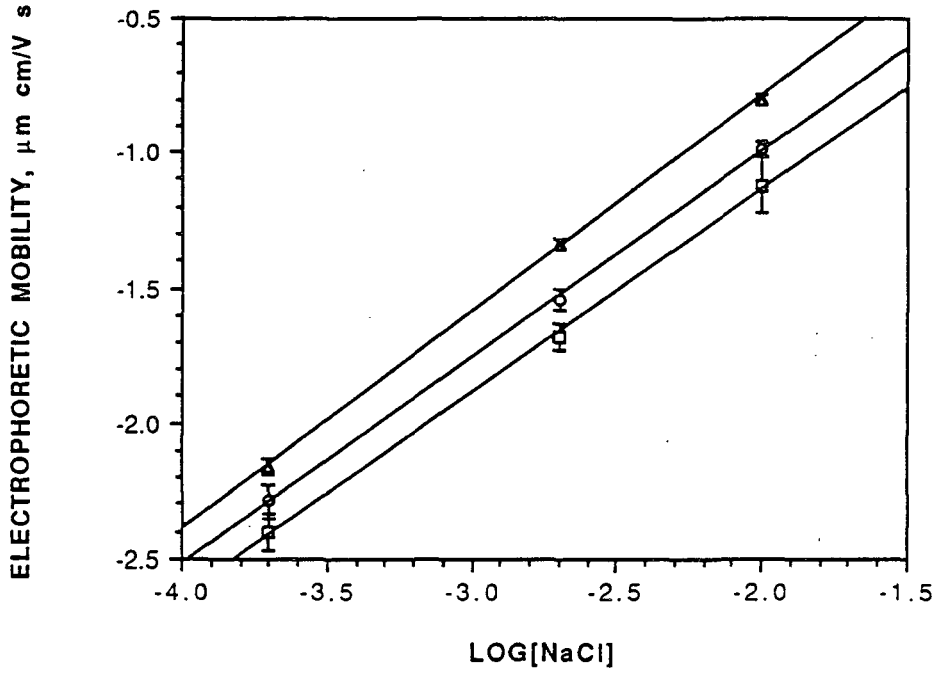

Figure 32. Electrophoretic mobility versus log[NaCl] for unbleached kraft fines: 7,500 revolutions (△ = 44.71% yield; ○ = 49.9% yield; □ = 54.4% yield).

Linear regression equations for Figure 32:

44.71% yield:	E.M. = 0.802(log[NaCl]) + 0.811	R^2 = 1.000
49.92% yield:	E.M. = 0.764(log[NaCl]) + 0.532	R^2 = 1.000
54.35% yield:	E.M. = 0.751(log[NaCl]) + 0.369	R^2 = 0.999

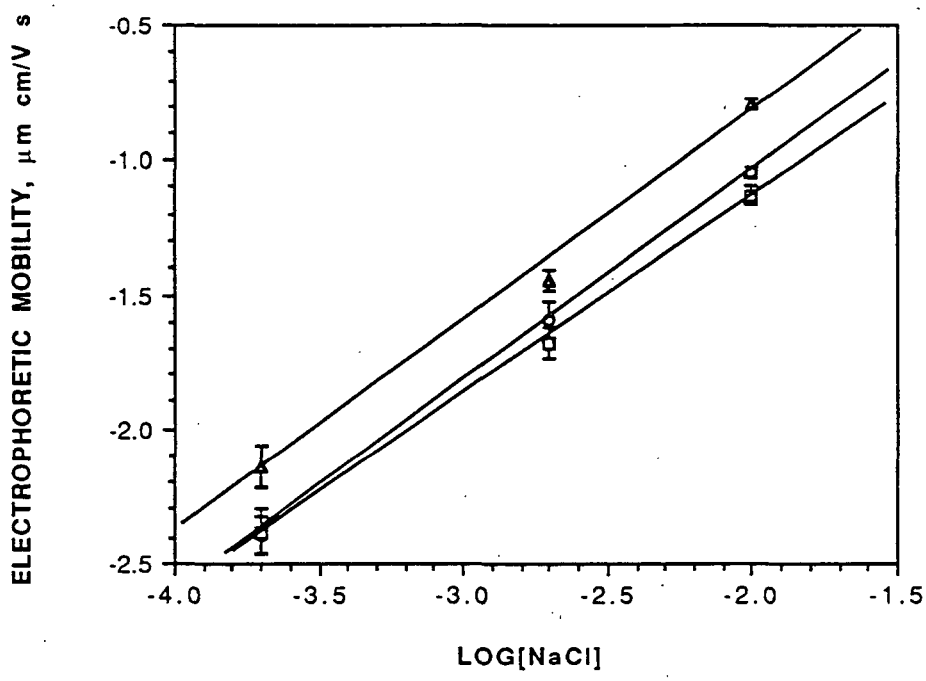

Figure 33. Electrophoretic mobility versus log[NaCl] for unbleached kraft fines: 15,000 revolutions (△ = 44.71% yield; ○ = 49.9% yield; □ = 54.4% yield).

Linear regression equations for Figure 33:

44.71% yield:	E.M. = 0.787(log[NaCl]) + 0.744	R^2 = 0.992
49.92% yield:	E.M. = 0.789(log[NaCl]) + 0.533	R^2 = 1.000
54.35% yield:	E.M. = 0.733(log[NaCl]) + 0.323	R^2 = 0.999

Once the pulps have been bleached the effect of yield on the average electrophoretic mobility becomes slightly less pronounced, as shown in Figs. 34 and 35. Nevertheless, the trend of decreasing pulp yield resulting in a less negative electrophoretic mobility is the same as the unbleached data.

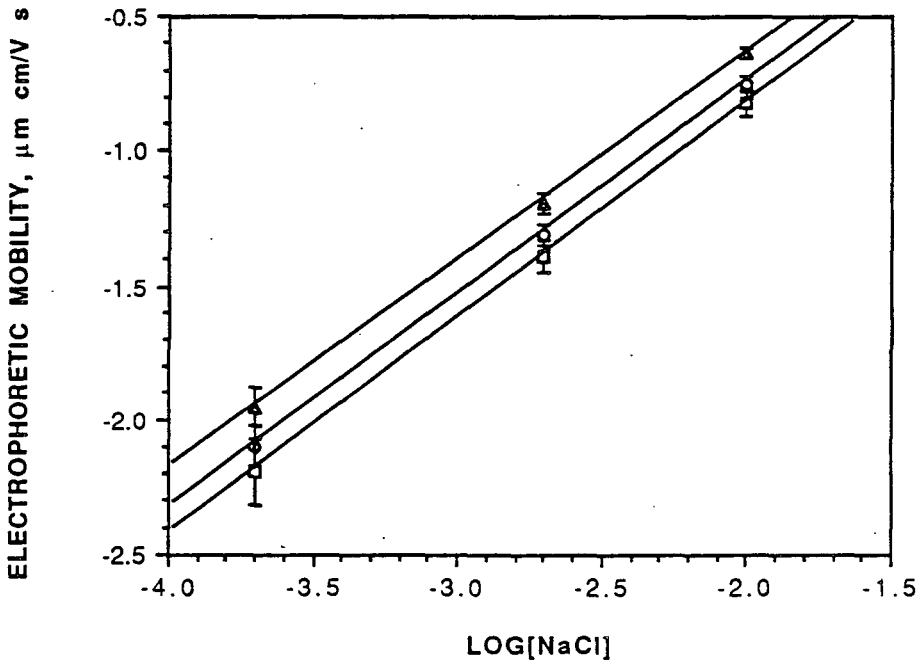

Figure 34. Electrophoretic mobility versus log[NaCl] for bleached kraft fines: 7,500 revolutions (△ = 44.71% yield; ○ = 49.9% yield; □ = 54.4% yield).

Linear regression equations for Figure 34:

44.71% yield:	E.M. = 0.770(log[NaCl]) + 0.896	R^2 = 1.000
49.92% yield:	E.M. = 0.794(log[NaCl]) + 0.837	R^2 = 1.000
54.35% yield:	E.M. = 0.806(log[NaCl]) + 0.789	R^2 = 1.000

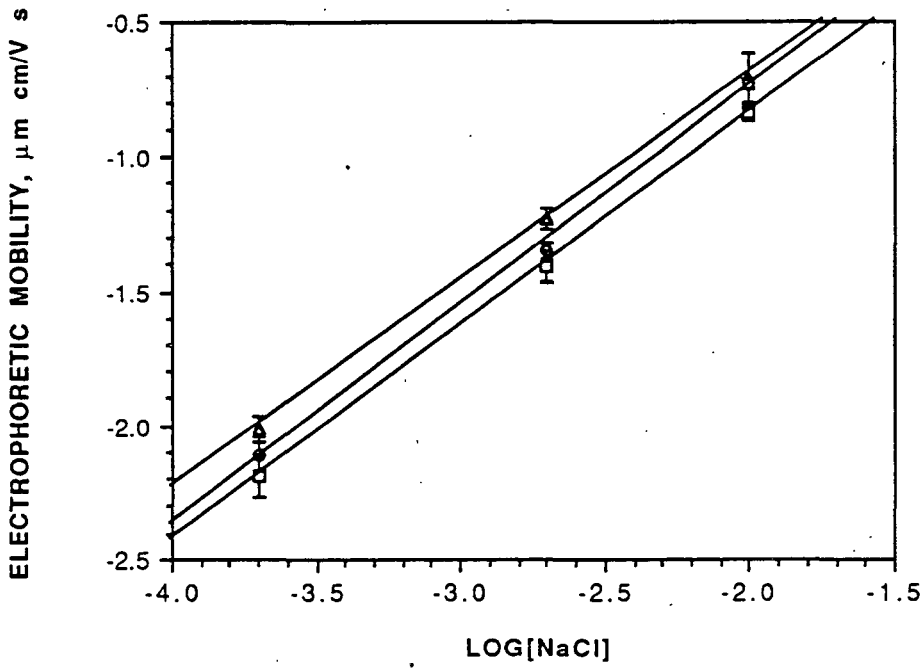

Figure 35. Electrophoretic mobility versus log[NaCl] for bleached kraft fines: 15,000 revolutions (Δ = 44.71% yield; o = 49.9% yield; □ = 54.4% yield).

Linear regression equations for Figure 35:

44.71% yield:	E.M. = 0.766(log[NaCl]) + 0.828	R^2 = 1.000
49.92% yield:	E.M. = 0.809(log[NaCl]) + 0.867	R^2 = 0.998
54.35% yield:	E.M. = 0.794(log[NaCl]) + 0.742	R^2 = 1.000

The distribution standard deviation results for kraft fines are plotted in Figures 36 - 39 versus the logarithm of the NaCl concentration. The data points in each grouping have been separated for clarification. Each point corresponds to the indicated value along the x-axis.

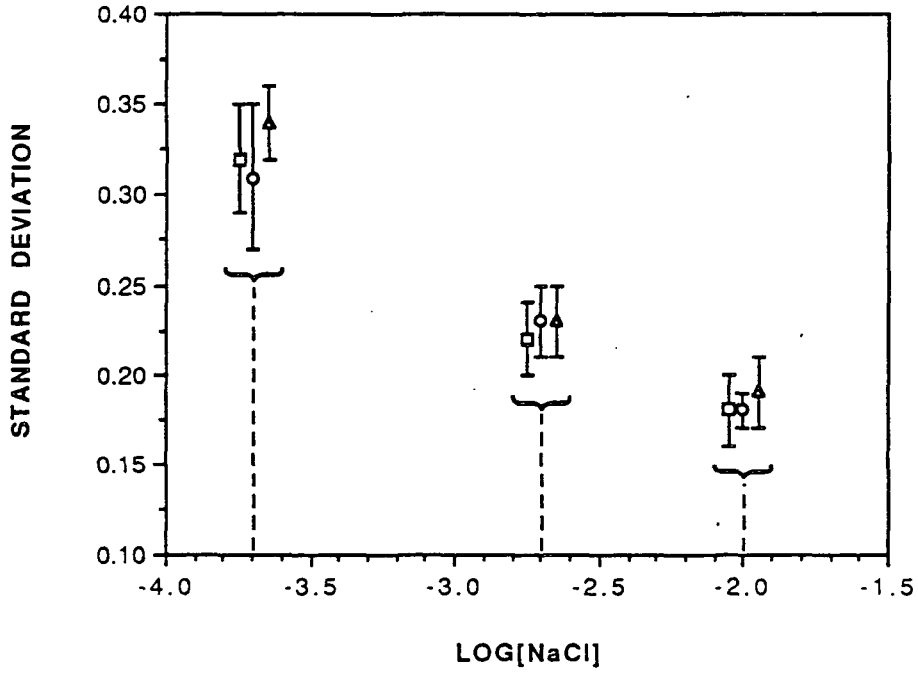

Figure 36. Unbleached kraft fines: 7,500 rev. (△ = 44.71%; ○ = 49.9%; □ = 54.4% yield).

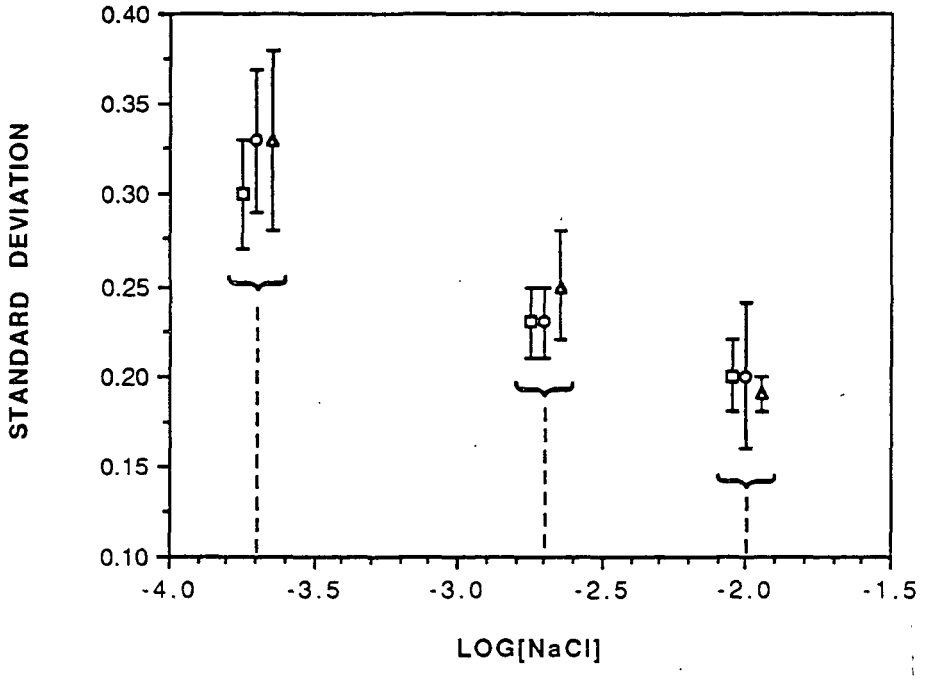

Figure 37. Unbleached kraft fines: 15,000 rev. (△ = 44.71%; ○ = 49.9%; □ = 54.4% yield).

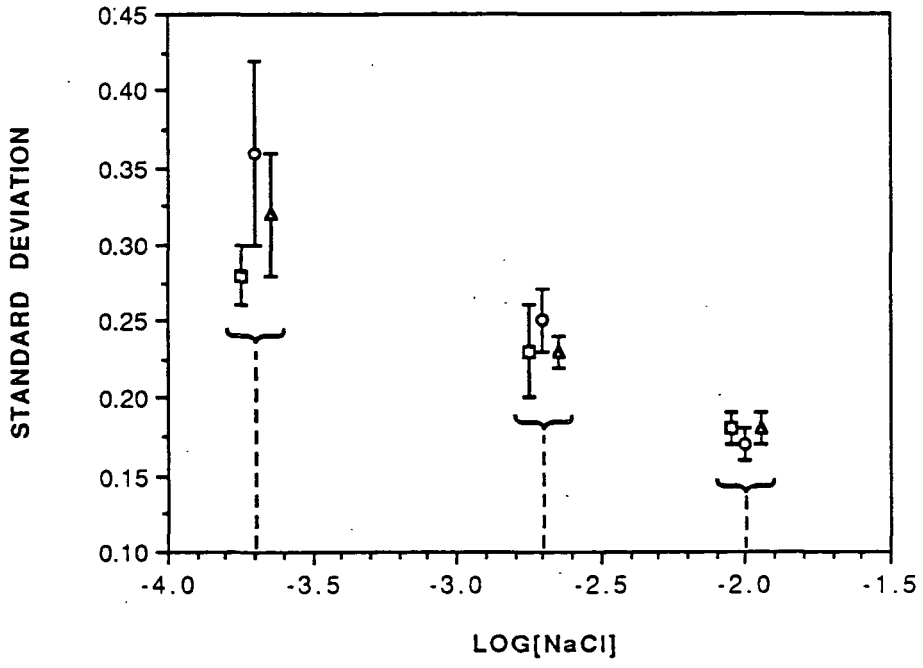

Figure 38. Bleached kraft fines: 7,500 rev. (△ = 44.71%; ○ = 49.9%; □ = 54.4% yield).

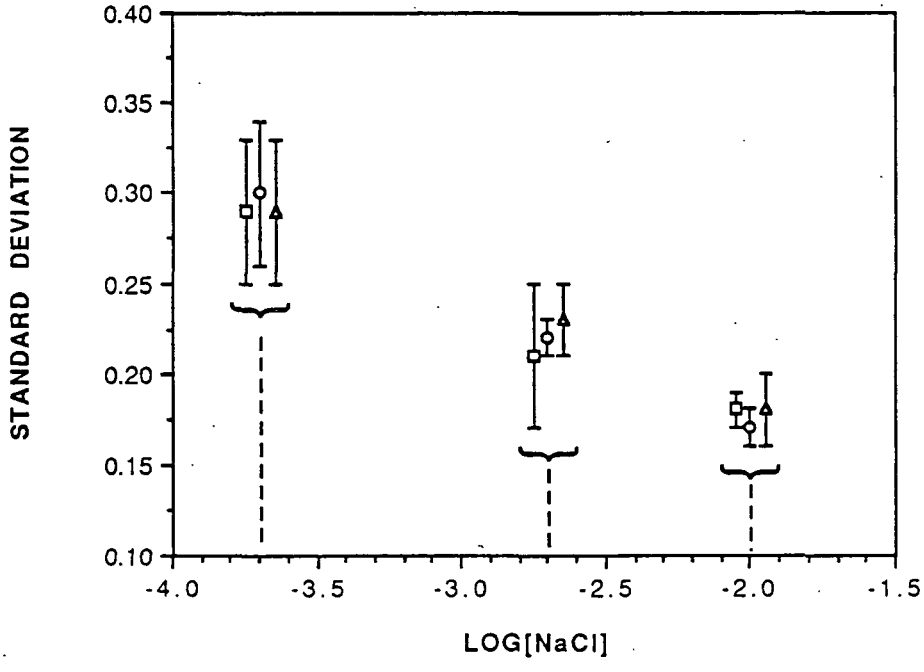

Figure 39. Bleached kraft fines: 15,000 rev. (△ = 44.71%; ○ = 49.9%; □ = 54.4% yield).

All of the electrophoretic mobility distributions were unimodal, and resembled a Gaussian distribution. The standard deviations of the distributions for kraft pulp fines were not significantly affected by changes in pulp yield. Bleaching the pulp did not have a large effect on the standard deviations of the distributions, but may have reduced them somewhat.

The standard deviations of the electrophoretic mobility distributions decreased with increasing electrolyte concentration, as shown in Figs 36 - 39. One possible explanation for this decrease is the collapse of the electric double layer with increasing electrolyte concentration. The decrease in double layer thickness reduces both the magnitude of the zeta potential and the difference in zeta potential between particles with different surface potentials. Therefore, the distribution of potentials within a system of particles, measured some distance from the surface (i.e., at the shear plane), would become smaller with increasing electrolyte concentration.

Using Equation 4, (p. 7) the electric potential decay across the double layer was calculated for particles with surface potentials of -20mV and -50mV in aqueous (1:1) electrolyte solutions of 0.0002M, 0.002M, and 0.01M. The results, presented in Figs. 40 - 42, show that the difference in electric potential between particles with different surface potentials decreases with distance from the surface. The effect is more pronounced at high electrolyte concentrations and at greater distances from the surface.

The electrophoretic mobility is an indirect measurement of the potential (ζ) at some distance from the surface corresponding to the shear plane, or surface of shear. The theoretical minimum shear-plane distance is approximately one hydrated counterion radius[3] (i.e., the location of the Stern plane). For the electrolyte used in this study, aqueous NaCl, the Stern plane would be approximately

0.2562nm[102] from the surface (the radius of a hydrated sodium ion). As previously discussed, the exact location of the shear plane is unknown. In addition to counterions in the Stern layer, the surface will probably contain bound solvent molecules. It is reasonable,therefore, to assume that the shear plane is located further out from the surface than the Stern plane.[5] Surface roughness effects (such as would be expected for refined wood pulp) can also have an effect on the exact position of the shear surface.[3]

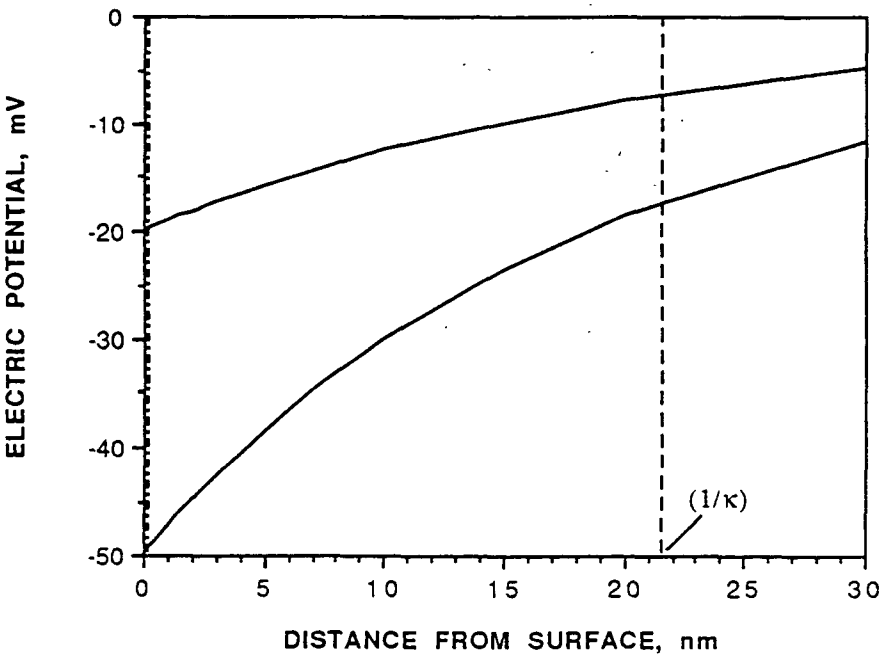

Figure 40. Electric potential as a function of distance from surface in 0.0002M NaCl, calculated from Gouy-Chapman theory assuming surface potentials of -20mV and -50mV. ("·····" = radius of hydrated sodium ion)

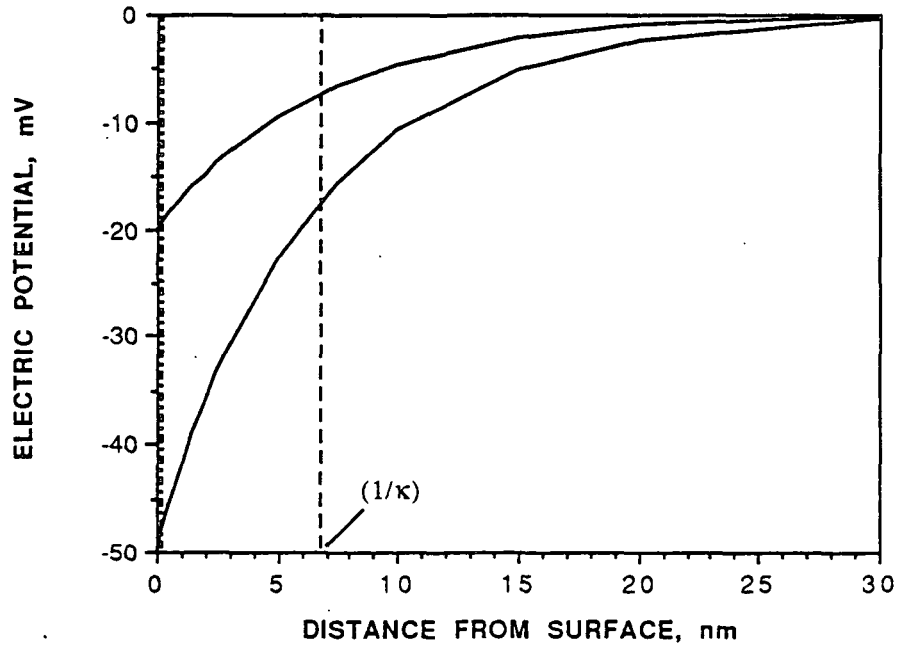

Figure 41. Electric potential as a function of distance from surface in 0.002M NaCl, calculated from Gouy-Chapman theory assuming surface potentials of -20mV and -50mV. ("·····" = radius of hydrated sodium ion)

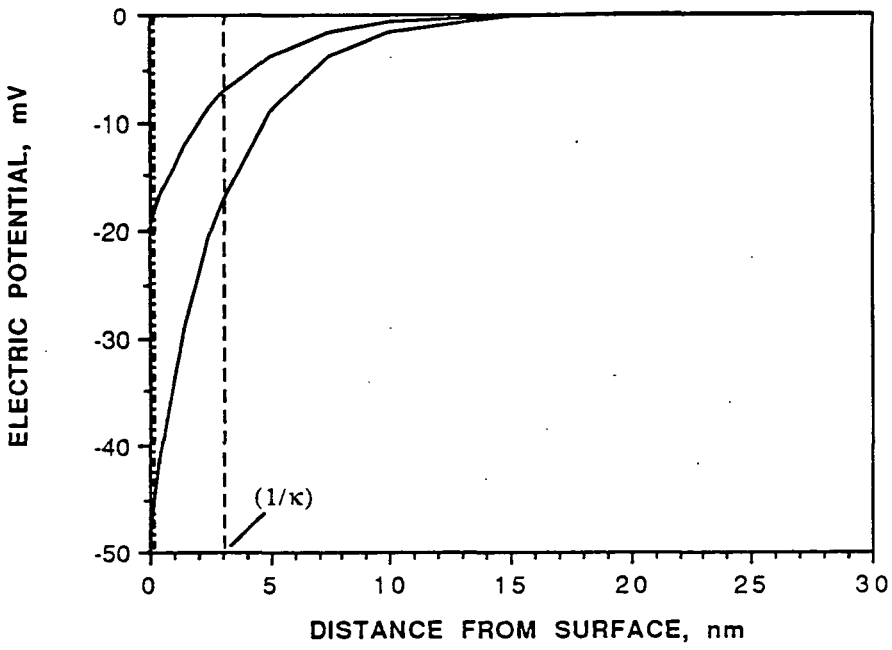

Figure 42. Electric potential as a function of distance from surface in 0.01M NaCl, calculated from Gouy-Chapman theory assuming surface potentials of -20mV and -50mV. ("·····" = radius of hydrated sodium ion)

The effect of bleaching on the electrophoretic mobility of kraft fines is shown in Figs. 43 and 44 for the low and high refining level samples, respectively. Linear regression lines have been drawn through the unbleached data only. The effect of bleaching can be seen by comparing filled (unbleached) and open (bleached) symbols of similar shape. Bleaching the kraft pulps using a CEDED sequence resulted in a less negative electrophoretic mobility of the fines. McKenzie[38] reported similar results with unbleached and bleached sulfate pulps. The major constituents removed during bleaching were lignin and hemicelluloses, specifically galactan. Another result of the bleaching process was a significant decrease in the weak acid content of the pulp. The decrease in weak acid content, resulting from changes in

(or modification of) the lignin and hemicellulose fractions, is believed by the present author to be responsible for the change in electrophoretic mobility.

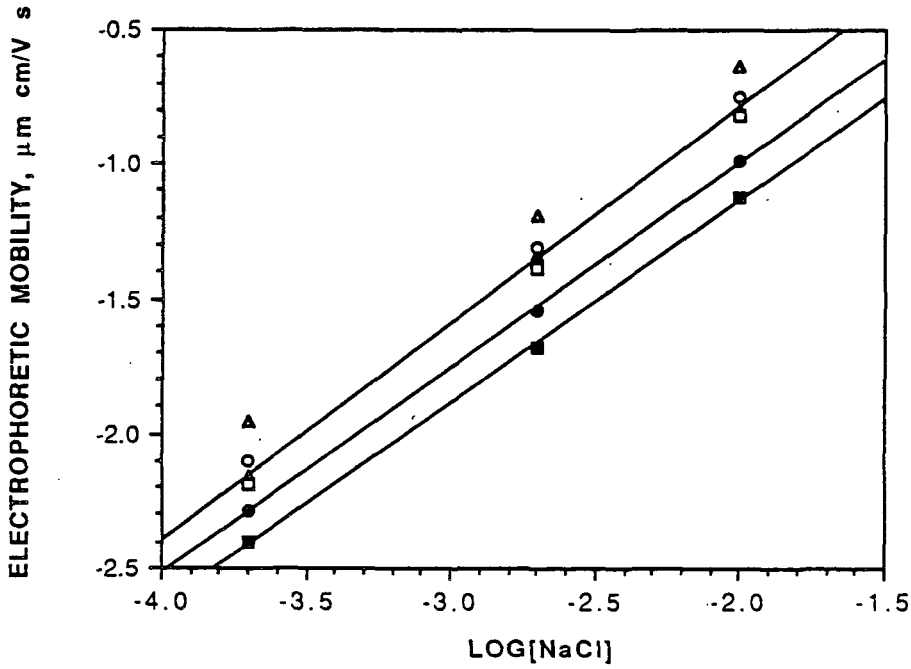

Figure 43. Effect of bleaching on the electrophoretic mobility of kraft fines: 7,500 rev. [▲ = 44.71% (unbl.); △ = 44.71% (bl.); ● = 49.92% (unbl.); ○ = 49.92% (bl.); ■ = 54.4% (unbl.); □ = 54.4% (bl.)].

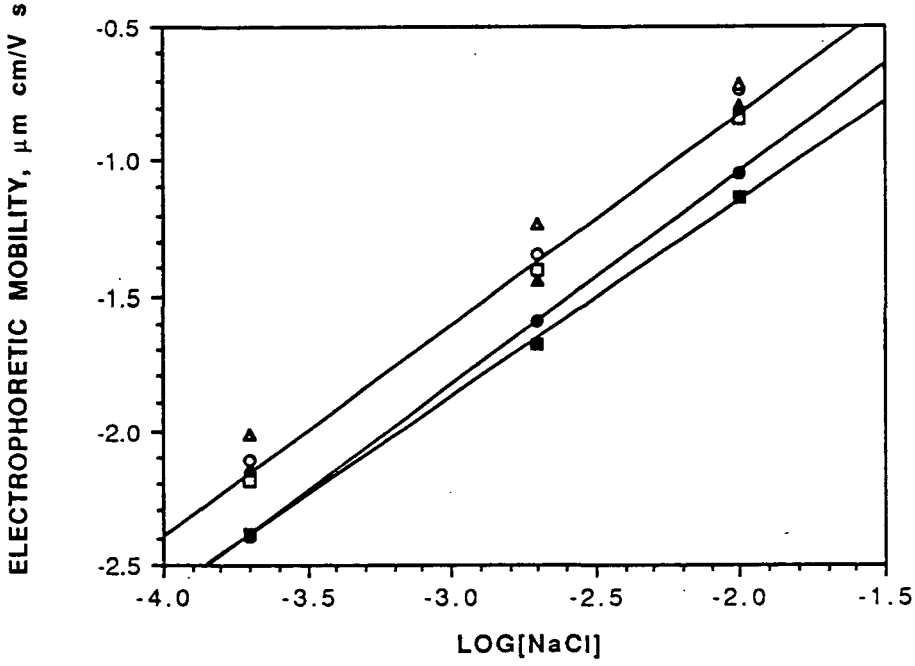

Figure 44. Effect of bleaching on the electrophoretic mobility of kraft fines: 15,000 rev. [▲ = 44.71% (unbl.); △ = 44.71% (bl.); ● = 49.92% (unbl.); ○ = 49.92% (bl.); ■ = 54.4% (unbl.); □ = 54.4% (bl.)].

Very little difference in electrophoretic mobility was observed between fines from pulps refined at the two levels used in this study. In some samples, fines from the highest refining level were slightly more negative than those from the low level. Nevertheless, the effect was small compared to the effect of pulp yield and bleaching, leading to the conclusion that refining had only a minor effect on the electrophoretic mobility of kraft fines. The electrophoretic mobility results are summarized in Table 18 (p. 71). The effect of increased refining level on the electrophoretic mobility of unbleached fines can be determined by comparing U_{i1} and U_{i2}. A similar comparison can be made between B_{i1} and B_{i2} to determine the effect on refining on the electrophoretic mobility of bleached fines.

Jaycock and Pearson[33] have reported that increased refining produced a more negative zeta potential for bleached pulps. The authors used a rotary blender to refine the pulp at 2% consistency and measured the zeta potential using the streaming potential technique. The kraft pulps in the present study were refined at 10% consistency using a PFI Mill refiner, and microelectrophoresis was used to measure the electrophoretic mobility of the fines fraction (recall that the electrophoretic mobility and zeta potential are related through the Smoluchowski equation). Differences in the consistency during refining may have contributed to the conflicting results, but the present author believes that differences in the technique used to measure the electrokinetic potential is primarily responsible for the conflicting results. The application of streaming potential to pads of compressible fibers (such as wood fibers) has been questioned by Stratton and Swanson,[11] and the differences in fiber pad density that would be expected over the freeness range used by Jaycock and Pearson may have accounted for the observed difference in zeta potential.

In direct contrast to Jaycock and Pearson, Anderson and Penniman[39] used both a Valley beater and a Waring high-shear blender to refine spruce sulfite pulp and report no change in the zeta potential with increased refining over the freeness range of 800mL CSF to 200mL CSF. Davison and Cates[40] also report no effect of refining on the zeta potential of bleached kraft fines refined in a Valley beater. The consistency during refining was not reported by either of the above authors and both authors used microelectrophoresis to measure the electrophoretic mobility of the fines fraction.

COMPARISON OF WEAK ACID CONTENT AND ELECTROPHORETIC MOBILITY

If the surface charge of wood fibers originates through ionization of acidic (i.e., carboxyl) groups, it is logical to assume that a relationship exists between

weak acid content and electrophoretic mobility. Some researchers have reported that increasing carboxyl content results in a more negative zeta potential,[29,32] while others have found just the opposite trend.[14,16,103] To examine this relationship, the electrophoretic mobility of kraft fines (<400-mesh) is plotted versus the weak acid content of the fines fraction (<200-mesh) in Figs. 45 - 47. The data points correspond to the average electrophoretic mobility values for both bleached and unbleached kraft fines at the two refining levels used in this study. For each of the three electrolyte concentrations, the electrophoretic mobility of kraft fines became more negative with increasing weak acid content. At low values of weak acid content the electrophoretic mobility decreased sharply with increasing weak acid content. However, at higher values of weak acid content, the electrophoretic mobility leveled off and appeared to approach some limiting value.

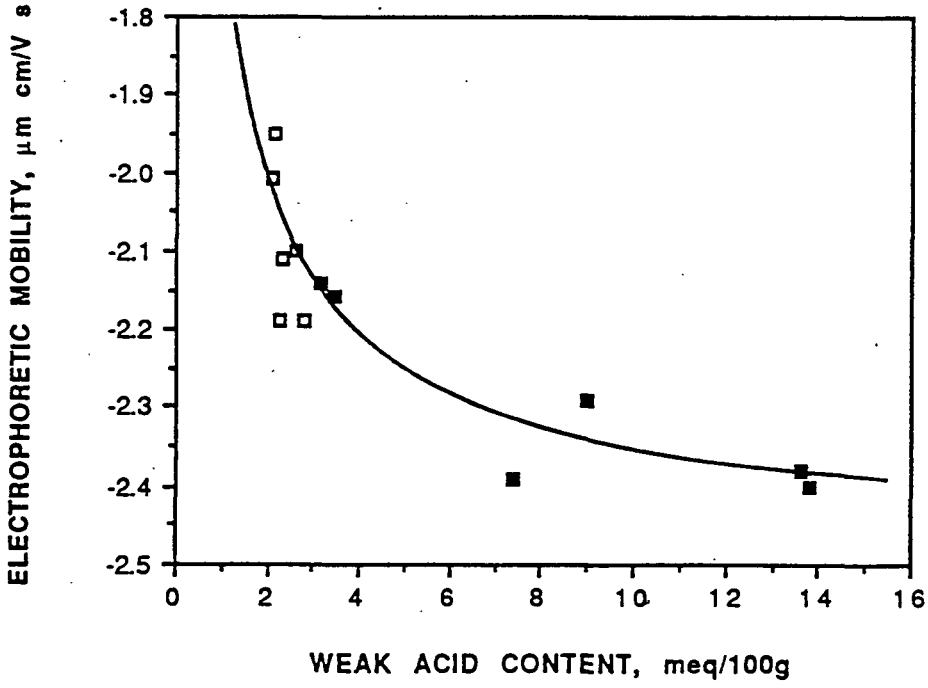

Figure 45. Kraft fines in 0.0002M NaCl (■ = unbleached; □ = bleached). Line calculated from Eq. 9.

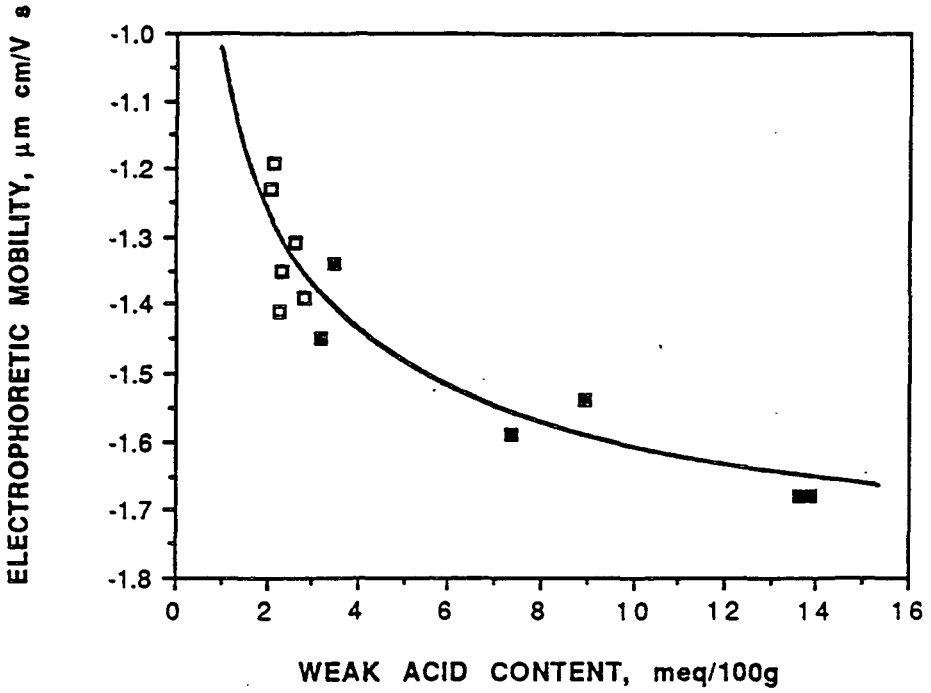

Figure 46. Kraft fines in 0.002M NaCl (■ = unbleached; □ = bleached). Line from Eq. 9.

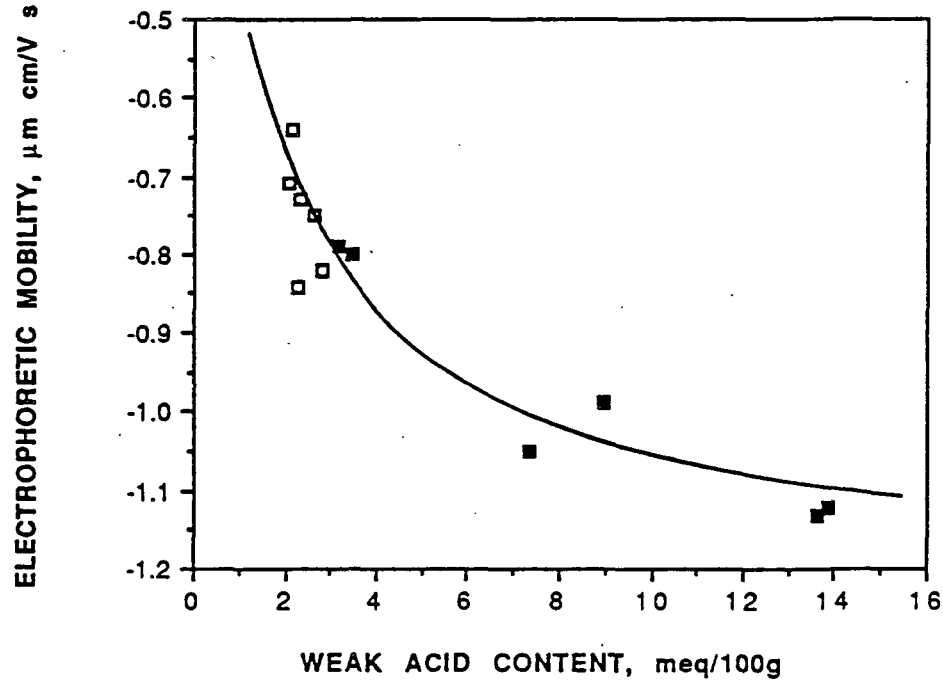

Figure 47. Kraft fines in 0.01M NaCl (■ = unbleached; □ = bleached). Line from Eq. 9.

An empirical expression of the form of the Langmuir adsorption isotherm was used to calculate the curves shown in Figs. 45-47. This form of equation was chosen because it satisfies the assumption that the electrophoretic mobility would be "zero" when the weak acid content is "zero", and because the equation predicts some limiting value of electrophoretic mobility (B) as the weak acid content becomes very large. The equation had the following general form:

$$E.M. = aBW/(1 + aW) \qquad [9]$$

where: a = constant
B = constant
W= weak acid content of fines fraction (<200-mesh)

The constants "a" and "B" were determined from linear plots of 1/E.M. vs. 1/W. The slope of such plots is equal to (1/aB) and the y-axis intercept equals (1/B). The "a" and "B" constants obtained for each electrolyte concentration are presented in Table 19, and are plotted versus the logarithm of the sodium chloride concentration in Fig. 48.

Table 19. Values of "a" and "B" for kraft fines in various electrolytes.

Electrolyte	a*	B**	R^2
0.0002M NaCl	2.31	-2.46	0.811
0.002M NaCl	1.25	-1.75	0.819
0.01M NaCl	0.638	-1.22	0.856

* (cg/meq)
**(μm cm/V s)

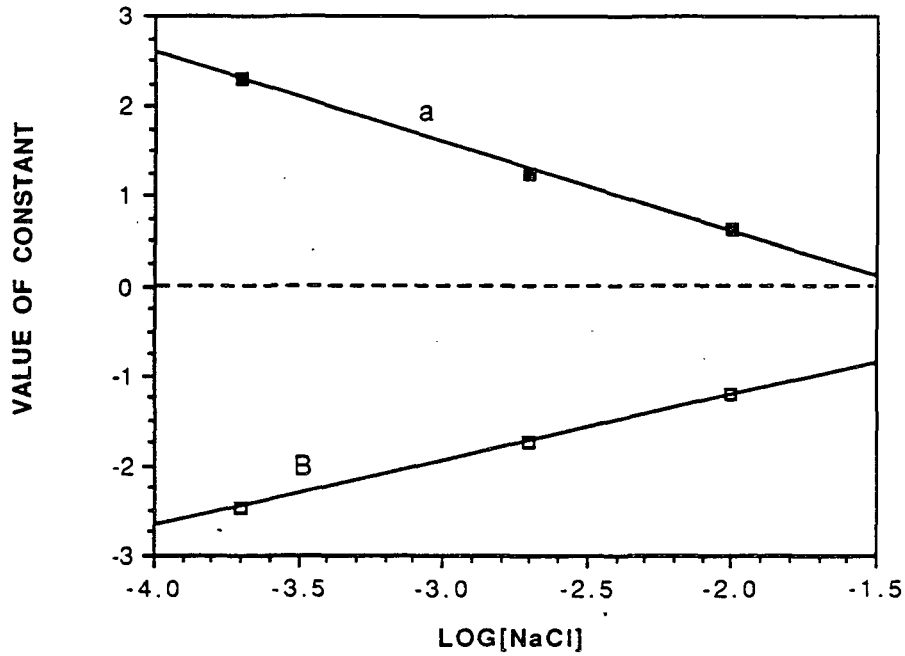

Figure 48. Values of "a" and "B" for Equation 9, as a function of log[NaCl] (■ = "a";□ = "B").

It is clear from Fig. 48 that a linear relationship exists between the constants "a" and "B" and log[NaCl]. The linear regression equations are shown below:

$$a = (-0.989)\log[NaCl] - 1.37 \qquad R^2 = 0.997 \qquad [10]$$

$$B = (0.728)\log[NaCl] + 0.229 \qquad R^2 = 1.000 \qquad [11]$$

The ability to calculate values for "a" and "B" allows one to estimate the electrophoretic mobility of spruce kraft fines in any concentration of NaCl, providing the weak acid content of the fines is known. Substitution of Eqs. 10 and 11 for "a" and "B" into Eq. 9 gives Eq. 12.

$$E.M. = W\{-0.720(\log[NaCl])^2 - 1.22\log[NaCl] - 0.314\} / \{1 + W(-0.989\log[NaCl] - 1.37)\}^4 \quad [12]$$

Equation 12 is plotted in Fig. 49 over the following variable limits:

log[NaCl]: min. = -3.70, max. = -2.0

W: min. = 2.00, max. = 14.00

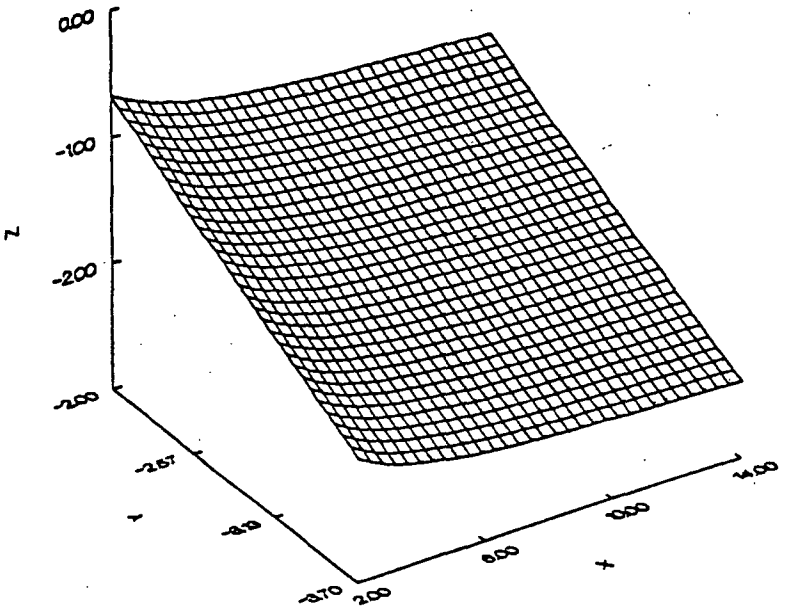

Figure 49. Three-dimensional plot of Eq. 12, derived from data of bleached and unbleached kraft fines {Axes: Z = Electrophoretic Mobility (μm cm/V s); Y = log[NaCl]; X = Weak Acid Content (meq/100g)}.

Equation 12 was used to calculate the electrophoretic mobility of both unbleached and bleached kraft fines for the specific conditions used in this work. The calculated values are compared with experimental measurements in Fig. 50. The results demonstrate the ability of the empirical equation to predict the electrophoretic mobility of spruce kraft fines in sodium chloride solutions at pH 6.0.

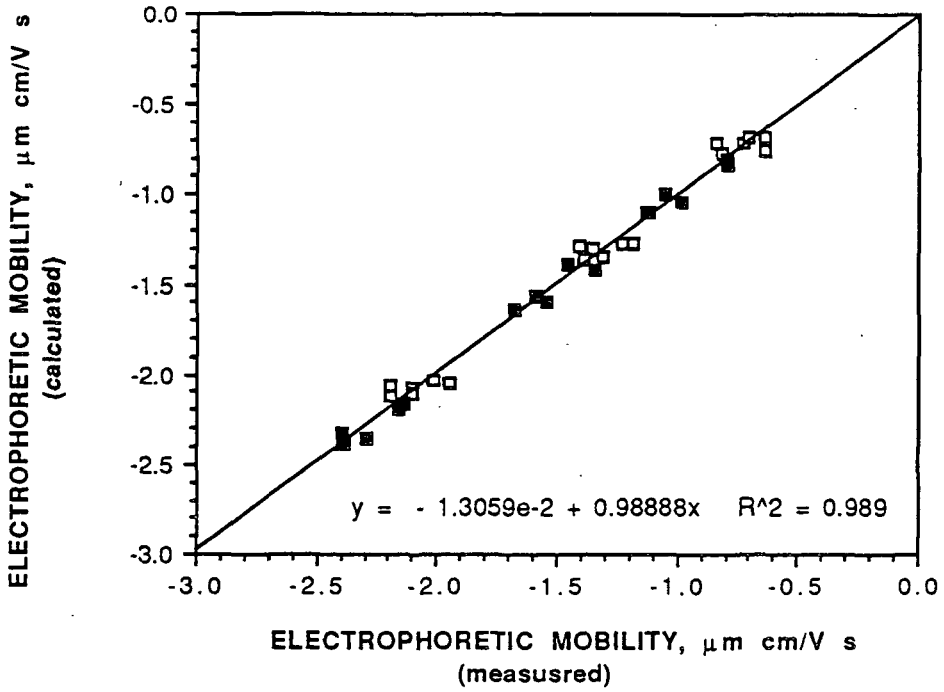

Figure 50. Electrophoretic mobility calculated from Eq. 12 versus measured values (■ = unbleached kraft; □ = bleached kraft).

Since a linear relationship was found between the weak acid content of the fines and the unbleached, unscreened pulp yield (as shown in Fig. 51), it should be possible to estimate the electrophoretic mobility of spruce kraft fines from any pulp yield in any concentration of aqueous NaCl at pH 6.0.

The applicability of Equations 9 - 12 to kraft fines in general, or to spruce kraft fines in other electrolytes, is not known and beyond the scope of the thesis objectives. Future research to address these and other questions concerning these relationships is warranted.

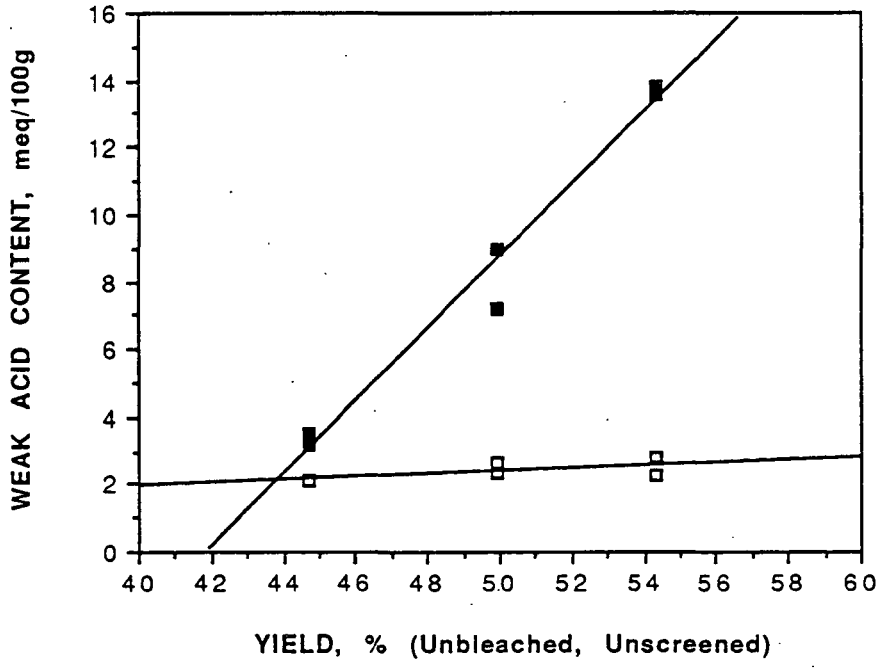

Figure 51. Weak acid content of spruce kraft fines (<200-mesh) versus unbleached, unscreened pulp yield (■ = unbleached; □ = bleached).

The linear regression equations for the lines in Fig. 51 are shown below:

Unbleached: W.A.C. = 1.07(% yield) - 44.85 R^2 = 0.975

Bleached: W.A.C. = 0.0423(% yield) + 0.273 R^2 = 0.439

In Fig. 52, the electrophoretic mobility and weak acid content data from the TMP fines are added to the kraft data from Figs. 45 - 47. The curves in Fig. 52 are calculated from Eq. 9 for the kraft data only.

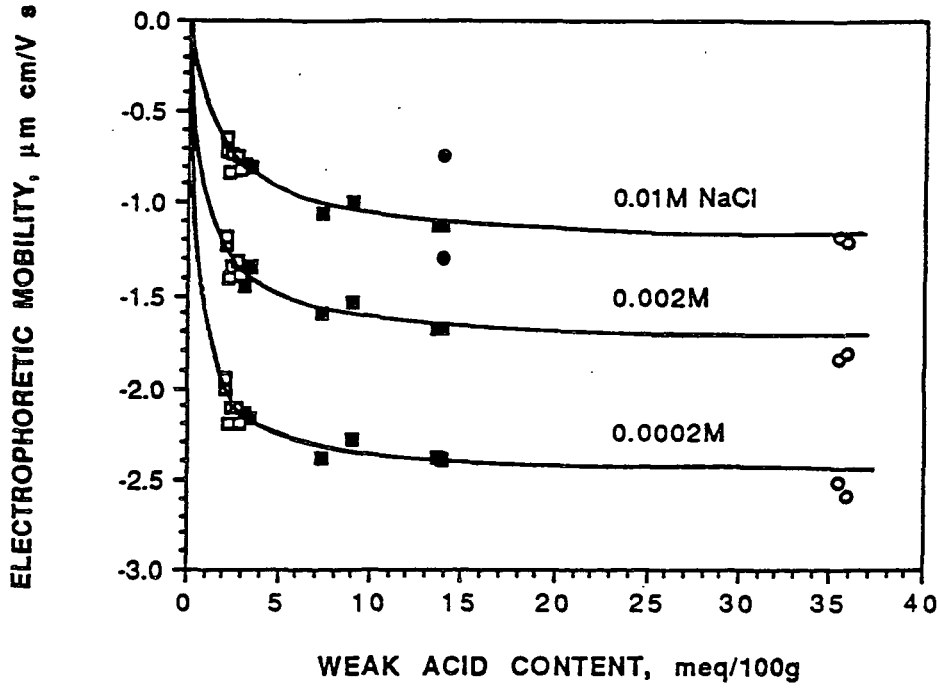

Figure 52. Electrophoretic mobility versus weak acid content for both kraft and TMP fines (■ = unbleached kraft; □ = bleached kraft; • = unbleached TMP; ○ = bleached TMP; —— = calculated from Eq. 9, for kraft data only).

The bleached TMP data points, at approximately 36meq/100g, appear to fit the curves derived for the kraft data. However, the unbleached TMP data points (14meq/100g) do not appear to fit at the higher electrolyte concentrations. There are too few data points within the TMP pulps to accurately estimate the type of relationship that may exist between the electrophoretic mobility and the weak acid content. However, the same trend of increasing weak acid content resulting in a more negative electrophoretic mobility was observed.

When measuring the weak acid content of wood fibers and fiber fines, every acidic site accessible to the methylene blue dye molecule within the particle is measured. The electrophoretic mobility, on the other hand, is an indirect

measurement of only those (ionized) acid groups on the surface of the particle. Since all kraft fines were similar in shape (within each pulp yield), relating the electrophoretic mobility to the total weak acid content is valid if a uniform distribution of weak acids throughout the particle is assumed. Because of morphological differences between kraft and TMP fines, a different relationship would be expected for mobility versus the weak acid content, as it was measured in this study.

COMPARISON OF RESULTS WITH ELECTROKINETIC THEORY

The theoretical relationship between surface charge density and zeta potential can be derived from Eq. 1 (p. 4) and Eq. 4 (p. 7). Solving Eq. 1 for the surface potential (φ_o) gives Eq. 13.

$$\varphi_o = (2kT/ze)\sinh^{-1}[\sigma_o\pi^{0.5}/(2\varepsilon\varepsilon_o\kappa N_A Tc)^{0.5}] \qquad [13]$$

Rearranging Eq. 4 to solve for φ_x, the potential at a distance "x" from the surface, gives Eq. 14.

$$\varphi_x = (4kT/ze)\tanh^{-1}[e^{-\kappa x}\tanh(ze\varphi_o/4kT)] \qquad [14]$$

The relationship between the zeta potential (ζ) and the surface potential (φ_o) is given by Eq. 14 if the distance from the surface to the shear plane (δ) is substituted for x. By making this substitution, and substituting Eq. 13 for φ_o in Eq. 14, the relationship between zeta potential and surface charge density is obtained. This expression is given in Eq. 15 for particles suspended in a 1:1 electrolyte at 25°C:

$$\zeta = (102.8)\tanh^{-1}\{e^{-\kappa\delta}\tanh[(0.5)\sinh^{-1}(30.18\sigma_o c^{-0.5})]\} \quad [15]$$

Equation 15 is plotted in Fig. 53 for electrolyte concentrations of 0.0002M, 0.002M and 0.01M NaCl. The value of "δ" was assumed to be 0.5124nm, corresponding to the diameter of a hydrated sodium ion.[102]

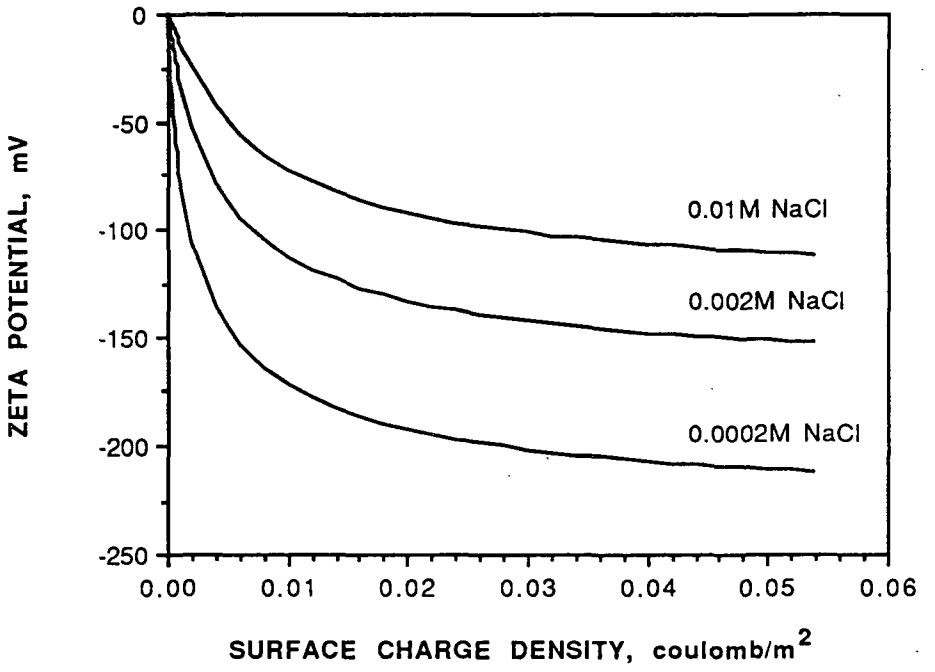

Figure 53. Zeta potential as a function of surface charge density (from Eq. 15).

The surface charge density of fiber fines is at present very difficult to determine for two reasons: (1) the porous nature of fiber fines makes it difficult to differentiate between acid groups on the surface and those contained below the surface, and (2) the irregular shape and porous nature also makes it difficult to obtain an accurate surface area measurement, over which the surface charge is distributed. Because of these difficulties, no attempt was made to measure the surface charge density of the fiber fines used in this study. Published values for the surface charge density of wood and cotton fibers are summarized in Table 20.

Table 20. Literature values for the surface charge density of cotton and wood fibers.

Sample Description	$-\sigma_o$ (Coulomb/m^2)	Reference
Cotton linters	0.0032 - 0.0085	24
Bleached sulfate	0.0137 - 0.0206	24
Unbleached sulfate	0.0315 - 0.0403	24
Oxidized cotton linters	19.294 - 106.12	29

The values reported by Rozalinov[29] are extremely high, and differ from those of Herrington[24] by at least a factor of 1,000. Rozalinov[29] calculated the surface charge density by dividing the weak acid content, measured via calcium ion exchange, by the hydrodynamic surface area, obtained using a Canadian Pulmac apparatus. The calcium ion exchange technique measures essentially all weak acid groups accessible to calcium ions, while the hydrodynamic surface area is a measure of external surface only. Calculation of the surface charge density in this manner leads to inaccurately high values because it assumes all weak acids are present on the external surface. This is the most likely explanation for the difference between the data of Rozalinov and Herrington, and Rozalinov's data should be disregarded for purposes of comparison.

Herrington[24] also calculated the surface charge density by dividing the measured weak acid content by the measured surface area. The weak acid content was determined by potentiometric titration. Every acidic group accessible to H^+ and OH^- ions is measured with this technique. The surface area was measured by two different techniques: (1) nitrogen gas adsorption, and (2) negative adsorption of chloride ions. Both methods measure the surface area of internal pores within the fiber in addition to the external surface area. Calculating the external surface charge density from these two measurements may also be erroneous because it is assumed

that the ratio of weak acid groups to "surface" area is the same for the true external surface as it is for the total surface measured by nitrogen gas adsorption.

A new technique described by Wågberg and coworkers[104] has also been used to measure the weak acid content of fiber surfaces. The technique involves adsorption of well characterized cationic polyelectrolytes onto fiber surfaces and assumes a 1:1 relationship between the moles of cationic charge on the adsorbed polymer and the moles of negative charge present on the fiber surface. The authors report a ratio of surface charge to bulk charge of 0.17 for bleached sulfate pulp, although they admit this value may be very high.

The surface area of wood fiber fines is also difficult to measure because of the porous nature of the particles. Marton[105] measured the surface area of fines from a 70:30 hardwood-softwood bleached pulp blend using both a drainage rate method and nitrogen gas adsorption. With the drainage rate method, Marton obtained a hydrodynamic surface area of 8.0 m^2/g for the fines fraction (<200-mesh). The BET nitrogen adsorption technique, conducted on fines dried after sequential solvent exchange to preserve the internal pore structure, gave a surface area of 46.8 m^2/g.[105] The hydrodynamic surface area may underestimate the actual surface area somewhat while the BET nitrogen adsorption results certainly overestimate the external surface area. It is interesting to note that the ratio of the hydrodynamic surface area/BET nitrogen surface area (0.17) equals the value obtained by Wågberg[104] for the ratio of surface acid groups to total acid groups.

Evaluation of the data from the present study in terms of electrokinetic theory will require an assumption of the surface charge density because there is not an acceptable method for accurately determining the surface charge density of wood fibers or fiber fines. The surface charge density was calculated by dividing the weak

acid content values obtained from methylene blue dye adsorption by 46.8m^2/g (the surface area of fines reported by Marton[105] measured using nitrogen adsorption). The results are shown in Table 21.

Table 21. Calculated surface charge densities for kraft and TMP fines.

Sample	Weak Acid (meq/100g)	σ_o (coulomb/sq. meter)
U11	13.83	-0.284
U12	13.61	-0.279
U21	8.95	-0.183
U22	7.17	-0.147
U31	3.51	-0.0720
U32	3.17	-0.0650
B11	2.78	-0.0570
B12	2.26	-0.0463
B21	2.64	-0.0541
B22	2.33	-0.0478
B31	2.14	-0.0439
B32	2.10	-0.0430
TMP-U	13.88	-0.284
TMP-B1	35.88	-0.736
TMP-B2	35.33	-0.724

Zeta potential values for the experimental results were calculated from electrophoretic mobility data using Eq. 5. For aqueous electrolytes at 25 °C, Eq. 5 reduces to the following[5] (for $|\zeta| < 25mV$):

$$\zeta = 12.85(E.M.) \qquad [16]$$

The zeta potential of kraft fines in 0.01M NaCl is plotted versus the calculated surface charge density in Figs. 54. The theoretical zeta potential, calculated from Eq. 15 assuming a shear plane distance (δ) of 0.5124nm, is also shown in Fig. 54.

The theoretical zeta potential at the assumed shear plane distance is extremely negative over the range of surface charge densities calculated for the kraft fines. The experimental zeta potential data, calculated using Eq. 16, are much less negative than the theory predicts. Similar results were obtained for kraft fines in 0.0002M and 0.002M NaCl.

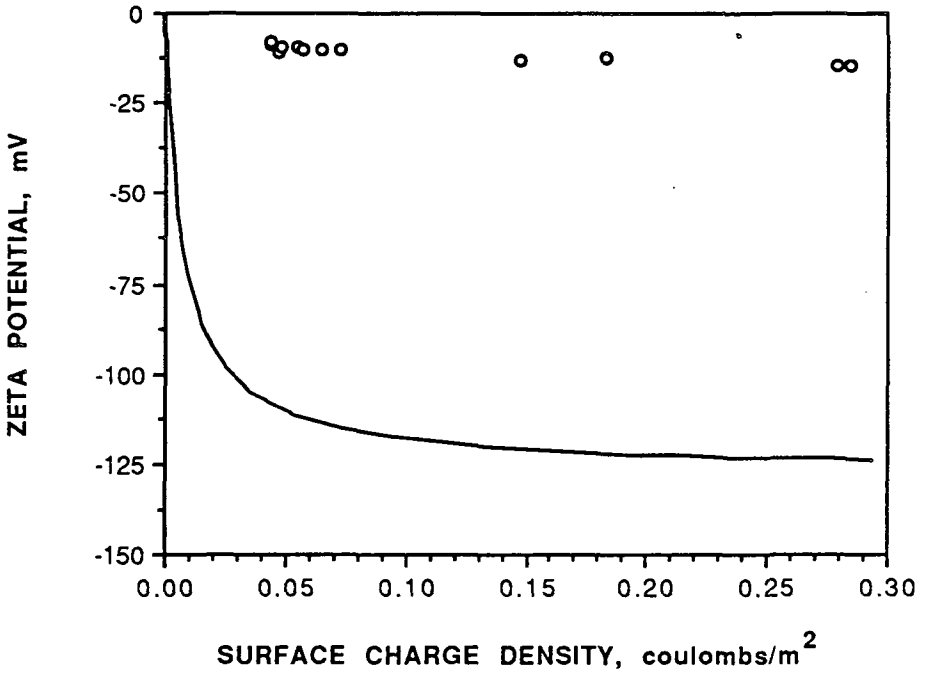

Figure 54. Zeta potential versus surface charge density, kraft fines in 0.01M NaCl (o = experimental data; —— = calculated from Eq. 15 for δ = 0.5124nm).

By increasing the assumed value for "δ" (i.e., moving the shear plane farther out from the particle surface) it is possible to bring the line calculated from Eq. 15 closer to the experimental data. The value of δ required to "approximate" the data in 0.01M NaCl was 6.5nm. Figure 55 is a plot of the experimental data and the curve generated from Eq. 15 using δ = 6.5nm. Larger values of δ are required to approximate the zeta potential data in 0.0002M ($\delta \cong$ 28nm) and 0.002M NaCl ($\delta \cong$ 12nm).

As discussed previously, the exact location of the shear plane is not known, but is usually assumed to be slightly larger than the radius of a hydrated counterion.

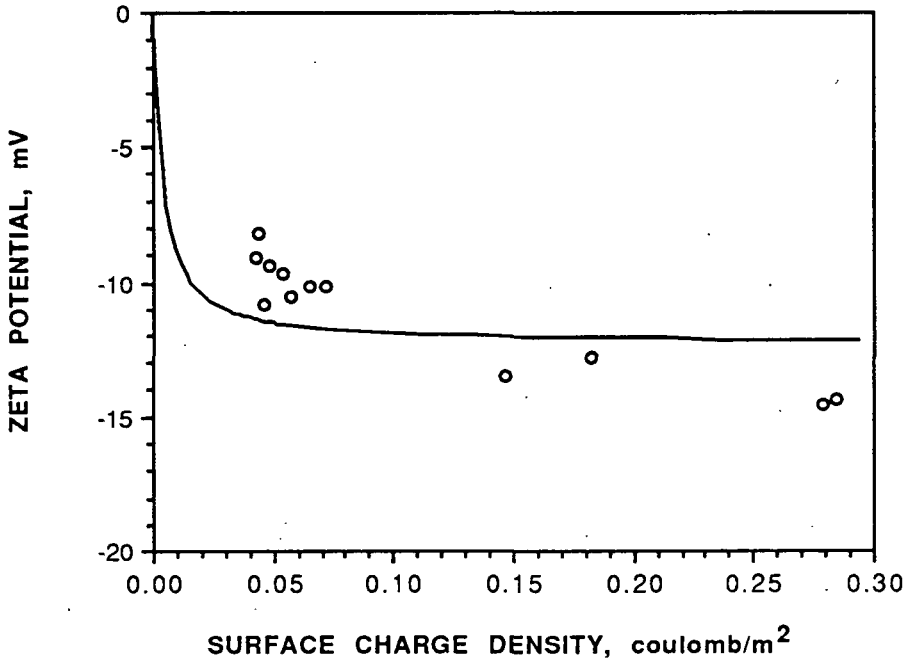

Figure 55. Zeta potential versus surface charge density for kraft fines, δ = 6.5nm.

The shear plane distance needed to produce the curve in Fig. 55 is much greater than would be expected. Eversole and coworkers,[8,9] however, have also reported large values of the shear plane distance from glass and ceramic surfaces, ranging from 0.8nm to 11nm. Shear plane distances in low electrolyte concentrations were found to be greater than those measured in higher concentrations. Bikerman[106] postulates that surface roughness effects may result in shear plane distances on the order of 1nm to 10nm away from the surface. He suggests that the slip plane should not be thought of as a rigid monolayer, but rather as an enveloping surface around the protrusions of the particle surface. This idea could probably be applied to wood fiber fines, since scanning electron photomicrographs of wood fiber fines reveal the surface to be very rough.

It is evident from Fig. 55 that Eq. 15, derived from Gouy-Chapman theory, does not fit the data generated in this study as well as the empirical relationship given in Eq. 9 does. An underlying assumption of the overall theoretical evaluation is that the theory developed by Gouy and Chapman is sophisticated enough to accurately predict the relationship between the zeta potential and surface charge density for the system under study. Several researchers have made modifications to the basic equations derived by Gouy and Chapman for application to specific systems,[4] however, the equations used in the present evaluation have also been used by other researchers[7] in the study of wood fiber systems. The application of Eq. 15 for systems of wood fiber fines involves many other assumptions, some of which are listed below:

1. The surface charge density calculation includes an assumption that the ratio of acid groups to "surface" area is the same on the true external surface as on the total surface.

2. The surface area of fiber fines was assumed to be equal to the value published by Marton[105] using a BET nitrogen adsorption technique. This may not be the correct value to use in this type of calculation as it is a measure of the surfaces available for nitrogen adsorption, while the weak acid content measures only those acids accessible to the methylene blue dye molecule.

3. The dielectric constant and viscosity of the solution adjacent to the particle were assumed to be equal to the value for distilled water at the same temperature. Within the Stern layer the concentration of counterions is extremely high. The high ionic concentrations will increase the viscosity and decrease the dielectric properties of the solution in this region.[3,4]

4. The nonspherical nature of the fines also presents a problem, however, if the product of the double layer thickness (κ) and the local particle radius (r) is greater than 100, application of the Smoluchowski equation is valid. For fiber fines suspended in systems of moderate ionic strength, the value of ($\kappa \cdot r$) can be assumed to be greater than 100.[11]

It should be restated that an accurate measurement of the surface charge density of wood fiber fines is needed before a theoretical evaluation of electrokinetic data can be made with any degree of confidence.

The surface charge density can also be calculated from Gouy-Chapman theory. Rearrangement of Eq. 15 to solve for the surface charge density (σ_o) gives:

$$\sigma_o = (c^{0.5}/30.18)\sinh[2\tanh^{-1}\{e^{\kappa\delta}\tanh(\zeta/102.8)\}] \qquad [17]$$

Equation 17 was applied to the data from this study for the purpose of calculating the surface charge density of the fines from the zeta potential data. A constant shear plane distance of 0.5124nm was assumed for each electrolyte concentration. The results appear in Table 22.

It is evident from Table 22 that the surface charge density calculated from zeta potential measurements is much smaller than that presented in Table 21. In general, the two values differ by at least one order of magnitude. This same situation has also been reported by Hunter[4] (p. 307). It is interesting to note that the surface charge density in Table 22 is dependent upon the electrolyte concentration, and increases with increasing electrolyte concentration.

Table 22. Calculated surface charge densities for kraft and TMP fines.

Sample	Weak Acid (meq/100g)	$\sigma_o \times 10^4$ (coulomb/sq. meter) 0.0002M	0.002M	0.01M
U11	13.83	-3.07	-6.96	-11.2
U12	13.61	-3.04	-6.96	-11.3
U21	8.95	-2.91	-6.33	-9.90
U22	7.17	-3.05	-6.57	-10.5
U31	3.51	-2.73	-5.48	-7.80
U32	3.17	-2.70	-5.95	-7.80
B11	2.78	-2.77	-5.68	-8.12
B12	2.26	-2.77	-5.78	-8.36
B21	2.64	-2.64	-5.34	-7.42
B22	2.33	-2.66	-5.51	-7.21
B31	2.14	-2.44	-4.84	-6.31
B32	2.10	-2.52	-5.01	-7.01
TMP-U	13.88	-3.06	-5.31	-7.32
TMP-B1	35.88	-3.35	-7.54	-12.3
TMP-B2	35.33	-3.24	-7.67	-11.8

There are several possible explanations for the observed differences between the data presented in Tables 21 and 22, in addition to the previously discussed assumptions implicit in applying Eq. 15. One possible explanation is that the method used to calculate the surface charge density values presented in Table 21 assumes that all acidic groups are ionized, and this may not be the case. The pK values of carboxyl groups on cellulose and bleached sulfate fibers published in the literature range from 3.6 to 5.1,[107] while the pK of aliphatic carboxyl groups on lignin is between 4 and 5.[108] Because the electrophoretic mobility studies were conducted at pH 6.0, it can be assumed that a significant fraction of the acid groups were ionized. Herrington and Midmore[107] calculated a degree of dissociation (α) of 0.893 for bleached sulfate fibers in 0.01M NaCl at pH 6.03. Significantly lower values were calculated below pH 4.83 for cotton linters in the same electrolyte concentration.[7]

Factors other than pH, including neighboring group interactions and electrolyte concentration, can also affect the degree of dissociation. The general equation describing the relationship between pH and the degree of dissociation, taking into account neighboring group effects, is presented in Eq 18.[107]

$$pH = pK_o - \log[(1-\alpha)/\alpha] + 0.434\Delta G_{el}(\alpha)/RT \qquad [18]$$

where: pK_o = characteristic dissociation constant of ionizing group when electrostatic interactions with other ionizing groups are absent

α = degree of dissociation (no. of groups dissociated/total no.)

$\Delta G_{el}(\alpha)$ = required electrostatic Gibbs energy for the removal of a molar equivalent of protons at a given degree of ionization

For polyelectrolytes containing a monobasic acid, the Henderson-Hasselbach equation (Eq. 19) can be used as an approximation of the relationship between pH, pK, and the degree of dissociation.

$$pH = pK - \log[(1 - \alpha)/\alpha] \qquad [19]$$

Katchalsky and Spitnik[109] published the following empirical relationship (Eq. 20) based on potentiometric titration data for polymethacrylic acid in the presence of neutral salts. The constant, *n*, was found to decrease with increasing electrolyte concentration. Equation 20 reduces to Eq. 19 when "*n*" is equal to 1.0.

$$pH = pK - n\log[(1 - \alpha)/\alpha] \qquad [20]$$

where: n = empirical constant

Table 23 contains values of "*n*" published by Herrington[107] for cotton linters and bleached sulfate fibers. From the data presented in Table 23, the effect of increasing electrolyte concentration on the pK value, calculated from Eq. 20, can be clearly seen. The trend of decreasing pK with increasing electrolyte concentration is consistent with the data shown in Table 22, indicating an increasing surface charge density with increasing electrolyte concentration.

Table 23. Values of *n* and pK obtained for cotton linters and bleached sulfate fibers.[107]

Sample	[NaCl] (molar)	*n*	pK
cotton linters	0.001	1.97	5.15
cotton linters	0.01	1.44	4.20
cotton linters	0.1	1.0	3.95
cotton linters	1.0	1.0	3.65
bleached sulfate	0.001	2.05	5.10
bleached sulfate	0.01	1.92	4.35
bleached sulfate	0.1	1.58	3.85
bleached sulfate	1.0	1.26	3.75

The effect of neighboring group interaction on the ionization constants of soluble polyelectrolytes has also been reviewed in a series of articles by Bloys von Treslong.[110-112] Functional groups in both charged and uncharged states have been shown to have an effect. Interaction between uncharged groups may affect the determination of pK_o, which is estimated by extrapolation of pK to zero degree of ionization. Charged functional groups will affect the value of the ionization constant for functional groups in close proximity. The data in Table 24 demonstrate the effect of increasing distance between functional groups of dicarboxylic acids on the ionization constants. With increasing distance between ionizing groups the first ionization constant becomes larger, indicating the effect on uncharged groups. By increasing the separation distance from $(CH_2)_2$ to $(CH_2)_3$, the pK of the second

ionizing group decreases. Further increases in separation distance, up to $(CH_2)_6$, did not affect pK_{II}, suggesting the influence of an ionized neighboring group is only a short-range effect.

Table 24. Values of pK for difunctional carboxylic acids.[110]

Sample	pK_I*	pK_{II}**	pK***
$HOOC(CH_2)_2COOH$	4.21	5.64	4.51
$HOOC(CH_2)_3COOH$	4.34	5.41	4.64
$HOOC(CH_2)_4COOH$	4.43	5.41	4.73
$HOOC(CH_2)_5COOH$	4.51	5.42	4.81
$HOOC(CH_2)_6COOH$	4.52	5.40	4.82

* = pK of first ionizing group
** = pK of second ionizing group
*** = pK of difunctional carboxylic acid

Although the data presented in Table 24 are for soluble polyelectrolytes, the results are consistent with those of Neale and Stringfellow[113] for oxidized cotton fibers. These authors report a decrease in the pK_a value of oxidized cellulose from 4.21 to 2.94 as the weak acid content was increased from 3.69 to 20.0meq/100g. When the weak acid content increases the average distance between carboxylic acid groups decreases, and thus one would expect a lower pK_a value based on the results presented in Table 24. These same effects have also been cited to explain the interaction of direct dyes with oxidized cotton fibers.[48,114]

Employing the procedure outlined by Ottewill and Shaw,[115] the data in Table 9 were used to calculate a value of 2.89 for the pK_a of unbleached TMP fines in 0.004M NaCl. Although this value appears to be somewhat low, the weak acid content of the fines fraction was 13.88meq/100g. On the basis of the results obtained

by Neale and Stringfellow,[113] this may be within the range of expected values. Using the value of 2.89 for the pK of unbleached TMP, and an "*n*" value of 2.0 for 0.004M NaCl (from Table 23), the degree of dissociation (α) at pH = 6.0 was calculated using Eq. 20. A value of $\alpha = 0.97$ was obtained, indicating a very high degree of dissociation. This is regarded as only an approximation, however, as many assumptions have been made in arriving at this value. Nevertheless, it is an indication that the degree of dissociation is not significantly less than 1.0 at pH 6.0. Variations in degree of dissociation, therefore, probably are not responsible for the differences between the surface charge density values presented in Tables 21 and 22.

One final possible explanation for the difference in surface charge density values will be briefly discussed, and that is the phenomenon known as counterion condensation, or binding of counterions to charged functional groups. Counterion condensation theory has been reviewed, in terms of soluble polyelectrolytes, by Ikegami[116] and Manning.[117-119] The theory assumes two distinct ion binding states: (1) site bound ions, or those counterions which are in direct contact with one or more charged groups on the polyion, with no intervening water molecules, and (2) territorial bound ions, used to describe bound counterions that are not site bound. Territorial bound counterions are drawn to the polyion by the strong anionic field, but are essentially free to move about the surface and are not held in place by any specific charged site. Binding of ions in either state will result in a net reduction of the surface charge resulting from ionized functional groups.

Monovalent counterions are generally considered to be territorially bound, as are divalent counterions on surfaces of low charge density. Other ion types are usually site bound. There is at present no theory for site binding, nor are the quantitative molecular criteria known for the distribution of bound counterions between the two populations.[119]

The fundamental (empirical) equation in counterion condensation theory is the charge fraction rule. The charge fraction, f, of a polyion is equal to the ratio of its structural charge which is uncompensated by bound counterions to its total structural charge. The charge fraction rule is presented in Eqs. 21a and 21b.

$$f = (N\xi)^{-1} \quad \ldots \quad \text{for } \xi > N^{-1} \qquad \text{(condensation)} \qquad [21a]$$

$$f = 1 \quad \ldots\ldots\ldots \quad \text{for } \xi < N^{-1} \qquad \text{(no condensation)} \qquad [21b]$$

where: N = counterion valence
ξ = charge density parameter

The charge density parameter, ξ, is a dimensionless measure of the linear polyion charge density, defined by Eq. 22.

$$\xi = e^2/\varepsilon kTb \qquad [22]$$

where: b = average linear charge spacing

The charge fraction rule states that for dilute solutions containing monovalent ions, sufficiently many counterions will "condense" on the polyion to lower the charge density parameter to the value of 1.0. In other words, if $\xi < 1$ then $f = 1$, and the polyion has its maximum effective charge. However, if $\xi > 1$ then $f = 1/\xi$. That is, for systems in which $\xi > 1$, sufficient counterions will condense onto the polyion to increase the value of "b" such that $\xi = 1$. When counterion condensation occurs, the polyion is no longer at the maximum effective charge (i.e., $f < 1$).

Klein and Ware[120] studied counterion condensation onto 6,6-ionene (a polyelectrolyte with a linear charge spacing of 0.87nm) by measuring the electrophoretic mobility as a function of ξ. The charge density parameter was varied between 0.82 and 1.85 through modification of the dielectric constant with methanol. The authors observed a decrease in the electrophoretic mobility by greater than a factor of 2 at precisely the conditions where $\xi = 1.0$. The decrease in the electrophoretic mobility was presumably the result of increased association of counterions with the polyion, thus providing direct experimental evidence of counterion condensation.

Several other soluble polyelectrolyte systems have been studied, including polyacrylic acid, chondroitin, and carboxymethylcellulose, and are reviewed in Ref. 119. Counterion condensation theory has also been applied to systems of micelles,[121,122] although to date no research has been conducted with larger particles such as latices or wood fiber fragments.

Condensation of counterions onto the surface of wood fiber fines will result in a lower effective surface charge and could explain the difference between the surface charge values reported in Tables 21 and 22. Recall that the values in Table 21 were calculated from the measured weak acid content of the fines. The methylene blue dye used to measure the weak acid content would displace any adsorbed counterions on the acid groups, and therefore counterion condensation would not affect these values. The surface charge densities reported in Table 22 were calculated from Gouy-Chapman theory using measured values of electrophoretic mobility. Counterion condensation could reduce the electrophoretic mobility, thus reducing the calculated surface charge density values reported in Table 22. Surface charge density values in Table 22 were at least one order of magnitude smaller than

than those reported Table 21. The effect of counterion condensation on wood fiber fines cannot be quantitatively evaluated without making major assumptions regarding the value of the charge spacing parameter. An accurate measurement technique to determine the surface charge density and surface area of fiber fines must be developed before the counterion condensation theory outlined for soluble polyelectrolytes can be applied to fiber fines.

CONCLUSIONS

The most significant finding of this thesis was the identification of a relationship between the weak acid content of fiber fines and their electrophoretic mobility. As a result, fiber modification processes that increase the weak acid content of the pulp (i.e., bleaching with hydrogen peroxide) produce fines with a more negative electrophoretic mobility. Processes that reduce the weak acid content (i.e., decreasing kraft pulp yield and bleaching of kraft pulp using a CEDED bleaching sequence) produce fines with a less negative electrophoretic mobility. Increasing the level of refining did not appreciably affect the weak acid content, and also had little effect on the electrophoretic mobility.

The following conclusions were drawn on the basis of results obtained, and are limited to the specific conditions used in this work. Similar trends might be expected for other pulp types measured in different electrolytes.

1) Hydrogen peroxide bleaching of spruce TMP produces an increase in the weak acid content. The increase in weak acid content results in a more negative electrophoretic mobility of the fines fraction.

2) The standard deviation of the electrophoretic mobility distribution of TMP fines is not affected by bleaching.

3) For spruce kraft pulps, decreasing the pulp yield results in a decrease in the weak acid content, as does bleaching with a CEDED sequence. This is primarily a result of decreasing lignin content and removal or modification of the hemicelluloses during these operations. The decrease in weak acid content results in a less negative electrophoretic mobility of the fines fraction.

4) Increasing the level of refining does not have a significant effect on the weak acid content or electrophoretic mobility over the range studied in this work.

5) No significant change in the standard deviation of the electrophoretic mobility distribution was observed in the kraft fines with decreasing pulp yield, bleaching, or increased refining. However, increasing the electrolyte concentration does reduce the standard deviation of the electrophoretic mobility distribution for both kraft and TMP fines.

6) A relationship exists between the weak acid content and the electrophoretic mobility of wood fiber fines and can be approximated using an empirical expression of the form of the Langmuir adsorption isotherm.

There are several practical implications from the results obtained by this study, two examples of which are described below. It is apparent, however, that much additional research will be required to fully understand how electrokinetic theory can be successfully applied to papermaking operations.

1) With knowledge of the effect of pulp yield, bleaching, and refining on the electrophoretic mobility of the fines, it should be possible for mill personnel to predict *a priori* how changes in these process operations will affect the electrokinetic properties of the pulp. The appropriate actions could then be taken regarding levels of additive addition, etc., to ensure continued operation with a minimum effect on product quality.

2) Currently, the electrokinetic properties of the pulp are monitored and modified at the wet end of the papermachine. By identifying the relationship between weak acid content and electrophoretic mobility, it should be possible to control the electrokinetic properties of the pulp during fiber processing operations (or by additional fiber modification treatments). This provides the opportunity for decreased use of additives designed to modify these same properties at the wet-end of the papermachine (i.e., alum and cationic polymers), thus simplifying the system.

SUGGESTIONS FOR FUTURE RESEARCH

The purpose of this work was to investigate the effects of various pulp processing operations on the electrokinetic properties of spruce fiber fines and to identify the chemical changes responsible for these effects. Although an empirical relationship was derived between the weak acid content and the electrophoretic mobility of fiber fines, direct application of available electrokinetic theory was possible only after assumptions regarding the surface charge density of the fines had been made. The irregular shape and porous nature of fiber fines make direct measurement and/or calculation of the surface charge density difficult. Future work should concentrate on developing methods for determining the surface charge density of fiber fines.

Surface charge density determination of fiber fines will involve accurate measurement of two parameters: (1) the average surface area of fiber fines, and (2) the weak acid content of the surface. Methods commonly used to measure the surface area of wood pulps may or may not be adequate. The pressure drop across a pad of fibers has been used to calculate the hydrodynamic surface area of fibers and fines.[123] Other common methods involve adsorption of an inert gas onto dry fibers[124] and the negative adsorption of bound ions in solution.[125] Polymer adsorption has also been used to measure the surface area of pulp fibers, with limited success.[126] Each of these techniques has its limitations and, in general, will give different values for the surface area of the same sample. An accurate technique for measuring the external surface area of fiber fines suspended in water does not exist at the present time.

The porous nature of wood fiber fines makes it difficult to measure the weak acid content of the surface (i.e., the acidic groups responsible for surface charge development). Typical methods used to measure the carboxyl content of pulp, such as methylene blue dye adsorption and conductometric titration, measure every acidic group within the particle accessible to either the methylene blue dye molecule or the titrant used in the conductometric titration (usually NaOH). A recently developed technique,[104] however, may make it possible to determine the surface charge of porous particles such as wood fibers and fiber fines. The method involves adsorption of various molecular weight cationic polymers, thus making it possible to estimate the charge at different structural levels within the porous material. By combining this technique with electrokinetic measurements it should be possible to determine the surface charge responsible for electrokinetic property development (i.e., the amount of cationic charge adsorbed when $\zeta = 0$).

An accurate estimate of the surface charge density will allow the electrokinetic results to be evaluated using existing theoretical relationships. Application of Eq. 1 will enable the surface potential (φ_o) to be calculated, and by knowing ζ and φ_o, an estimate of the shear plane distance (δ) can be calculated from Eq. 4. The effect of cation type (i.e., Na^+, Ca^{+2}, Al^{+3}) and surface roughness on the calculated shear plane distance is just one of the many interesting experiments that would be possible.

An investigation into the effect of counterion condensation on the electrokinetic properties of fiber fines should also be pursued. It may be desirable to conduct the initial work on a series of well characterized polystyrene latices covering a wide range of surface charge densities. This would allow the fiber fines results to be interpreted on the basis of the results obtained with a model colloid system.

ACKNOWLEDGEMENTS

The guidance of my thesis advisory committee: Dr. Robert A. Stratton; Dr. Terrance E. Conners; and Dr. Dwight B. Easty is gratefully acknowledged. I would especially like to thank the chairman of my thesis committee, Dr. Stratton, for the many stimulating conversations that helped give direction to my project and for the genuine interest he has shown, both in me and in my work.

I would like to express my appreciation to The Institute of Paper Chemistry and its member companies for providing the financial support for me to conduct research in this unique environment.

I would like to thank Dr. Sheng Hu of Consolidated Papers, Inc., for donating the fiber resources used in this study.

Many faculty, staff, and students of IPC have also contributed to the success of this project and deserve recognition. In particular: Tom Paulson of the IPC pulp lab provided direction during the pulping, bleaching, and refining phases of the study; Sally Berben, Randy Paff, and Art Webb of the analytical department conducted various pulp analyses; Mary Block and Sara Spielvogel of the electron microscopy laboratory prepared and photographed the wood fiber and fiber fines samples; Norm Colson and Don Gilbert of the paper materials division provided general assistance in the laboratory; and Dr. Thomas McDonough suggested the statistical analysis approach used to evaluate the data.

I would like to thank my wife, and best friend, Christine. Chris provided an endless supply of love, support, and encouragement to me during the course of this research, for which I am sincerely grateful. And finally, I would like to dedicate this work, with love, to my parents, Edward and Lois Goulet.

GLOSSARY OF SYMBOLS

a = empirical constant

b = average linear charge spacing

B = empirical constant

c = molar ion concentration in the bulk of the electrolyte

e = electron charge

E.M. = electrophoretic mobility

f = charge fraction

$\Delta G_{el}(\alpha)$ = electrostatic Gibbs energy required to remove one mole of protons at a given degree of ionization

k = Boltzmann's constant

n = number of observations

n = empirical constant

N = counterion valence

N_A = Avagadro constant

$p(E.M._i)$ = percentage of particles having electrophoretic mobility "i"

r = local particle radius

S^2 = sample variance

T = absolute temperature

V_f = velocity of fringe pattern

W = weak acid content

x = distance from surface of particle

z = electrovalence of ion

GLOSSARY OF SYMBOLS

α = degree of dissociation

δ = distance from particle surface to shear plane

ε = dielectric constant of the medium

ε_o = permittivity of free space

ζ = zeta potential (or electrokinetic potential)

η = viscosity of medium surrounding particle

κ = Debye-Huckel parameter

ν = degrees of freedom

ξ = charge density parameter

σ_e = electrokinetic charge density

σ_o = surface charge density

φ_d = Stern potential

φ_o = surface potential

φ_x = potential of the double layer at distance "x" from surface

LITERATURE CITED

1. Verwey, E. J. W.; Overbeek, J. T. G. Theory of the Stability of Lyophobic Colloids. New York, NY, Elsevier Publishing Co., 1948:250 p.

2. Kruyt, H. R. (Ed.) Colloid Science. Vol. 1. New York, NY, Elsevier Publishing Co., 1952:115-243.

3. Matijevic, E. (Ed.) Surface and Colloid Science. Vol. 7. New York, NY, John Wiley & Sons, 1974:356 p.

4. Hunter, R. J. Zeta Potential in Colloid Science: Principles and Applications. New York, NY, Academic Press, 1981:386 p.

5. Shaw, D. J. Electrophoresis. London, England, Academic Press, 1969:6, 1.

6. Hunter, R. J. The interpretation of electrokinetic potentials. Journal of Colloid and Interface Science 22:231-239(1966).

7. Herrington, T. M.; Midmore, B. R. Adsorption of ions at the cellulose/aqueous electrolyte interface. Part 3. Calculation of the potential at the surface of cellulose fibers. Journal of the Chemical Society, Faraday Transactions 1 80:1553-1566(1984).

8. Eversole, W. G.; Lahr, P. H. Evidence for a rigid multilayer at a solid-liquid interface. Journal of Physical Chemistry 9:530-534(July, 1941).

9. Eversole, W. G.; Boardman, W. W. The effect of electrostatic forces on electrokinetic potentials. Journal of Physical Chemistry 9:798-801 (November, 1941).

10. Sprycha, R.; Matijevic, E. Electrokinetics of uniform colloidal dispersions of chromium hydroxide. Langmuir 5(2):479-485(1989).

11. Stratton, R. A.; Swanson, J. W. Electrokinetics in papermaking. Tappi 64(1): 79-83(January, 1981).

12. Wiersema, P. H.; Loeb, A. L.; Overbeek, J. Th. G. Calculation of the electrophoretic mobility of a spherical colloid particle. Journal of Colloid and Interface Science 22:78-99(1966).

13. Loeb, A. L.; Overbeek, J. Th. G.; Wiersema, P. H. The Electrical Double Layer Around a Spherical Colloid Particle. Cambridge, MA, The M.I.T. Press, 1961, 375p.

14. Neale, S. M.; Peters, R. H. Electrokinetic measurements with textile fibers in aqueous solutions. Transactions of the Faraday Society 42:478-487(1946).

15. Aksel'rod, G. Z. The nature of the electrokinetic potential of cellulose. Sb. Tr. Vses. Nauch-Issled. Inst. Tsellyul.-Bumazh. Prom. :69-77(1973).

16. Clapp, R. T. An Investigation of the Relation Between Carboxyl Content and Zeta Potential. Doctoral Dissertation, Appleton, WI, The Institute of Paper Chemistry, 1972. 138p.

17. Stamm, A. J. Wood and Cellulose Science. New York, NY, The Ronald Press Co., 1964:378-384.

18. Balodis, V. Electrokinetic properties of fiber surfaces. Appita 21(3):96-103 (November, 1967).

19. Ingruber, O. V. The behavior of wood and wood constituents as acid-buffering systems. Pulp and Paper Magazine of Canada 59(11):135-141(November, 1958).

20. Calkin, J. B. The system cellulose-sodium hydroxide-water: determination of the ionization constant of cellulose. Tappi 34(9):108A-112A(September, 1951).

21. Saric, S. P.; Schofield, R. K. The dissociation constants of the carboxyl and hydroxyl groups in some insoluble and sol-forming polysaccharides. The Proceedings of the Royal Society of London (A) 185:431-447(1946).

22. Rydholm, S. A. Pulping Processes. New York, NY, Interscience Publishers, 1965:153.

23. Ivancic, A.; Rydholm, S. A. Technical color reactions in lignin. Svensk Papperstidning 62(16):554-566(August 31, 1959).

24. Herrington, T. M. The surface potential of cellulose. Paper Technology and Industry. 26(8):383-387(Dec. 85/Jan. 86).

25. Nevell, T. P.; Zeronian, S. H. (Eds.) Cellulose Chemistry and its Applications. Chichester, England, Ellis Horwood, Ltd., 1985:365.

26. Jacquelin, G.; Bourlas, H. Measurement of the zeta potential of papermaking fibers: effects of preliminary treatments. Techniques et. Recherches Papertieres 3:49-58(1964).

27. Gossens, J. W. S.; Luner, P. Flocculation of microcrystalline cellulose suspensions with cationic polymers: effect of agitation. Tappi 59(2): 89-94(February, 1976).

28. Lindström, T.; Söremark, C.; Heingård, C.; Martin-Löf, S. The importance of electrokinetic properties of wood fibre in papermaking. Tappi 57(12):94-96 (December, 1974).

29. Rozalinov, D. Electrical surface characteristics of various oxycellulose fractions. Papir Celoloza 41(7/8):V36-40(1986) (IPC translation T-6696).

30. Neale, S. M.; Standring, P. T. The measurement of Donnan potentials with cellulose and aqueous solutions. The Proceedings of the Royal Society of London (A) 213:530-545(1952).

31. Strazdins, E. Factors affecting the electrokinetic properties of cellulose fibers. Tappi 55(12):1691-1695(December, 1972).

32. Strazdins, E. Surface chemical aspects of polymer retention. Tappi 57(12):76-80 (December, 1974).

33. Jaycock, M. J.; Pearson, J. L. Colloidal aspects of paper formation. Part 1: factors affecting the electrokinetic properties of cellulose fibers. Svensk Papperstidning 78(5):167-171(1975).

34. Hinton, A. J.; Quinn, M. Fibre surface characteristics as they affect two sided dyeing of paper. Paper Technology 5(1):60-64(1964).

35. Branion, R.; Arcelus, M. Effect of particle size on electrophoretic mobility of cellulose pulp fibers. Transactions of the Technical Section. Canadian Pulp and Paper Association. 5(1):TR1-3(March, 1979).

36. Morrison, F. A. Electrophoresis of particle of arbitrary shape. Journal of Colloid and Interface Science. 34(2):210-214(October, 1970).

37. Smith, M. K. Surface charges on mechanical pulp fibers and their effects on drainage and retention on newsprint machines. in TAPPI, Retention and Drainage Technology in Paper Manufacturing. Atlanta, GA, TAPPI (1977):62-67.

38. McKenzie, A. W. The application of zeta potential measurements to pulping and bleaching operations. Appita 22(3):82-86(November, 1968).

39. Anderson, R.; Penniman, J. How to maximize drainage through zeta potential control. Paper Trade Journal 38(16):22-25(September 23, 1974).

40. Davison, R. W.; Cates, R. E. Electrokinetic effects in papermaking systems: theory and practice. Paper Technology and Industry 16(2):107-114(April, 1975).

41. Lindström, T.; Ljunggren, S.; de Ruvo, A.; Söremark, C. Dissolution of carbohydrates and lignin during beating of kraft pulps. Svensk Papperstidning 81(12):397-402(1978).

42. Bryson, H. R. Four years experience with zeta potential control. International Seminar on Paper Mill Chemistry. Amsterdam, Netherlands: no. 3 (September 11-13, 1977).

43. Jaycock, M. J.; Pearson, J. L.; Counter, R.; Husband, F. W.; Effect of cellulose fibre fines on the retention of fillers. Journal of Applied Chemistry and Biotechnology 26:370-374(1976).

44. Chang, Y. C.; Henderson, K.; Matters, J. F. The application of zeta potential for filler retention optimization. Tappi Papermakers Conference Proceedings, New Orleans, LA, :331-336(April 14-16, 1986).

45. Jaycock, M. J.; Pearson, J. L. A study of the retention of pigment during paper formation. Journal of Colloid and Interface Science 55(1):181-190(April, 1976).

46. Melzer, J. Zeta potential and its importance in the manufacture of paper. Das Papier 26:305-332(1972).

47. Strazdins, E. Factors affecting retention of wet-end additives. Tappi 53(1): 80-83(January, 1970).

48. Daruwalla, E. H.; Kangle, P. J.; Nabar, G. M. Adsorption of direct cotton dyes by chemically modified celluloses. Textile Research Journal 31(8):712-721 (August, 1961).

49. Strazdins, E. Significance of electrokinetic charge in polymer adsorption. International Seminar on Paper Mill Chemistry, Amsterdam, Netherlands: no. 5(September 11-13, 1977).

50. Gillham, P. J. The papermaker's appreciation of polyelectrolytes. Appita 34(1):57-60(July, 1980).

51. Marton, J. Surface chemical role of fines in papermaking furnish. Industrial and Engineering Chemistry Product Research and Development 21: 146-150(1982).

52. Ampulski, R. S. The influence of fiber surface charge on tensile strength. Tappi Papermakers Conference Proceedings, Denver, CO, :9-16 (April 15-17, 1985).

53. Britt, K. Sheet formation - advances in retention and drainage concepts. Pulp and Paper Canada 80(6):67-71(June, 1979).

54. Poppel, E.; Bicu, I. Zeta potential and rheological behavior of paper pulp suspensions. Papier 26(4):162-173(April, 1972).

55. Chang, M. Y.; Robertson, A. A. Flocculation studies of fibre suspensions: influence of zeta potential. Pulp and Paper Magazine of Canada 68(9): T-438-444(September, 1967).

56. Grutsch, J. F. Optimization of wastewater treatment processes requires electrokinetic data. The Second International Seminar on Paper Mill Chemistry, New York, NY, :no. 9(September 11, 1978).

57. Frankle, W. E.; Penniman, J. G. Zeta potential measuring by laser: the key to one-pass retention? Paper Trade Journal 157(32):30-38(August 6, 1973).

58. Penniman, J. G. The measurement and control of zeta potential to improve papermaking. Southern Pulp and Paper 40(11):32-40(November, 1977).

59. McKague, J. F.; Etter, D. O.; Pilgrim, J. O.; Griggs, W. H. Practical applications of the electrokinetics of papermaking. Tappi, 57(12):101-103(December, 1974).

60. Melzer, J. Measurement of zeta potential and its practical application in paper mills. Papier 28(10A):V33-39(October, 1974) (IPC translation T-1169).

61. Schmut, R. Zeta potential measurement: applications in the paper industry. Industrial and Engineering Chemistry 56(10):28-33(October, 1964).

62. Sanders, N. D.; Schaefer, J. H. Zeta potential distributions in pulp/PCC mixtures. Tappi Papermakers Conference Proceedings, Washington, D.C.,: 69-74(April 10-12, 1989).

63. Hu, S. Consolidated Papers, Inc., personal communication, 1986.

64. Isenberg, I. H. Pulpwoods of United States and Canada. Appleton, WI, The Institute of Paper Chemistry, 1951:45,51.

65. TAPPI Test Method. T 261 pm-80, 1980.

66. Drain, L. E. The Laser Doppler Technique. New York, NY, John Wiley & Sons, 1980:241 p.

67. The Institute of Paper Chemistry Pulping Group Procedure 73. unpublished work (December, 1958).

68. MacDonald, K. G.; Franklin, J. N. (Eds.) The Pulping of Wood. New York, NY, McGraw-Hill Book Co., 1969:563, 422, 38.

69. Singh, R. P. (Ed.) The Bleaching of Pulp. Atlanta, GA, Tappi Press, 1979:24.

70. Paulson, T. The Institute of Paper Chemistry, personal communication, 1987.

71. TAPPI Test Method. T 248 cm-85, 1985.

72. TAPPI Test Method. T 253 om-86, 1986.

73. TAPPI Test Method. T 236 cm-85, 1985.

74. TAPPI Test Method. T 452 om-87, 1987.

75. Effland, M. J. Modified procedure to determine acid-insoluble lignin in wood. Tappi 60(10):143-144(October, 1977).

76. Berben, S. A.; Rademacher, J. P.; Sell, L. O.; Easty, D. B. Estimation of lignin in wood pulp by diffuse reflectance Fourier-transform infrared spectrometry. Tappi Journal 70(11):129-133(November, 1987).

77. Borchardt, L. G.; Piper, C. V. A gas chromatographic method for carbohydrates as alditol-acetates. Tappi 53(2):257-260(February, 1970).

78. TAPPI Test Method. T204 om-88 (1988).

79. TAPPI Test Method. T 237 om-88, 1988.

80. Katz, S.; Beatson, R. P.; Scallan, A. M. The determination of strong and weak acidic groups in sulfite pulps. Svensk Papperstidning 87(6):R48-53(1984).

81. Wilson, W. K.; Mandel, J. Determination of carboxyl in cellulose. Tappi 44(2):131-137(February, 1961).

82. Davies, J. T.; Rideal, E. K. Interfacial Phenomena. New York, NY, Academic Press, 1963:147.

83. Anderson, P. J. The characteristics of ζ-potential against concentration relations. Transactions of the Faraday Society 54:562-572(1958).

84. Mohlin, U. B. Distinguishing character of TMP. Pulp and Paper Canada 78(12):83-88(December, 1977).

85. Hawes, J. M. Characterization of the Fines Fraction of Papermaking Pulps. A-291 Independent Study. Appleton, WI, The Institute of Paper Chemistry, 1984:63p.

86. Gierer, J. The chemistry of delignification: a general concept, part II. Holzforschung 36(1):55-64(1982).

87. Gierer, J.; Imsgard, F. The reactions of lignins with oxygen and hydrogen peroxide in alkaline media. Svensk Papperstidning 80(16):510-518(1977).

88. Hamilton, J. K. The behaviour of wood carbohydrates in technical pulping processes. Pure and Applied Chemistry 5:197-217(1962).

89. Meier, H. The distribution of polysaccharides in wood fibers. Journal of Polymer Science 51:11-18(1961).

90. Kibblewhite, R. P.; Brookes, D. Distribution of chemical components in the walls of kraft and bisulphite pulp fibers. Wood Science and Technology 10:39-46(1976).

91. Willis, J. M.; Herring, F. G. Carbon-13 CP/MAS nuclear magnetic resonance study of the peroxide bleaching of thermomechanical pulp from white spruce. Holzforschung 41(6):379-382(1987).

92. Sjöström, E. Wood Chemistry: Fundamentals and Applications. New York, NY, Academic Press, 1981:208.

93. Whiting, P.; Goring, D. A. I. Chemical characterization of tissue fractions from the middle lamella and secondary wall of black spruce tracheids. Wood Science and Technology 16:261-267(1982).

94. Westermark, U.; Hardell H.; Iversen, T. The content of protein and pectin in the lignified middle lamella/primary wall of spruce fibers. Holzforschung 40:65-68(1986).

95. Wise, L. E. Wood Chemistry. New York, NY, Reinhold, 1944:470.

96. Marton, J. in K. V. Sarkanen and C. H. Ludwig: Lignins. New York, NY, Wiley Interscience, 1971:676.

97. Marton, J.; Adler, E. Reactions of lignin with methanolic hydrochloric acid: a discussion of some structural questions. Tappi 46(2):92-98(February, 1963).

98. Allan, G. G. in K. V. Sarkanen and C. H. Ludwig: Lignins. New York, NY, Wiley Interscience, 1971:537.

99. Webb, A. A. The Institute of Paper Chemistry, personal communication, 1989.

100. Berben, S. A. The Institute of Paper Chemistry, personal communication, 1989.

101. Proctor, A. R.; Yean, W. Q.; Goring, D. A. I. The topochemistry of delignification in kraft and sulfite pulping of spruce wood. Pulp and Paper Magazine of Canada 68(9):T-445-460(September, 1967).

102. Harned, H. S.; Owen, B. B. The Physical Chemistry of Electrolytic Solutions. New York, NY, Reinhold Publishing Corporation, 1958:217.

103. Rabinov, G.; Heymann, E. Electrokinetic properties and surface conductivity of cellulose and oxycellulose, with reference to the carboxyl group content. The Journal of Physical Chemistry 47(9):655-668(1943).

104. Wågberg, L.; Ödberg, L.; Glad-Nordmark, G. Charge determination of porous substrates by polyelectrolyte adsorption. Part 1. carboxymethylated bleached cellulosic fibers. Nordic Pulp and Paper Research Journal (submitted for publication) 1988.

105. Marton, J. The role of surface chemistry in fines-cationic starch interactions. Tappi 63(4):87-91(April, 1980).

106. Bikerman, J. J. Immobile layer at the solid-liquid interface. Journal of Physical Chemistry 9:880(December, 1941).

107. Herrington, T. M.; Midmore, B. R. Adsorption of ions at the cellulose/aqueous electrolyte interface. Part 1. charge/pH isotherms. Journal of the Chemical Society, Faraday Transactions 1 80:1525-1537(1984).

108. Allan, G. G. in K. V. Sarkanen and C. H. Ludwig: Lignins. New York, NY, Wiley Interscience, 1971:537.

109. Katachalsky, A.; Spitnik, P. Potentiometric titrations of polymethacrylic acid. Journal of Polymer Science 2(4):432-446(1947).

110. Bloys van Treslong, C. J. Interaction between functional groups in low-molecular-weight polyfunctional compounds. Recuil, Journal of the Royal Netherlands Chemical Society 97(1):9-13(January, 1978).

111. Bloys van Treslong, C. J. Evaluation of potentiometric data of weak polyelectrolytes taking account of nearest-neighbour interaction. Recuil, Journal of the Royal Netherlands Chemical Society 97(1):13-21(January, 1978).

112. Bloys van Treslong, C. J.; Moonen, P. Distribution of counterions in solutions of weak polyelectrolytes: A study to the effects of neighbour interactions between charged sites and the structure of the macromolecule. Recuil, Journal of the Royal Netherlands Chemical Society 97(1):22-27(January, 1978).

113. Neale, S. M.; Stringfellow, W. A. The determination of the carboxylic acid group in oxycelluloses. Transactions of the Faraday Society 33:881-889(1937).

114. Iyer, S. R. S.; Jayaram, R. Zeta potential studies in cellulose fibre-aqueous electrolyte solution systems. Journal of the Society of Dyers and Colourists 87(10):338-342(1971).

115. Ottewill, R. H.; Shaw, J. N. Studies on the preparation and characterization of monodisperse polystyrene latices. Part 2: Electrophoretic characterization of surface groupings. Kolloid-Zeitschrift und Zeitschrift fur Polymere 218(1): 34-40(1967).

116. Ikegami, A. Hydration and ion binding of polyelectrolytes. Journal of Polymer Science: Part A 2:907-921(1964).

117. Manning, G. S. Limiting laws and counterion condensation in polyelectrolyte solutions. I Colligative properties. The Journal of Chemical Physics 51(3): 924-933(August 1, 1969).

118. Manning, G. S. Limiting laws and counterion condensation in polyelectrolyte solutions. II Self-diffusion of the small ions. The Journal of Chemical Physics 51(3):934-938(August 1, 1969).

119. Manning, G. S. Counterion binding in polyelectrolyte theory. Accounts of Chemical Research 12:443-449(1979).

120. Klein, J. W.; Ware, B. R. Direct observation of the transition to counterion condensation. Journal of Chemical Physics 80(3):1334-1339(February 1, 1984).

121. Bostrom, G.; Bachlind, S.; Blokhus, A. M.; Hoiland, H. Counterion association to aqueous sodium dodecyl sulfate micelles in the presence of organic additives. Journal of Colloid and Interface Science 128(1):169-175 (March 1, 1989).

122. Treiner, C.; Khodja, A. A.; Fromon, M. Counterion condensation on mixed anionic/nonionic surfactant micelles: Bjerrum's limiting condition. Journal of Colloid and Interface Science 128(2):416-421(March 15, 1989).

123. Ingmanson, W. L.; Andrews, B. D. The effect of beating on filtration resistance and its components of specific surface and specific volume. Tappi 42(1): 29-35(January, 1959).

124. Thode, E. F.; Swanson, J. W.; Becher, J. J. Nitrogen adsorption on solvent-exchanged wood cellulose fibers: Indications of "total" surface area and pore size distribution. Journal of Physical Chemistry 62:1036-1039(1958).

125. Schofield, R. K.; Talibuddin, O. Measurement of internal surface by negative adsorption. Discussions of the Faraday Society 3:51-56(1948).

126. Standley, J. R. Pulp Fiber Surface Area by Polymer Adsorption. A-190 Independent Study. Appleton, WI, The Institute of Paper Chemistry, 1986:54p.

127. Herren, B. J. Shafer, S. G.; VanAlstine, J.; Harris, J. M.; and Snyder, R. S. Control of electroosmosis in coated quartz capillaries. Journal of Colloid and Interface Science. 115(1):46-55(January, 1987).

128. Patterson, W. J. Development of polymeric coatings for control of electroosmotic flow in ASTP MA-011 electrophoresis technology experiment. National Aeronautics and Space Administration Technical Memorandum, NASA TM X-73311, Washington, D.C., The United States Government Printing Office, 1976:56p.

129. Montgomery, D. C. Design and Analysis of Experiments. New York, NY, John Wiley & Sons, 1984:28, 223.

APPENDIX I

THERMOMECHANICAL PULP BLEACHING

BLEACH LIQUOR PREPARATION

A hydrogen peroxide bleaching solution of approximately 9g/L was prepared in the following manner:

1. Add 10.0mL of magnesium sulfate ($MgSO_4$) solution (25g/L) to a 500-mL amber bottle.

2. Add 464mL of distilled water.

3. Add 11.25mL of NaOH solution (50g/L).

4. Add 15g of a 30% H_2O_2 solution, cap and mix thoroughly.

BLEACH LIQUOR ANALYSIS

The following procedure was used to analyze the hydrogen peroxide concentration of both freshly prepared and spent bleach liquors.

1. Pipette 5.0mL of peroxide bleach liquor into a 250-mL Erlenmeyer flask containing 100mL of distilled water saturated with KI crystals.

2. Add 3 mL of acetic acid.

3. Add 5 drops of 5% Ammonium molybdate solution.

4. Titrate the liberated Iodine with 0.10N sodium thiosulfate using a starch indicator.

Calculation: $$H_2O_2 = \frac{(17)(\text{mL thiosulfate})(\text{N of thiosulfate})}{(\text{mL of bleach liquor analyzed})}$$

BLEACHING

Calculations

The following set of calculations were made prior to bleaching the TMP:

1. The volume of bleach liquor required for a 2.0% hydrogen peroxide charge based on oven dry fiber was determined.

2. The quantity of magnesium sulfate entering the system with the bleach liquor was calculated as follows: g $MgSO_4$ = 0.0005 x mL bleach liquor.

3. The volume of additional magnesium sulfate solution required to reach a final concentration of 0.2 g/L in the liquid phase was calculated.

4. The quantity of sodium silicate (40°Be´solution) required for a 5% addition level on oven dry pulp was calculated.

5. The volume of distilled water required to give a final consistency of 5% after the addition of all other chemicals was calculated.

Procedure

1. Add the necessary additional magnesium sulfate to a 600-mL beaker in the form of a 25g/L solution.

2. Add the required sodium silicate.

3. Add the required quantity of water and adjust the pH to 11.5 with NaOH.

4. Add the hydrogen peroxide bleach liquor and mix thoroughly.

5. Weigh the pulp into a heat-sealable bag, add liquor, seal, and mix well.

6. Open bag, recheck pH, adjust if necessary, reseal ,and mix.
7. Place bag in a constant temperature water bath (35°C).

8. Repeat steps 6 and 7 periodically during the bleach trial.

9. At the end of the trial remove the bag, filter the residual liquor and wash the pulp thoroughly with distilled water using a Büchner funnel.

10. Analyze the residual liquor in the same manner as the original liquor. (Note: use a lower concentration of sodium thiosulfate).

APPENDIX II

WEAK ACID CONTENT ANALYSIS USING METHYLENE BLUE DYE ADSORPTION

The following procedure was used to measure the weak acid content of pulp fibers and fiber fines via methylene blue dye adsorption.

Solutions

Methylene Blue Dye Stock Solution (0.002M)

A methylene blue dye stock solution was prepared by dissolving 2.0 millimoles of methylene blue chloride (0.640g) in one liter of distilled water.

Buffer Stock Solution

A stock buffer solution was prepared by dissolving 6.25 millimoles of diethyl barbituric acid (1.150g) and 4.0 millimoles of sodium hydroxide (0.16g) in one liter of distilled water.

Procedure for Preparation of Calibration Curve

Step 1.

1. Add 25mL of buffer solution to 100mL distilled water in a 250-mL volumetric flask.

2. Add the desired volume of methylene blue dye stock solution and dilute to 250mL with distilled water. Invert 10 times.

Step 2.

1. Add 25mL of distilled water to a 100-mL volumetric flask.

2. Add 10.0mL of methylene blue solution prepared in step 1, and 10mL of 0.10M hydrochloric acid.

3. Fill to the mark with distilled water, cap and invert 10 times.

A series of ten standard methylene blue solutions were prepared ranging from 0.0 to 20×10^{-6}M were prepared following the above procedure. Solution absorptance was measured at 620nm in disposable polystyrene cuvettes using a Perkin-Elmer model 320 Spectrophotometer. The calibration curve shown in Fig. 56 was constructed from the standard solution absorptance data.

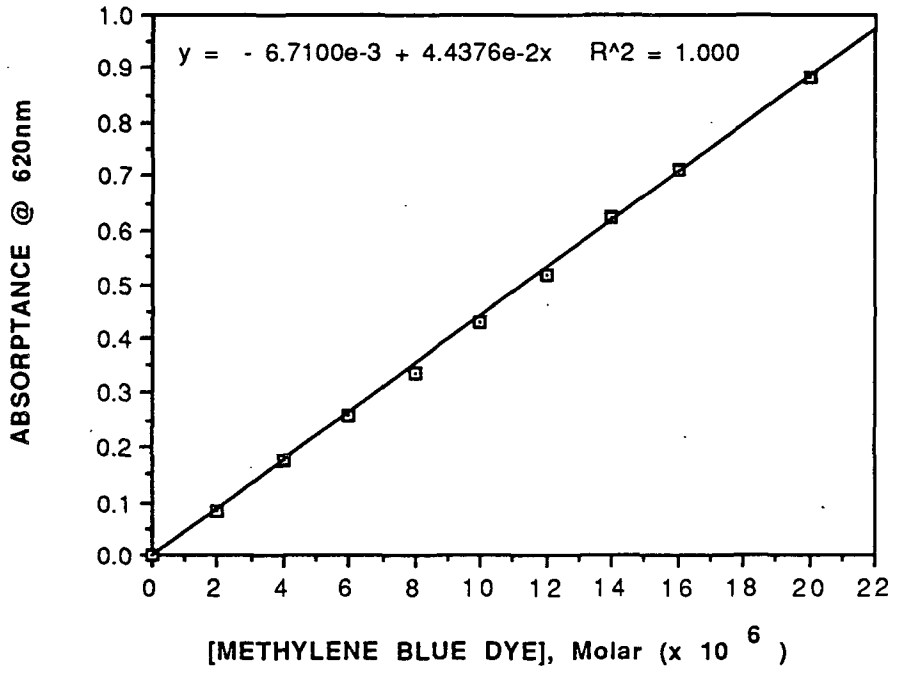

Figure 56. Methylene blue dye calibration curve.

Because of differences in the quantity of long fiber and fiber fines available, slightly different procedures were used during the dye adsorption and dye analysis phases of the technique. The following schematics illustrate the procedures used for each fraction.

Methylene Blue Dye Weak Acid Content Analysis Procedures

Step 1: Methylene Blue Dye Adsorption

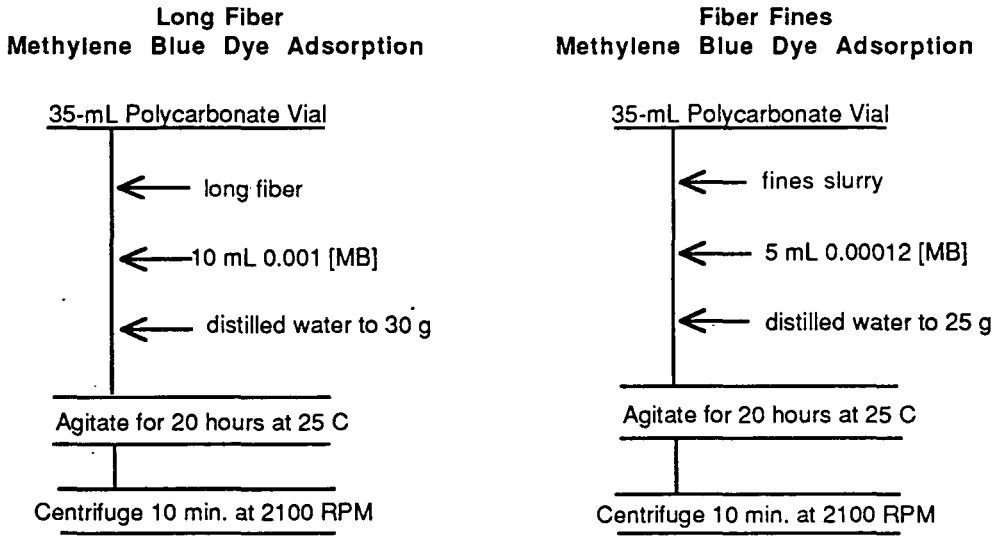

Step 2: Unadsorbed Methylene Blue Dye Analysis

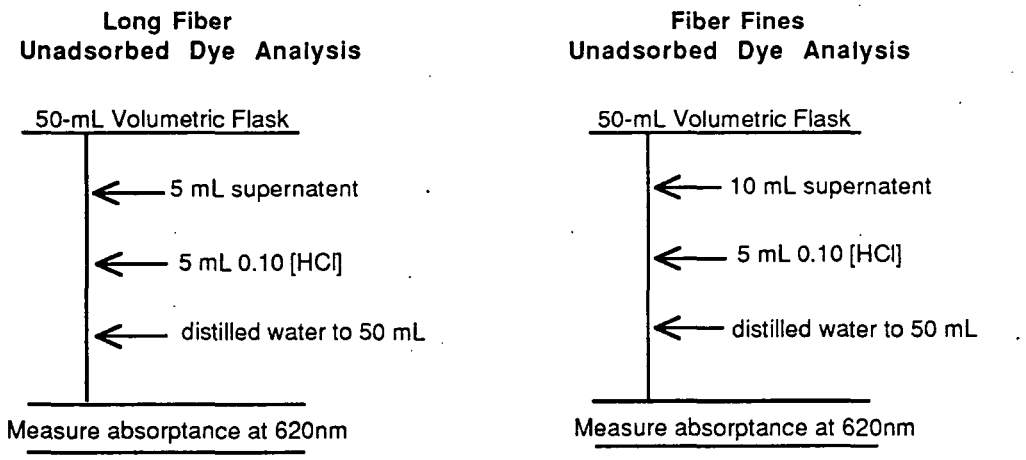

For each sample, a series of five adsorption vials were prepared containing equal amounts of dye and varying weights of fibers or fines. After

measuring the concentration of unadsorbed dye, the percent of dye consumed was calculated and plotted versus dry fiber (or fines) weight. Figures 57 and 58 are examples of such plots for bleached kraft fibers and fines (Sample B32).

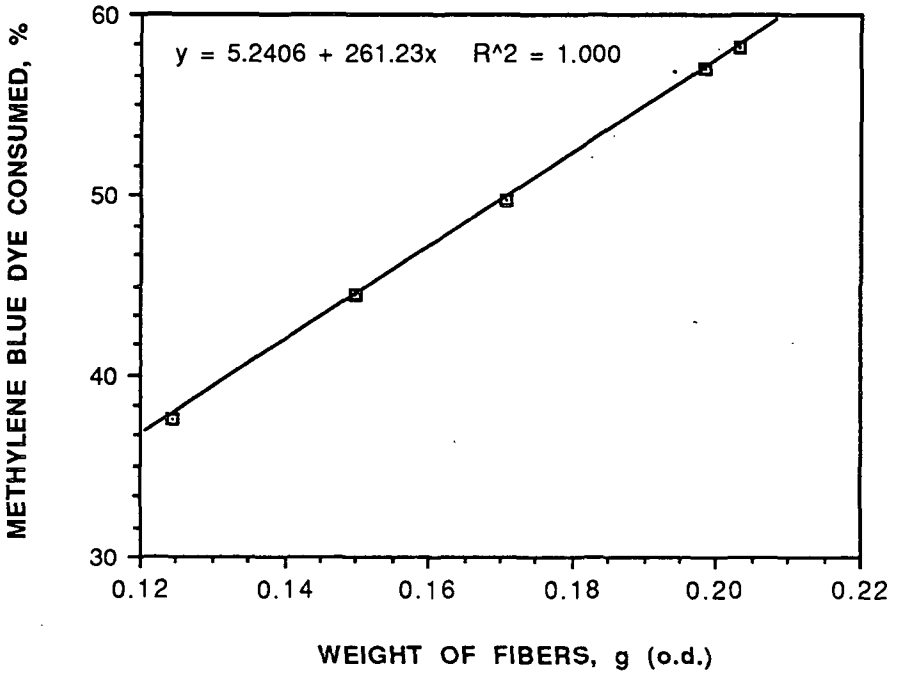

Figure 57. Percent methylene blue dye adsorbed versus dry fiber weight (Sample B32 - Long Fibers).

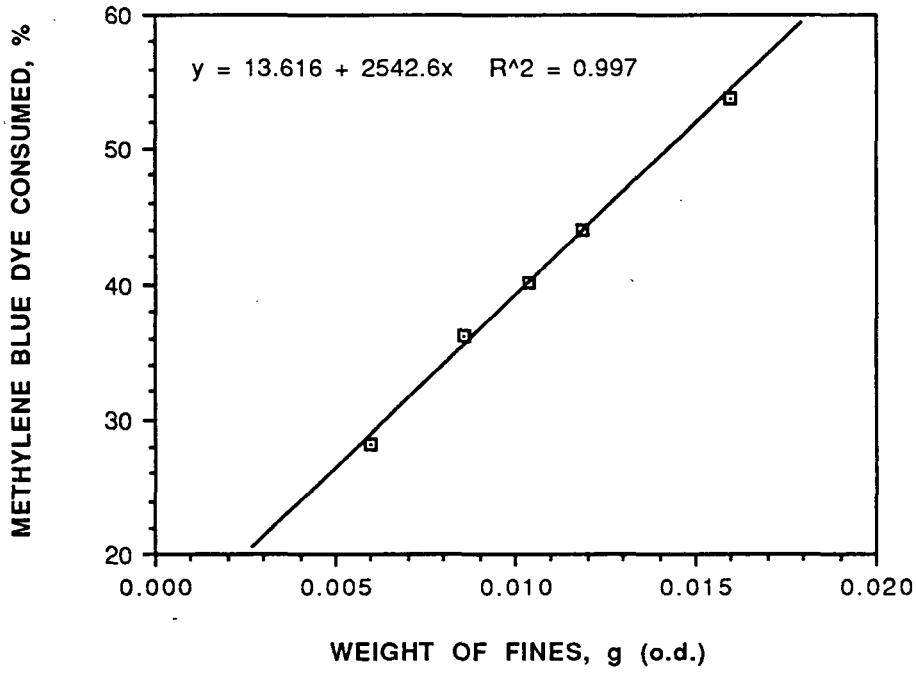

Figure 58. Percent methylene blue dye adsorbed versus dry fines weight (Sample B32 - Fines, < 200-mesh).

The weak acid content (meq/100g) was calculated using the following equation for both long fibers and fiber fines:

$$\text{Weak Acid Content} = \frac{\text{(milliequivalents consumed at 50\% consumption)}}{\text{(weight required for 50\% dye consumption)}} \times 100$$

APPENDIX III

COATING OF QUARTZ CAPILLARY WITH METHYLCELLULOSE

Coating a quartz microelectrophoresis capillary with methylcellulose has been reported in the literature to reduce the fluid velocity profile that develops during a measurement as a result of electroosmosis.[127,128] The high molecular weight polymer forms a film on the capillary wall that shields the surface charge, thus reducing the electroosmotic effect.

The initial work was conducted with Methocel HG (Dow Chemical Co.). The coating was applied by soaking a quartz capillary, cleaned in a chromic acid cleaning solution, in a solution of 0.10% Methocel HG for three days. Excess methylcellulose was removed from the capillary by rinsing with distilled water. The capillary was not allowed to dry prior to installation in the PC4 sample cell. The electrophoretic mobility of a dilute latex slurry (Interfacial Dynamics Corp., catalogue no. 2-27-92) was measured at various locations across the diameter of the capillary. The shape of the electrophoretic mobility profile was used as a measure of the fluid velocity profile. Electrophoretic mobility profile results before and after coating with Methocel HG are presented in Fig. 59. Decreasing the pH resulted in a less negative particle mobility, but did not change the shape of the profile. This indicates that essentially no carboxyl groups are present on the methylcellulose molecule.

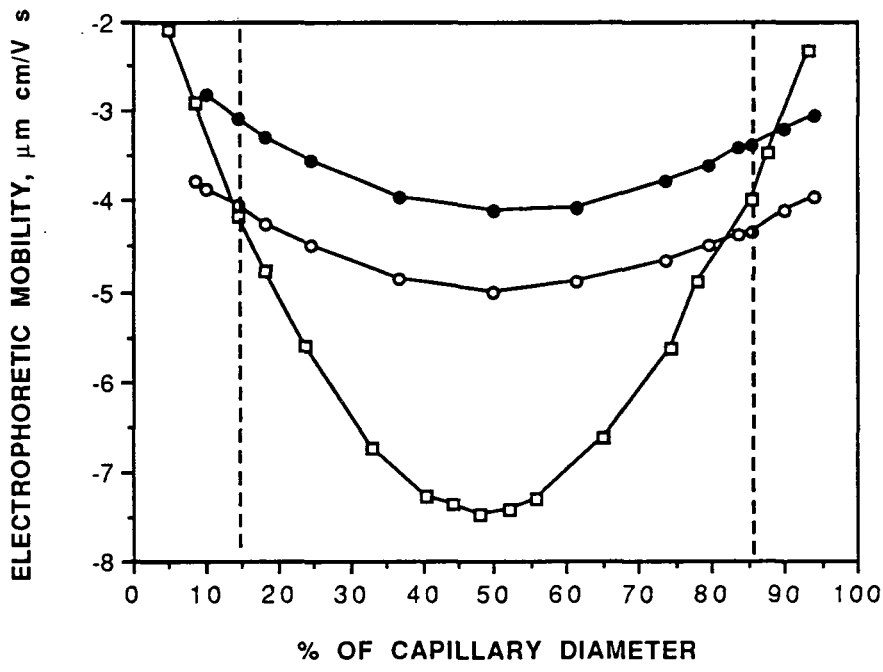

Figure 59. Electrophoretic mobility profile for latex 2-27-92 in 0.01M NaCl. (□ = uncoated: pH = 7.10; ○ = coated: pH = 7.05; ● = coated: pH = 4.03; "- - -" = stationary layer).

Methylcellulose coatings have been reported to desorb from a quartz capillary surface within a few days.[127] To test the durability of the methylcellulose coating, a series of velocity profiles were measured after flushing the capillary with 0, 100, 500, and 1,000mL of electrolyte solution. Flushing was conducted by repeated injections of 10mL volumes to simulate sample loading. No change in the velocity profile was observed, indicating a durable coating film.

Because the Methocel HG sample was quite old and somewhat difficult to solubilize a new methylcellulose sample was obtained from Dow Chemical Co., Methocel J75 MS-N. A new capillary was placed in a 0.10% solution of Methocel J75 for one hour, rinsed with distilled water, and installed in the PC4 cell. The

electrophoretic mobility profile of latex 2-27-92 was measured in a series of background electrolytes ranging from 0.0002M to 0.01M NaCl. The results are shown in Fig. 60.

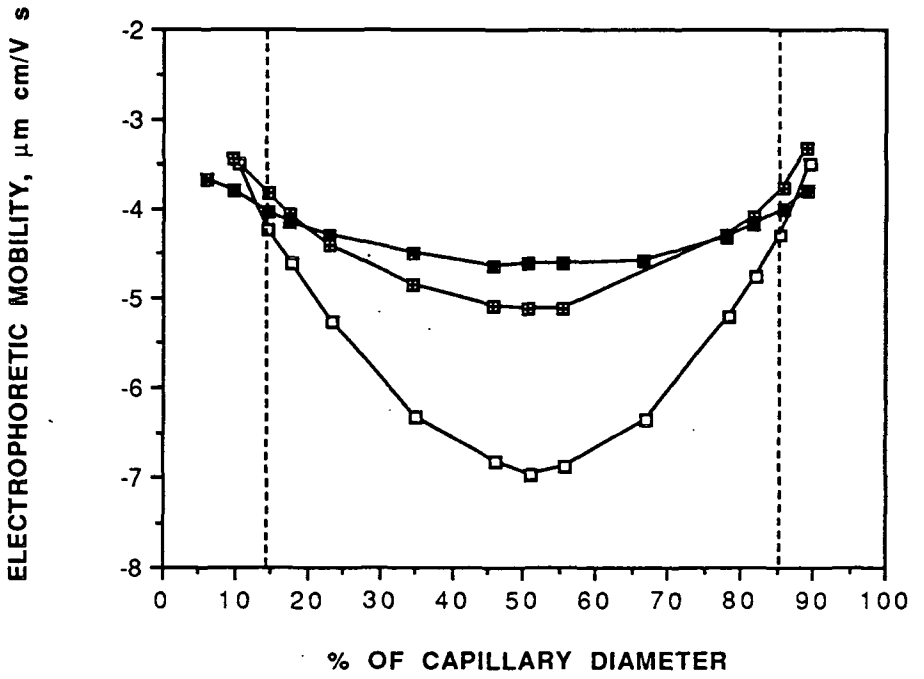

Figure 60. Electrophoretic mobility profile for latex 2-27-92 various electrolytes. (□ = 0.0002M NaCl; ▣ = 0.002M NaCl; ■ = 0.01M NaCl; "- - -" = stationary layer)

As the electrolyte concentration decreased the velocity profile became more severe. At high electrolyte concentrations the electrical double layer of the quartz capillary has been collapsed to within the film thickness of the methylcellulose coating, resulting in little if any net charge at the film surface. As the electrolyte concentration decreases the double layer expands past the film thickness and the net charge at the film surface gives rise to electroosmotic fluid flow. As a result, the velocity profile will remain relatively flat for the 0.002M and

0.01M samples but the 0.0002M measurements will be conducted in a system with a considerable velocity profile. When measuring wood fiber fines, all electrophoretic mobility measurements were made at one of the stationary layers.

The electrophoretic mobility profile present in the methylcellulose-coated capillary during testing of TMP and kraft fines is shown in Fig. 61 for 0.01M NaCl.

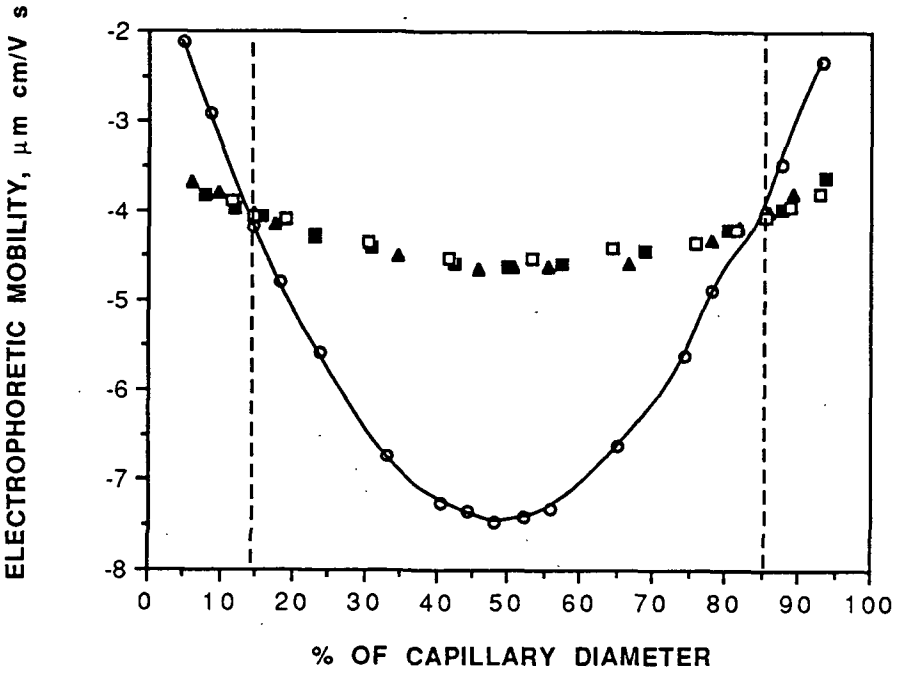

Figure 61. Electrophoretic mobility profile of latex 2-27-92 in 0.01M NaCl (o = uncoated; ■ = profile before testing TMP fines; ▲ = profile after testing TMP fines/before testing kraft fines; □ = profile after testing kraft fines).

APPENDIX IV

ELECTROPHORETIC MOBILITY RESULTS FOR THERMOMECHANICAL PULP FINES AND REPRESENTATIVE HISTOGRAMS

Spruce TMP Fines in 0.0002M NaCl

	Unbleached		Bleach 1		Bleach 2	
	E.M.	St. Dev.	E.M.	St. Dev.	E.M.	St. Dev.
	-2.79	0.28	-2.62	0.51	-2.50	0.44
	-2.17	0.43	-2.44	0.37	-2.27	0.30
	-2.34	0.39	-2.59	0.25	-2.71	0.38
	-2.34	0.39	-2.72	0.43	-2.53	0.50
	-2.57	0.44	-2.79	0.39	-2.44	0.47
	-2.47	0.52	-2.31	0.51	-2.61	0.56
	-2.39	0.38	-2.44	0.39	-2.85	0.37
	-2.19	0.46	-2.67	0.51	-2.42	0.41
	-2.29	0.19	-2.67	0.46	-2.45	0.31
	-2.33*	0.42	-2.65*	0.46	-2.42	0.30
Average:	-2.39	0.39	-2.59	0.43	-2.52	0.39
St. Dev.:	(0.19)	(0.10)	(0.16)	(0.09)	(0.17)	(0.08)

* indicates electrophoretic mobility histogram appears in Appendix.

Spruce TMP Fines in 0.002M NaCl

	Unbleached		Bleach 1		Bleach 2	
	E.M.	St. Dev.	E.M.	St. Dev.	E.M.	St. Dev.
	-1.41	0.25	-1.71	0.22	-1.93	0.26
	-1.20	0.32	-1.99	0.25	-1.85	0.19
	-1.38	0.28	-1.82	0.26	-1.80	0.19
	-1.18	0.23	-1.80	0.26	-1.97	0.22
	-1.37	0.24	-1.88	0.22	-1.87	0.20
	-1.49	0.32	-1.83	0.31	-1.80	0.22
	-1.39	0.28	-1.73	0.27	-1.90	0.23
	-1.02	0.18	-1.91	0.30	-1.69	0.25
	-1.28*	0.28	-1.85	0.30	-1.68	0.20
	-1.26	0.32	-1.57	0.26	-1.95	0.32
Average:	-1.30	0.27	-1.81	0.27	-1.84	0.23
St. Dev.:	(0.15)	(0.05)	(0.12)	(0.03)	(0.11)	(0.04)

Spruce TMP Fines in 0.01M NaCl

	Unbleached		Bleach 1		Bleach 2	
	E.M.	St. Dev.	E.M.	St. Dev.	E.M.	St. Dev.
	-0.73	0.20	-1.21	0.20	-1.08	0.21
	-0.65	0.18	-1.22	0.20	-1.15	0.22
	-0.80	0.23	-1.23	0.21	-1.24	0.24
	-0.79	0.22	-1.19	0.20	-1.27	0.22
	-0.68	0.19	-1.29	0.25	-1.21	0.21
	-0.82	0.23	-1.31	0.24	-1.15	0.18
	-0.80	0.21	-1.23	0.21	-1.13	0.18
	-0.70	0.22	-1.17	0.20	-1.15	0.20
	-0.73	0.25	-1.11	0.24	-1.24	0.22
	-0.74*	0.21	-1.21	0.23	-1.16	0.23
Average:	-0.74	0.21	-1.22	0.22	-1.18	0.21
St. Dev.:	(0.06)	(0.02)	(0.06)	(0.02)	(0.06)	(0.02)

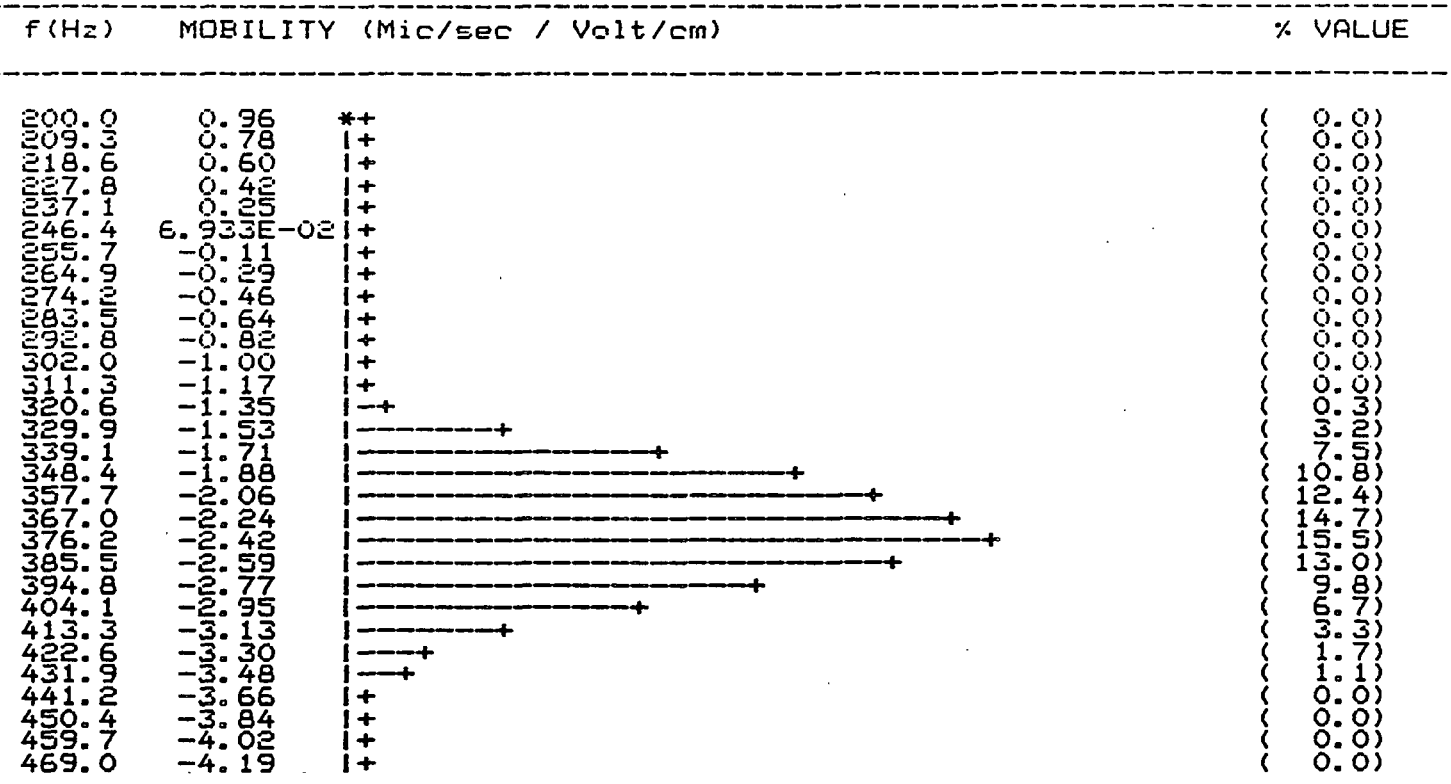

Figure. 62. Electrophoretic mobility histogram of unbleached TMP in 0.0002M NaCl.

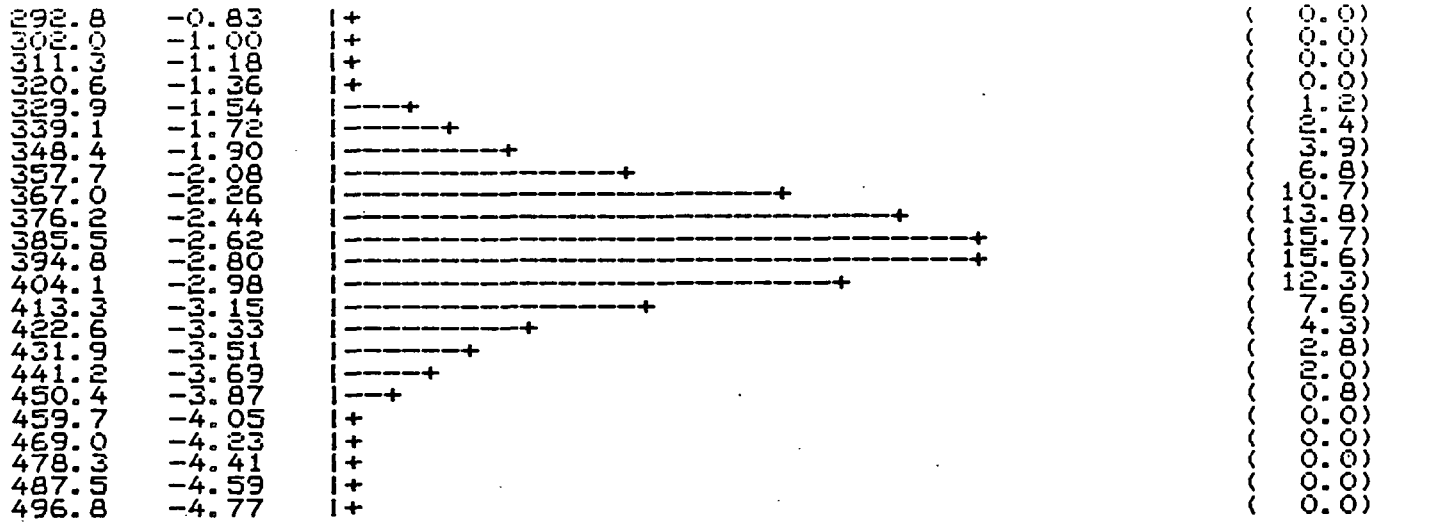

Figure. 63. Electrophoretic mobility histogram of bleached TMP in 0.0002M NaCl.

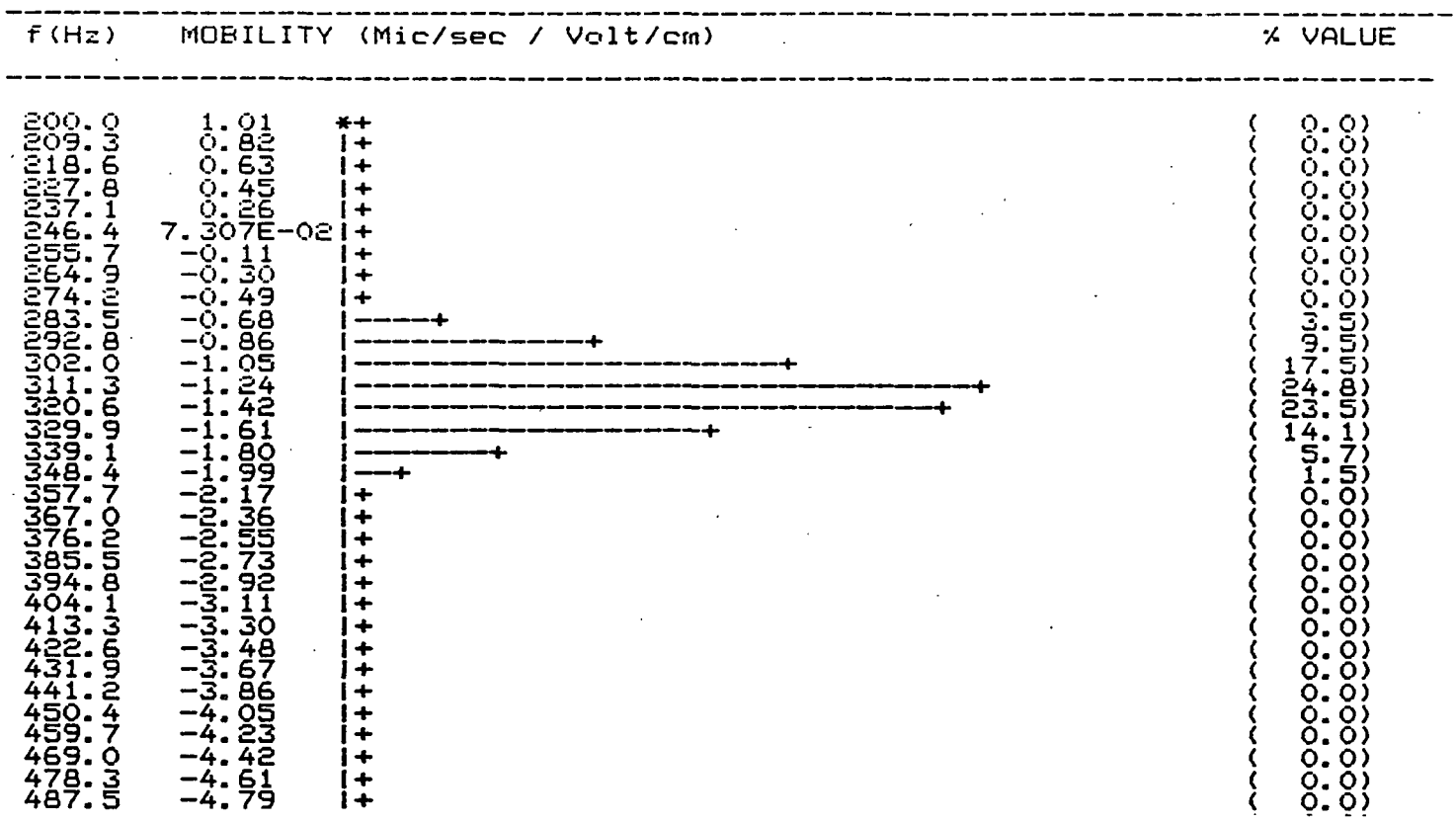

Figure. 64. Electrophoretic mobility histogram of unbleached TMP in 0.002M NaCl.

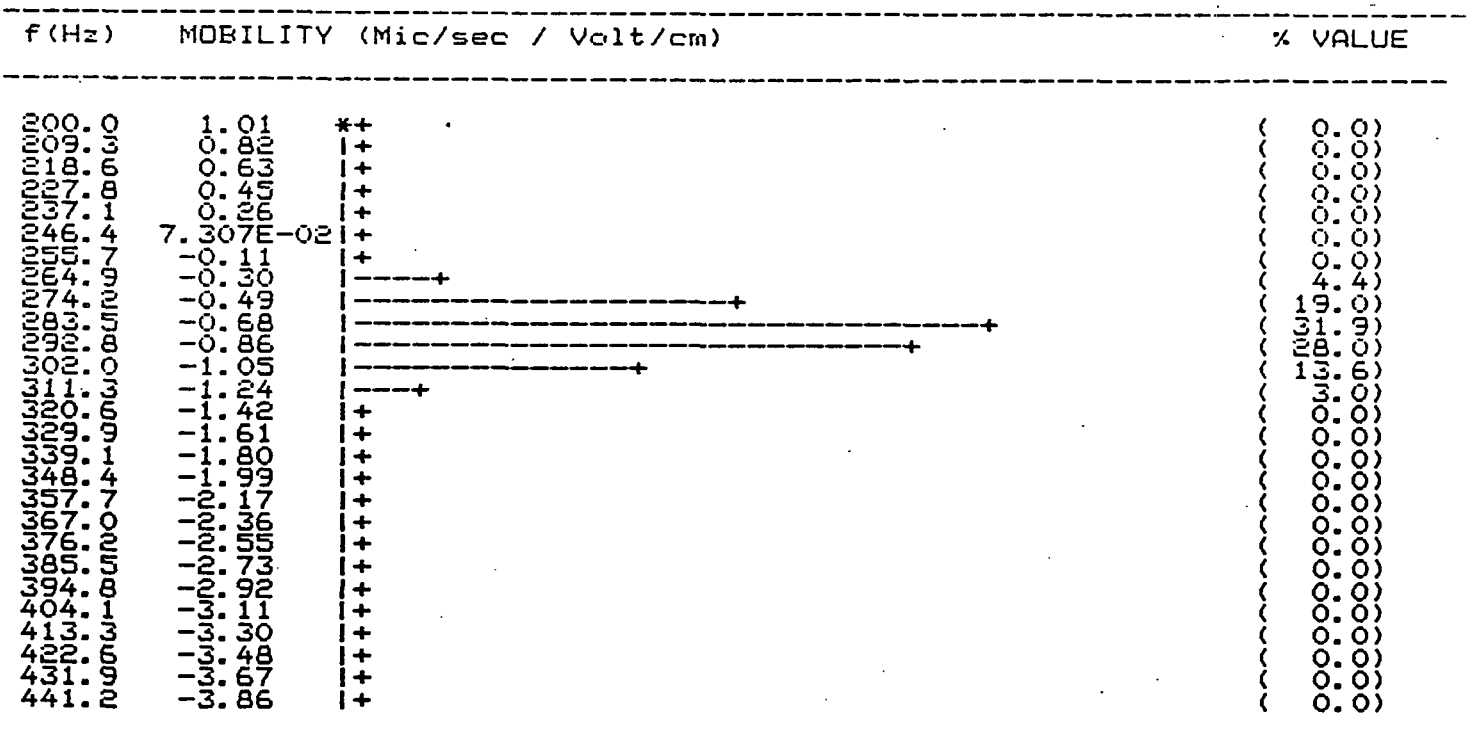

Figure. 65. Electrophoretic mobility histogram of unbleached TMP in 0.01M NaCl.

APPENDIX V

STATISTICAL ANALYSIS OF TMP ELECTROPHORETIC MOBILITY DATA

The effect of bleaching on the electrophoretic mobility of TMP fines was analyzed statistically using two-sample *t*-test. The mean unbleached electrophoretic mobility was compared to the mean electrophoretic mobility of each bleached samples using the following set of hypotheses:

Null hypothesis: H_0: $E.M._U = E.M._B$

Alternative hypothesis: H_1: $E.M._U \neq E.M._B$

where: $E.M._U$ = mean electrophoretic mobility of Unbleached fines

$E.M._B$ = mean electrophoretic mobility of Bleached fines

The variances of neither sample population were known, and were not assumed to be equal. Therefore, the test statistic used in the analysis was:[129]

$$t_o = (E.M._U - E.M._B)/[(S_U^2/n_U) + (S_B^2/n_B)]^{0.5} \quad [23]$$

where: S^2 = sample variance

n = number of observations

The test statistic, t_o, is not distributed exactly as *t*. However, the distribution of t_o is well-approximated by *t* if the following expression is used for the degrees of freedom, ν.[129]

$$\nu = \{[(S_U^2/n_U) + (S_B^2/n_B)]^2/[(S_U^2/n_U)^2/(n_U + 1) + (S_B^2/n_B)^2/(n_B + 1)]\} - 2 \quad [24]$$

The null hypothesis is rejected when $|t_o| > t_{\alpha/2}$. Rejection of the null hypothesis indicates the means of the two distributions are significantly different. The results of the statistical analysis are presented in Tables 25 and 26 below:

Table 25. Statistical comparison of unbleached and bleach 1 fines.

[NaCl]	E.M.$_U$	S_U	E.M.$_B$	S_B	ν	t_o	$t_{.025}$	Significant ?
0.0002	-2.39	0.19	-2.59	0.16	24.29	2.55	2.06	**Yes**
0.002	-1.30	0.15	-1.81	0.12	22.21	8.40	2.07	**Yes**
0.01	-0.74	0.06	-1.22	0.06	34.00	17.89	2.03	**Yes**

Table 26. Statistical comparison of unbleached and bleach 2 fines.

[NaCl]	E.M.$_U$	S_U	E.M.$_B$	S_B	ν	t_o	$t_{.025}$	Significant ?
0.0002	-2.39	0.19	-2.52	0.17	27.18	1.61	2.05	*No*
0.002	-1.30	0.15	-1.84	0.11	19.28	9.18	2.09	**Yes**
0.01	-0.74	0.06	-1.18	0.06	34.00	16.40	2.03	**Yes**

From the above analysis it is clear that the more negative electrophoretic mobility that results from bleaching TMP with hydrogen peroxide is statistically significant at a 95% confidence level. The results from the replicate bleach treatments were also compared using a similar analysis. The results, shown below, indicate the replicate treatments are not significantly different.

Table 27. Statistical comparison of bleach 1 and bleach 2 fines.

[NaCl]	E.M.$_B$	S_{B1}	E.M.$_B$	S_{B2}	ν	t_o	$t_{.025}$	Significant ?
0.0002	-2.59	0.16	-2.52	0.17	38.79	0.95	2.03	*No*
0.002	-1.81	0.12	-1.84	0.11	28.48	0.58	2.05	*No*
0.01	-1.22	0.06	-1.18	0.06	34.00	1.49	2.03	*No*

APPENDIX VI

ELECTROPHORETIC MOBILITY RESULTS FOR KRAFT PULP FINES AND REPRESENTATIVE HISTOGRAMS

Unbleached Kraft Fines (7,500 revolutions) in 0.0002M NaCl

	55.4% yield		49.9% yield		44.7% yield	
	E.M.	St. Dev.	E.M.	St. Dev.	E.M.	St. Dev.
	-2.50	0.36	-2.23	0.32	-2.13	0.32
	-2.47	0.31	-2.35	0.35	-2.18*	0.36
	-2.48	0.37	-2.35	0.37	-2.19	0.31
	-2.38	0.27	-2.32	0.28	-2.20	0.34
	-2.36	0.31	-2.22	0.27	-2.16	0.36
	-2.40	0.34	-2.25*	0.28	-2.17	0.38
	-2.37*	0.32	-2.34	0.35	-2.13	0.34
	-2.36	0.34	-2.30	0.29	-2.15	0.33
	-2.32	0.31	-2.25	0.31	-2.14	0.33
	-2.31	0.30	-2.24	0.31	-2.10	0.35
Average:	-2.40	0.32	-2.29	0.31	-2.16	0.34
St. Dev.:	(0.07)	(0.03)	(0.06)	(0.04)	(0.03)	(0.02)

Unbleached Kraft Fines (15,000 revolutions) in 0.0002M NaCl

	55.4% yield		49.9% yield		44.7% yield	
	E.M.	St. Dev.	E.M.	St. Dev.	E.M.	St. Dev.
	-2.47	0.32	-2.33	0.34	-2.07	0.29
	-2.40	0.30	-2.42	0.25	-1.97	0.31
	-2.45	0.31	-2.42	0.35	-2.14	0.38
	-2.47	0.25	-2.47	0.32	-2.18	0.40
	-2.44	0.31	-2.41	0.33	-2.22	0.32
	-2.36	0.30	-2.44	0.35	-2.19	0.36
	-2.33	0.28	-2.36	0.29	-2.12	0.39
	-2.40	0.33	-2.47	0.35	-2.16	0.29
	-2.24	0.34	-2.32	0.38	-2.17	0.36
	-2.28	0.30	-2.29	0.33	-2.22	0.24
Average:	-2.38	0.30	-2.39	0.33	-2.14	0.33
St. Dev.:	(0.08)	(0.03)	(0.07)	(0.04)	(0.08)	(0.05)

Unbleached Kraft Fines (7,500 revolutions) in 0.002M NaCl

	55.4% yield		49.9% yield		44.7% yield	
	E.M.	St. Dev.	E.M.	St. Dev.	E.M.	St. Dev.
	-1.69	0.20	-1.58	0.24	-1.33	0.22
	-1.72	0.21	-1.54	0.28	-1.33	0.23
	-1.74	0.18	-1.54	0.22	-1.34	0.22
	-1.65	0.22	-1.52	0.21	-1.37	0.24
	-1.70	0.20	-1.51	0.23	-1.32	0.24
	-1.73	0.25	-1.61	0.24	-1.34	0.26
	-1.66	0.23	-1.51	0.24	-1.35	0.23
	-1.68	0.23	-1.55	0.22	-1.32	0.22
	-1.58	0.23	-1.48	0.22	-1.34	0.22
	-1.64	0.26	-1.51	0.23	-1.32	0.27
Average:	-1.68	0.22	-1.54	0.23	-1.34	0.23
St. Dev.:	(0.05)	(0.02)	(0.04)	(0.02)	(0.02)	(0.02)

Unbleached Kraft Fines (15,000 revolutions) in 0.002M NaCl

	55.4% yield		49.9% yield		44.7% yield	
	E.M.	St. Dev.	E.M.	St. Dev.	E.M.	St. Dev.
	-1.73	0.24	-1.64	0.22	-1.43	0.26
	-1.73	0.21	-1.68	0.22	-1.42	0.24
	-1.69	0.23	-1.62	0.25	-1.45	0.28
	-1.66	0.22	-1.57	0.26	-1.46	0.21
	-1.70	0.28	-1.61	0.26	-1.46	0.22
	-1.77	0.22	-1.58	0.23	-1.40	0.23
	-1.57	0.24	-1.58	0.23	-1.42	0.28
	-1.65	0.22	-1.41	0.21	-1.48	0.21
	-1.61	0.26	-1.59	0.21	-1.54	0.30
	-1.67	0.22	-1.61	0.25	-1.41	0.26
Average:	-1.68	0.23	-1.59	0.23	-1.45	0.25
St. Dev.:	(0.06)	(0.02)	(0.07)	(0.02)	(0.04)	(0.03)

Unbleached Kraft Fines (7,500 revolutions) in 0.01M NaCl

	55.4% yield		49.9% yield		44.7% yield	
	E.M.	St. Dev.	E.M.	St. Dev.	E.M.	St. Dev.
	-1.17	0.18	-0.95	0.17	-0.81	0.20
	-1.21	0.19	-1.01	0.19	-0.81	0.17
	-1.15	0.19	-0.98	0.18	-0.80	0.17
	-0.84	0.14	-0.98	0.19	-0.80	0.17
	-1.12	0.21	-0.98	0.17	-0.77	0.18
	-1.15	0.18	-0.96	0.18	-0.80	0.18
	-1.14	0.19	-0.98	0.18	-0.83	0.22
	-1.15	0.20	-1.04	0.19	-0.79	0.19
	-1.10	0.19	-0.99	0.18	-0.78	0.20
	-1.14	0.19	-0.98	0.17	-0.82	0.19
Average:	-1.12	0.18	-0.99	0.18	-0.80	0.19
St. Dev.:	(0.11)	(0.02)	(0.03)	(0.01)	(0.02)	(0.02)

Unbleached Kraft Fines (15,000 revolutions) in 0.01M NaCl

	55.4% yield		49.9% yield		44.7% yield	
	E.M.	St. Dev.	E.M.	St. Dev.	E.M.	St. Dev.
	-1.15	0.21	-1.05	0.29	-0.80	0.18
	-1.13	0.20	-1.06	0.18	-0.82	0.17
	-1.14	0.19	-1.07	0.19	-0.77	0.19
	-1.15	0.19	-1.07	0.21	-0.76	0.18
	-1.09	0.19	-1.05	0.19	-0.81	0.19
	-1.13	0.20	-1.06	0.18	-0.79	0.17
	-1.19	0.23	-1.02	0.18	-0.77	0.20
	-1.11	0.19	-1.05	0.20	-0.79	0.19
	-1.13	0.22	-1.02	0.18	-0.78	0.20
	-1.12	0.18	-1.03	0.20	-0.78	0.18
Average:	-1.13	0.20	-1.05	0.20	-0.79	0.19
St. Dev.:	(0.03)	(0.02)	(0.02)	(0.04)	(0.02)	(0.01)

Bleached Kraft Fines (7,500 revolutions) in 0.0002M NaCl

	55.4% yield		49.9% yield		44.7% yield	
	E.M.	St. Dev.	E.M.	St. Dev.	E.M.	St. Dev.
	-2.20	0.27	-2.14*	0.37	-1.99	0.34
	-2.21*	0.28	-2.19	0.43	-2.04	0.33
	-2.35	0.29	-2.09	0.32	-1.97	0.35
	-2.31	0.27	-2.18	0.40	-1.94	0.34
	-2.13	0.26	-2.10	0.33	-1.86	0.23
	-2.27	0.25	-2.20	0.27	-1.97*	0.33
	-2.27	0.29	-2.06	0.37	-1.83	0.33
	-2.00	0.32	-1.99	0.37	-1.89	0.31
	-2.08	0.30	-1.98	0.28	-1.98	0.28
	-2.06	0.25	-2.08	0.45	-1.99	0.35
Average:	-2.19	0.28	-2.10	0.36	-1.95	0.32
St. Dev.:	(0.12)	(0.02)	(0.08)	(0.06)	(0.07)	(0.04)

Bleached Kraft Fines (15,000 revolutions) in 0.0002M NaCl

	55.4% yield		49.9% yield		44.7% yield	
	E.M.	St. Dev.	E.M.	St. Dev.	E.M.	St. Dev.
	-2.15	0.26	-2.18	0.29	-2.11	0.38
	-2.12	0.25	-2.10	0.39	-2.04	0.30
	-2.33	0.27	-2.15	0.28	-1.99	0.30
	-2.28	0.26	-2.06	0.32	-1.99	0.27
	-2.24	0.30	-2.06	0.30	-2.06	0.30
	-2.24	0.32	-2.18	0.32	-2.02	0.23
	-2.15	0.29	-2.18	0.32	-1.95	0.27
	-2.16	0.29	-2.12	0.28	-2.00	0.32
	-2.10	0.38	-2.05	0.28	-1.96	0.26
	-2.09	0.31	-1.98	0.25	-1.97	0.28
Average:	-2.19	0.29	-2.11	0.30	-2.01	0.29
St. Dev.:	(0.09)	(0.04)	(0.07)	(0.04)	(0.05)	(0.04)

Bleached Kraft Fines (7,500 revolutions) in 0.002M NaCl

	55.4% yield		49.9% yield		44.7% yield	
	E.M.	St. Dev.	E.M.	St. Dev.	E.M.	St. Dev.
	-1.50	0.23	-1.29	0.22	-1.18	0.23
	-1.44	0.25	-1.32	0.25	-1.25	0.24
	-1.36	0.20	-1.33	0.27	-1.21	0.23
	-1.31	0.22	-1.37	0.26	-1.17	0.22
	-1.34	0.22	-1.35	0.25	-1.22	0.23
	-1.44	0.24	-1.32	0.24	-1.21	0.25
	-1.41	0.22	-1.24	0.24	-1.14	0.23
	-1.39	0.19	-1.31	0.23	-1.23	0.25
	-1.35	0.29	-1.32	0.29	-1.13	0.24
	-1.34	0.23	-1.26	0.26	-1.15	0.22
Average:	-1.39	0.23	-1.31	0.25	-1.19	0.23
St. Dev.:	(0.06)	(0.03)	(0.04)	(0.02)	(0.04)	(0.01)

Bleached Kraft Fines (15,000 revolutions) in 0.002M NaCl

	55.4% yield		49.9% yield		44.7% yield	
	E.M.	St. Dev.	E.M.	St. Dev.	E.M.	St. Dev.
	-1.45	0.25	-1.33	0.21	-1.27	0.26
	-1.48	0.21	-1.37	0.23	-1.24	0.23
	-1.43	0.26	-1.37	0.23	-1.24	0.25
	-1.46	0.20	-1.34	0.23	-1.19	0.21
	-1.42	0.15	-1.37	0.22	-1.24	0.23
	-1.35	0.14	-1.34	0.22	-1.19	0.21
	-1.43	0.26	-1.41	0.25	-1.23	0.24
	-1.34	0.23	-1.30	0.22	-1.23	0.19
	-1.35	0.21	-1.34	0.22	-1.28	0.23
	-1.34	0.22	-1.31	0.21	-1.17	0.23
Average:	-1.41	0.21	-1.35	0.22	-1.23	0.23
St. Dev.:	(0.06)	(0.04)	(0.03)	(0.01)	(0.04)	(0.02)

Bleached Kraft Fines (7,500 revolutions) in 0.01M NaCl

	55.4% yield		49.9% yield		44.7% yield	
	E.M.	St. Dev.	E.M.	St. Dev.	E.M.	St. Dev.
	-0.85	0.18	-0.73	0.16	-0.65	0.19
	-0.89	0.18	-0.72	0.18	-0.65	0.17
	-0.84	0.17	-0.75	0.17	-0.64	0.18
	-0.86	0.18	-0.75	0.16	-0.67	0.19
	-0.84	0.18	-0.82	0.18	-0.61	0.19
	-0.81	0.17	-0.76	0.17	-0.63	0.18
	-0.79	0.19	-0.75	0.17	-0.64	0.20
	-0.72	0.19	-0.75	0.16	-0.61	0.17
	-0.79	0.20	-0.73	0.19	-0.64	0.18
	-0.79	0.17	-0.74	0.19	-0.64	0.18
Average:	-0.82	0.18	-0.75	0.17	-0.64	0.18
St. Dev.:	(0.05)	(0.01)	(0.03)	(0.01)	(0.02)	(0.01)

Bleached Kraft Fines (15,000 revolutions) in 0.01M NaCl

	55.4% yield		49.9% yield		44.7% yield	
	E.M.	St. Dev.	E.M.	St. Dev.	E.M.	St. Dev.
	-0.87	0.18	-0.71	0.18	-0.68	0.18
	-0.87	0.17	-0.75	0.18	-0.68	0.20
	-0.87	0.19	-0.74	0.17	-0.67	0.18
	-0.85	0.17	-0.72	0.18	-0.74	0.16
	-0.79	0.17	-0.74	0.16	-0.96	0.24
	-0.84	0.19	-0.75	0.17	-0.66	0.17
	-0.82	0.19	-0.75	0.18	-0.69	0.18
	-0.84	0.18	-0.72	0.18	-0.67	0.18
	-0.80	0.17	-0.70	0.16	-0.67	0.18
	-0.81	0.17	-0.73	0.17	-0.66	0.17
Average:	-0.84	0.18	-0.73	0.17	-0.71	0.18
St. Dev.:	(0.03)	(0.01)	(0.02)	(0.01)	(0.09)	(0.02)

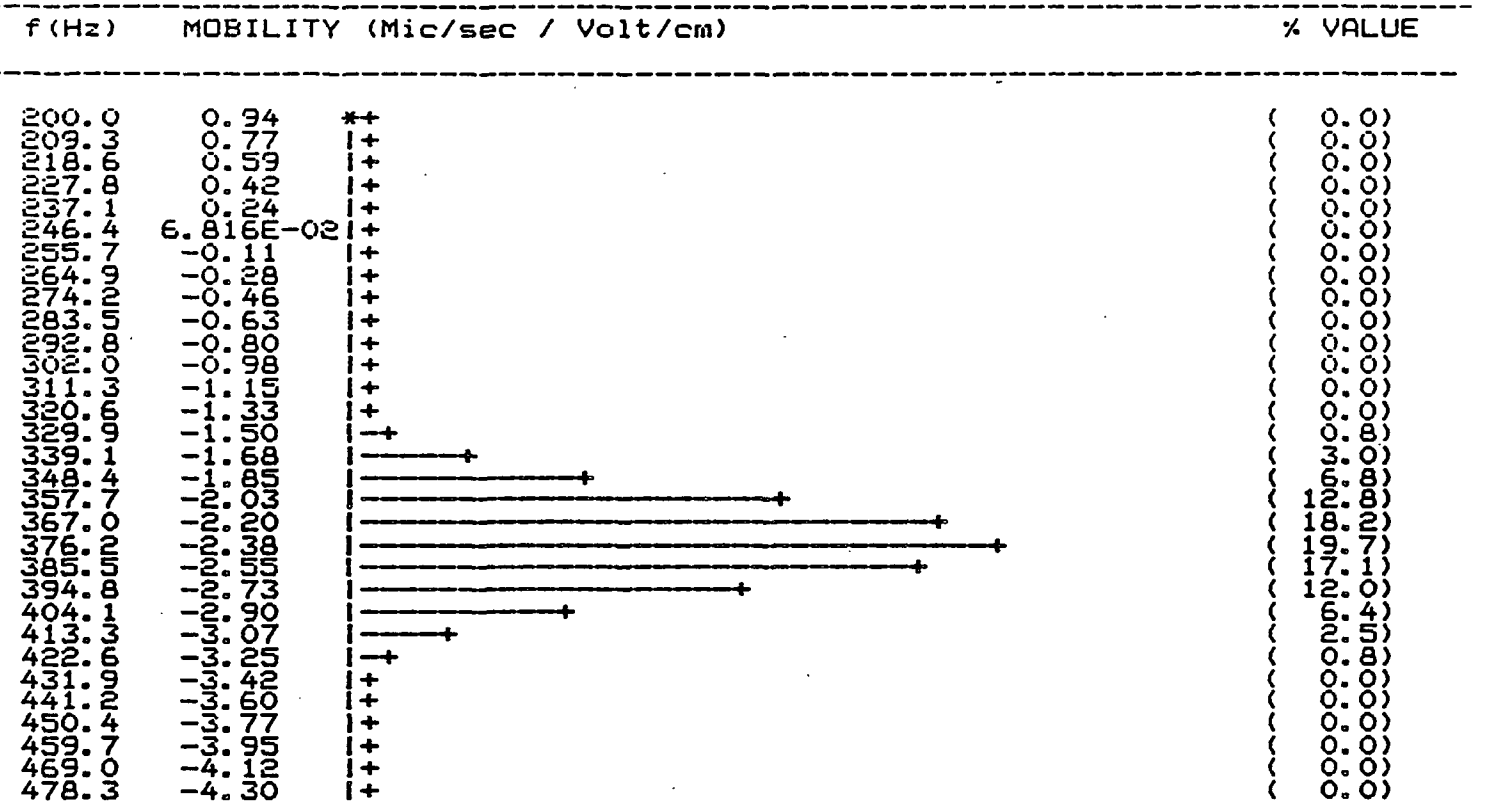

Figure. 66. Electrophoretic mobility histogram of unbleached kraft in 0.0002M NaCl (54.4% yield, 7,500 revolutions).

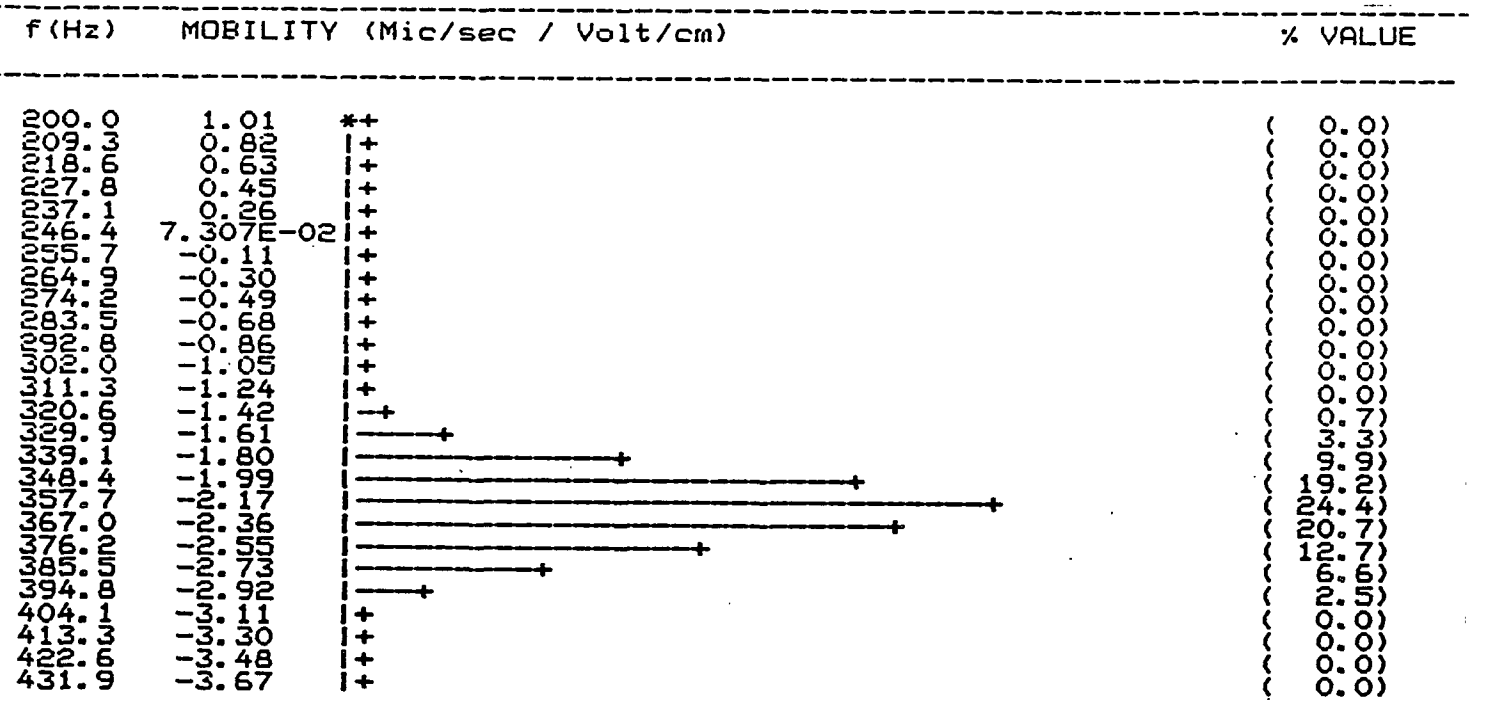

Figure. 67. Electrophoretic mobility histogram of bleached kraft in 0.0002M NaCl (54.4% yield, 7,500 revolutions).

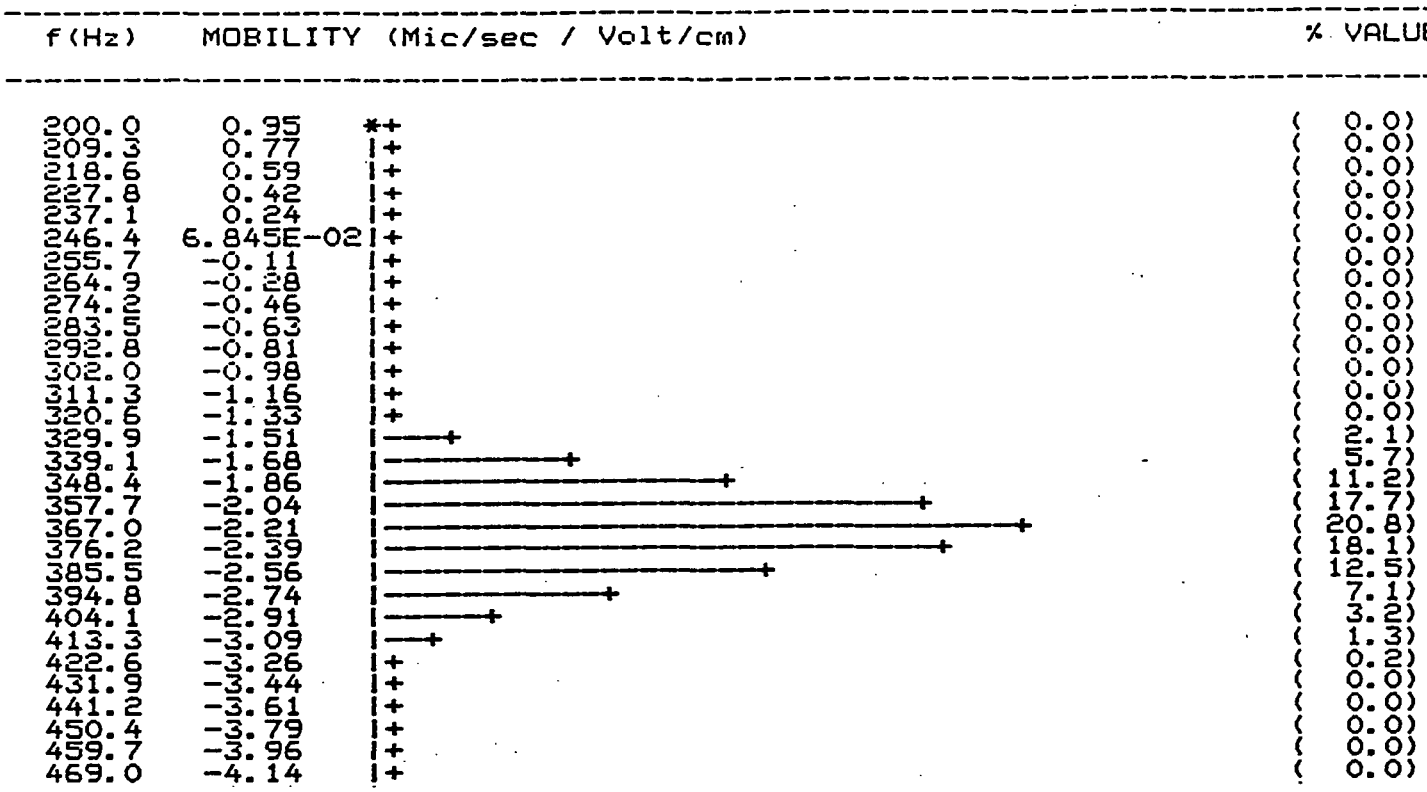

Figure. 68. Electrophoretic mobility histogram of unbleached kraft in 0.0002M NaCl (49.9% yield, 7,500 revolutions).

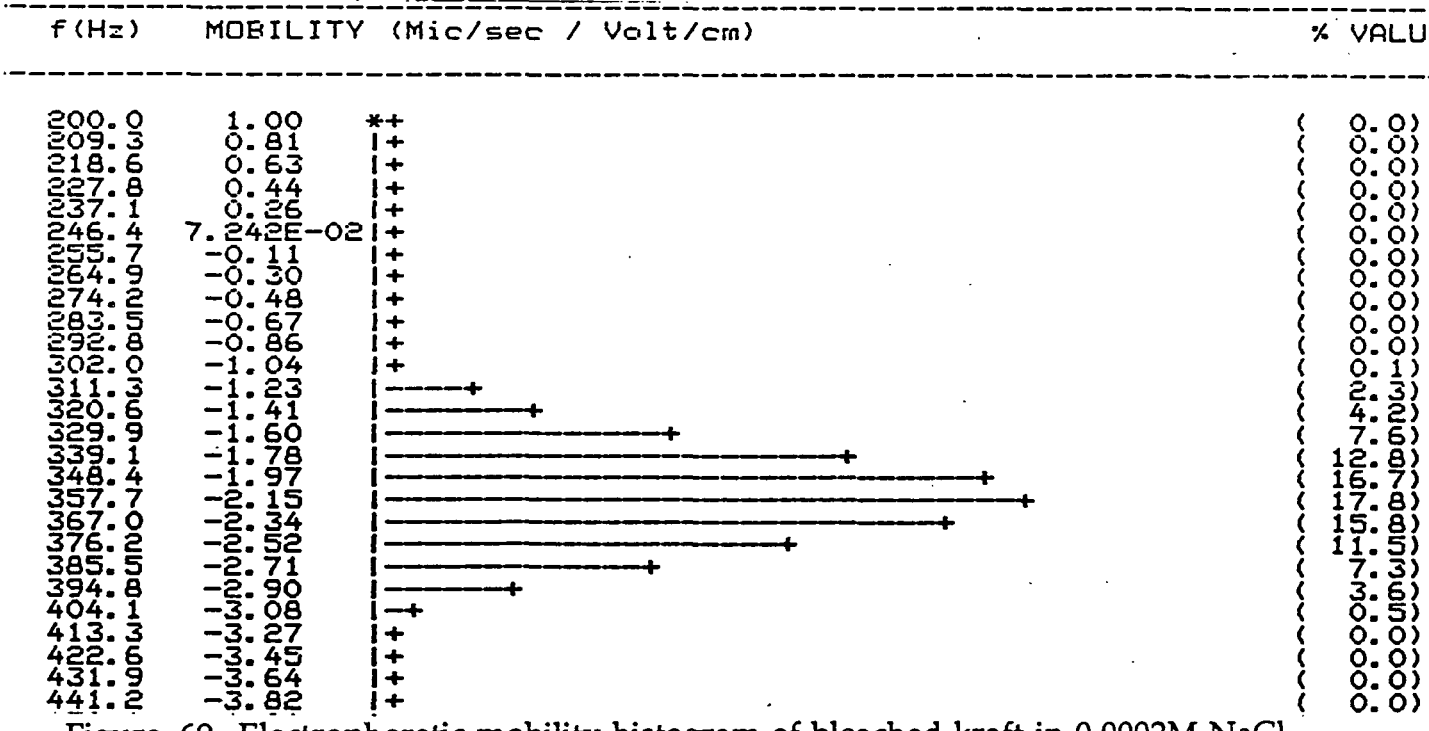

Figure. 69. Electrophoretic mobility histogram of bleached kraft in 0.0002M NaCl (49.9% yield, 7,500 revolutions).

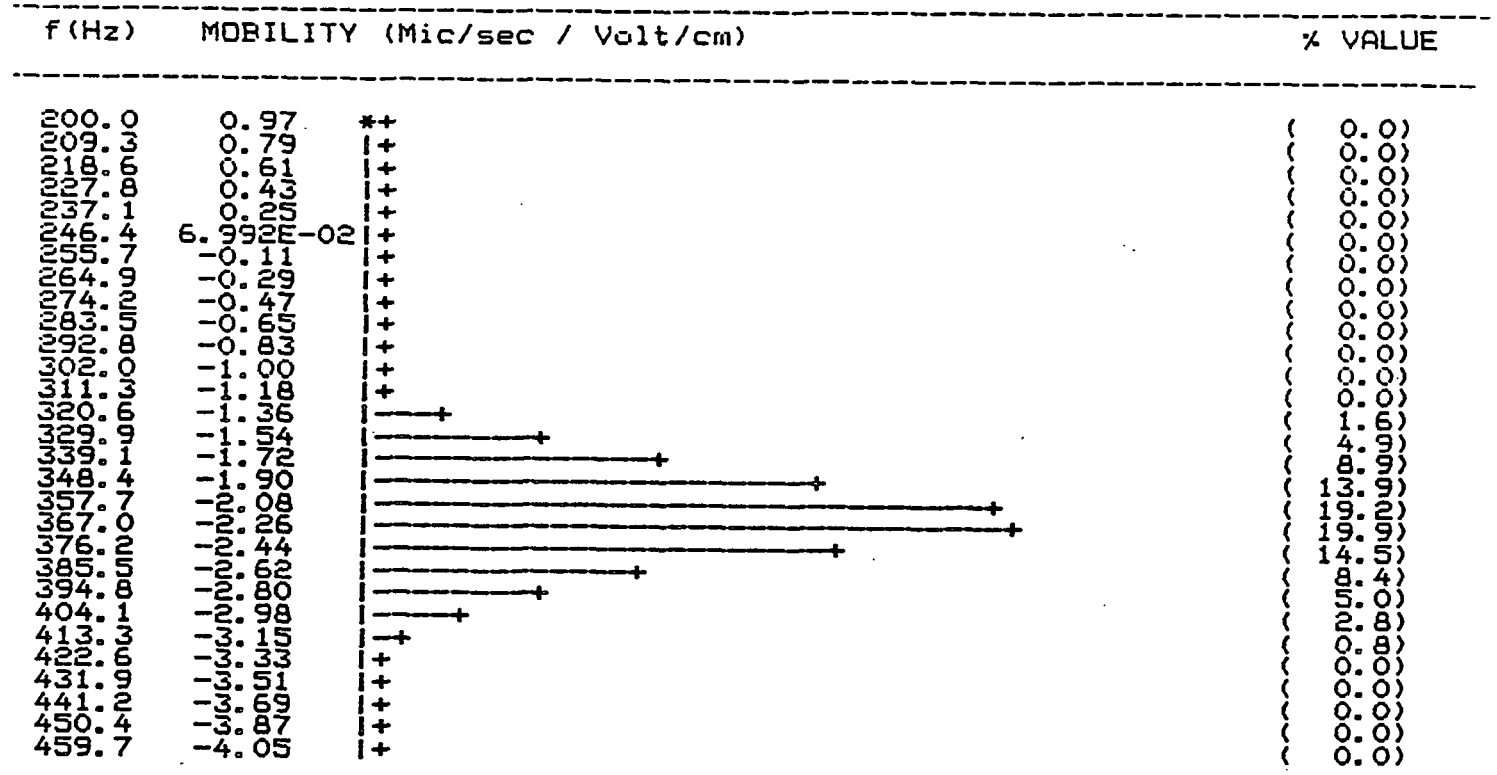

Figure. 70. Electrophoretic mobility histogram of unbleached kraft in 0.0002M NaCl (47.7% yield, 7,500 revolutions).

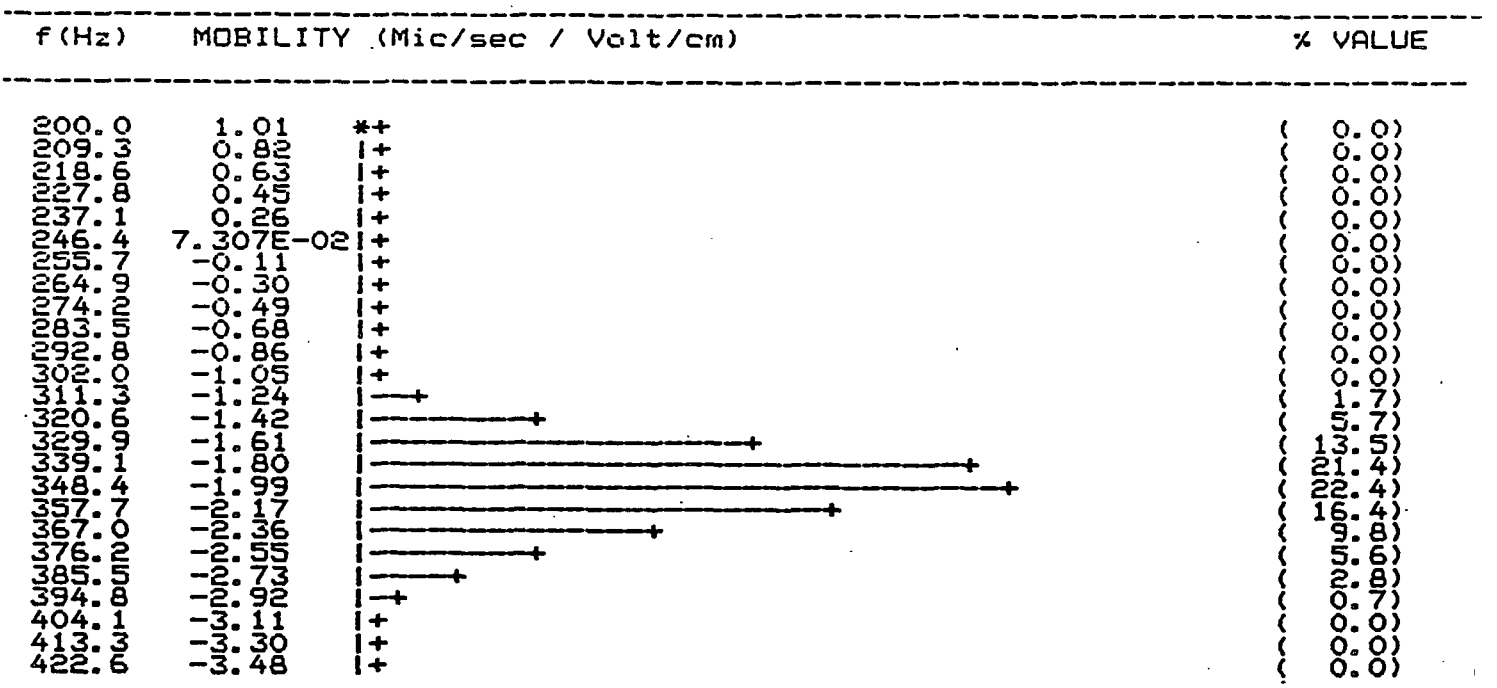

Figure. 71. Electrophoretic mobility histogram of bleached kraft in 0.0002M NaCl (47.7% yield, 7,500 revolutions).

APPENDIX VII

STATISTICAL ANALYSIS OF KRAFT ELECTROPHORETIC MOBILITY DATA

The statistical analysis to determine the effect of pulp yield, bleaching, and degree of refining on the electrophoretic mobility of kraft fines was carried out as if the experiment had been a 3 x 2 x 2 factorial design.[129] For a 3 x 2 x 2 factorial design, twelve individual kraft cooks would have had to have been produced, instead of the three shown in Fig. 5. This would have provided twelve independent kraft pulp samples for analysis.

Two major assumptions are implicit by proceeding with an analysis of this type: (1) the error associated with pulping is negligible; and (2) the error in bleaching is negligible. The ability to reproduce pulps with identical chemical and electrokinetic properties by pulping to the same H-Factor under identical conditions is not known. The reproducibility of the five-stage bleaching sequence, applied to similar pulps is also not known. For these reasons, the results of the statistical analysis can not be stated with any degree of statistical confidence. Nevertheless, the analysis was performed for purposes of ranking the mean squares to determine which effects would be expected to be statistically significant.

An estimate of the error mean square would have required an independent replicate of the experiment. Since this was not performed, the statistical analysis was carried out using the three factor interaction term, with two degrees of freedom (D.F.), as the estimate of the experimental error mean square. The analysis of variance tables calculated for each electrolyte concentration are presented below.

Table 28. Analysis of variance for kraft fines in 0.0002M NaCl

Source of Variation	Sum of Squares	D.F.	Mean Square	F-ratio*
Pulp Yield (A)	0.1066	2	0.0533	13.32[d]
Bleaching (B)	0.1220	1	0.1220	30.50[c]
Refining (C)	0.0014	1	0.0014	0.35
AB	0.0022	2	0.0011	0.28
AC	0.0021	2	0.0011	0.28
BC	0.0000	1	0.0000	0.00
ABC	0.0080	2	0.0040	

* = error assumed to be 3-factor interaction (M.S. = 0.0040, D.F. = 2)

Table 29. Analysis of variance for kraft fines in 0.002M NaCl

Source of Variation	Sum of Squares	D.F.	Mean Square	F-ratio*
Pulp Yield (A)	0.1146	2	0.0573	110.24[a]
Bleaching (B)	0.1633	1	0.1633	314.10[a]
Refining (C)	0.0056	1	0.0056	10.83[d]
AB	0.0045	2	0.0023	4.35[e]
AC	0.0021	2	0.0011	2.04
BC	0.0003	1	0.0003	0.59
ABC	0.0010	2	0.0005	

* = error assumed to be 3-factor interaction (M.S. = 0.0005, D.F. = 2)

Table 30. Analysis of variance for kraft fines in 0.01M NaCl

Source of Variation	Sum of Squares	D.F.	Mean Square	F-ratio*
Pulp Yield (A)	0.1176	2	0.0588	261.44[a]
Bleaching (B)	0.1875	1	0.1875	833.33[a]
Refining (C)	0.0048	1	0.0048	21.33[c]
AB	0.0262	2	0.0131	58.11[b]
AC	0.0020	2	0.0010	4.44[e]
BC	0.0012	1	0.0012	5.33[e]
ABC	0.00045	2	0.000225	

* = error assumed to be 3-factor interaction (M.S. = 0.000225, D.F. = 2)

An analysis of the mean squares indicates bleaching has the greatest effect on the electrophoretic mobility, followed by pulp yield. Refining, and the two- and three-factor interactions, had very small mean squares in most instances.

The F-ratio is calculated by dividing the treatment mean square by the error mean square. F-ratios are used to determine if a treatment effect is statistically significant. For reasons previously discussed, it is not valid to perform this analysis on my data unless the errors associated with the pulping and bleaching processes are known to be negligible. Nevertheless, the exercise was conducted to provide an indication of which effects might be considered significant. The F-ratios can be compared to a published table of values determined for the corresponding degrees of freedom associated with the treatment mean square, ν_1, and the error mean square, ν_2. A portion of an F-ratio table for the specific cases involved in this study is presented in Table 31. The superscript (a - e) associated with the F-ratios in Tables 28 - 30 indicate the significance of each source of variation based on the values presented in Table 31.

Table 31. Portion of $F_{v1,v2}$-ratio table for various degrees of significance.[129]

Percent Significance	$F_{1,2}$	$F_{2,2}$
1.0 (a)	98.50	99.00
2.5 (b)	38.51	39.00
5.0 (c)	18.51	19.00
10.0 (d)	8.53	9.00
25.0 (e)	2.59	3.00

It should be restated that the preceding statistical analysis is valid only if it is assumed that the errors associated with pulping and bleaching processes are negligible. One would not necessarily assume this to be so, given the complex chemical reactions occurring during these operations. However, chemical treatment of two TMP pulp samples with hydrogen peroxide, also a complex process, indicated excellent reproducibility.

On the basis of the above analysis it appears that both pulp yield and bleaching have a major effect on the electrophoretic mobility of fiber fines. Refining does not appear to have an effect on the electrophoretic mobility. The two-factor and three factor interactions also do not appear to have an effect on the electrophoretic mobility.